INVESTIGATION OF THE PERFORMANCE OF SOME CORROSION INHIBITORS IN AERATED ACID SOLUTIONS

A Thesis
Submitted to the College of Engineering
of Nahrain University in Partial Fulfillment of the
Requirements for the Degree of Master of Science in
Chemical Engineering

by

Hayder Mohammed Turkee
B.Sc. in Chemical Engineering 2006

Jumada Al-ula 1430
May 2009

Certification

We certify that this thesis entitled **“Investigation of the performance of some corrosion inhibitors in aerated acid solutions”** was prepared by **Hayder Mohammed Turkee** under our supervision at Nahrain University/College of Engineering in partial fulfillment of the requirements for the degree of Master of Science in Chemical Engineering.

Signature:
Name: **Prof. Dr. Qasim J. Slaiman**
(Supervisor)
Date: 24 / 5 / 2009

Signature:
Name: **Dr. Basim O. Hasan**
(Supervisor)
Date: 24 /5 /2009

Signature:
Name: **Prof. Dr. Qasim J. Slaiman**
(Head of Department)
Date: 1 / 6 / 2009

Certificate

We certify, as an examining committee, that we have read the thesis entitled "**Investigation of the performance of some corrosion inhibitors in aerated acid solutions**", examined the student **Hayder Mohammed Turkee**, in its content and found it meets the standard of thesis for the degree of Master of Science in Chemical Engineering.

Signature:
Name: **Prof. Dr. Qasim J. Slaiman**
(Supervisor)
Date: 24/5/2009

Signature:
Name: **Dr. Basim O. Hasan**
(Supervisor)
Date: 24/5/2009

Signature: Yaro
Name: **Assist. Prof. Dr. Aprael S. Yaro**
(Member)
Date: 26/5/2005

Signature: M. Sh
Name: **Assist. Prof. Dr. Muslet Sh. Hussain**
(Member)
Date: 26 / 5 / 2009

Signature: Mahmoud Omar Abdullah
Name: **Prof. Dr. Mahmoud O. Abdullah**
(Chairman)
Date: 27/5/2009

Approval of College of Engineering

Signature: M. J. Jweeg
Name: **Prof. Dr. Muhsin J. Jweeg**
(Dean)
Date: 7/6/2009

ABSTRACT

Corrosion tests on commercial carbon steel pipe in aerated 0.1N HCl solution under static and flow conditions with rotational speed range of 400–1400 rpm and temperature range 35 – 60ºC were curried out by weight loss techniques. Experiments were carried out in absence and presence of several inhibitors**:** thiourea, ethylene diamine, diethanol amine and formaldehyde as adsorption type inhibitors in concentration range 400 – 2000 ppm using rotating cylinder electrode technique.

The experimental results showed that corrosion rate in the absence and presence of inhibitors increased with increasing temperature of the corrosive solution and the rotational speed and decreased with increasing the inhibitor concentrations for the whole range of temperature and rotational speed. It was also found that order of corrosion inhibitors according to their inhibition efficiency was as follows: thiourea > ethylene diamine > diethanol amine > formaldehyde. The maximum inhibition efficiency obtained was for thiourea about 77.59% and the minimum inhibition efficiency for formaldehyde which is 37.12%.

Also the results revealed that increasing temperature and Reynolds number (or rotational speed) lead to increase the oxygen transport from the bulk solution to the metal surface, i.e. increase in the value of (i_{O2}), but it was observed that increasing Re have no clear effect on hydrogen evolution current (i_{H2}).

Arrhenius plots were performed in presence of thiourea at various Reynold numbers, concentrations, and the three temperatures of 35, 45, and 60ºC led to different values of activation energies.

List of Contents

Appendices

Nomenclature

Symbols	**Description**
A	Surface area of specimen (m^2)
C	The inhibitor concentration, ppm (mg/L)
C_b	Bulk concentration ($gmole/cm^3$)
CR	Corrosion rate ($gm/m^2.day$)
D	Diffusion coefficient of the reacting ions (m^2/s)
d	Outside diameter of cylindrical test specimen (m)
E, E_i	Electrode potential (mV), SHE or SCE
E_a	Activation energy (kJ/mol)
E_o	Standard potentials (mV)
E_p	Polarized potential (mV)
$E_{p,c}$	Cathodic polarized potential (mV)
E_r	Reversible potential (mV)
$E_{r,c}$	Cathodic reversible potential (mV)
F	Faradays constant (96487 Columb/equivelent)
i	Current density (A/m^2)
i_a	Anodic current density (A/m^2)
i_c	Cathodic current density (A/m^2)
i_{H2}	Current dencity of hydrogen evolution (A/m^2)
i_L	Limiting current density (A/m^2)
i_o	Exchange current density (A/m^2)
i_{O2}	Oxygen current dencity (A/m^2)
K	Mass transfer coefficient (m/s)
L	Length of cylindrical test specimen (mm)
N	Revolution per sec
N_A	Molar flux ($mol/m^2.s$)

Q	Heat of adsorption (Joule)
R	Gas constant (8.314 J/mol.K)
Re	Reynolds number
Sc	Schmidt number
Sh	Sherwood number
t	Time of exposure (h)
t_n	Transference number
U	Revolution per minute (rpm)
Z, n	Number of electrons transferred
ΔW	Weight loss (gm)

Greek Symbols

μ	Fluid viscosity (kg/m.s)
α_a, α_c	Transfer coefficient for anodic or cathodic reaction
α_{oxid}, $\alpha_{red.}$	Activities (concentrations) of the oxidized and reduced species
β	Tafel slope (mV/decade)
δ	Thickness of the diffusion layer (m)
η	Polarization overpotential (mV)
η^A	Activation overpotential (mV)
η^c	Concentration overpotential (mV)
η_T	Total overpotential (mV)
θ	Fraction of surface covered, i.e. degree of inhibition (or % protection)
ρ	Density of fluid (kg/m^3)

List of Tables

List of Figures

CHAPTER ONE

Introduction

1.1 Corrosion

The problem of metal corrosion by acids represents a wide range of corrosion problems in today's industrialized world. The present work deals with the corrosion of *Carbon Steel* in *Hydrochloric* acid; due to their wide spread use in industrial facilities [1].

Deterioration by physical causes is not called corrosion, but is described as erosion, galling, or wear. In some instances, chemical attack accompanies physical deterioration as described by the terms: corrosion-erosion, corrosive wear, or fretting corrosion. Nonmetals are not included in the present definition [2]. Environments that cause corrosion are called corrosive, while a metal that suffers corrosion is called corrodible [3].

Corrosion is defined as the destruction or deterioration of a material because of reaction with its environment. Some insist that the definition should be restricted to metals, but often the corrosion engineers must consider both metals and nonmetals for solution of a given problem [4].Or it is an interaction of a metal with its surroundings [5].

Corrosion in aqueous environment and atmospheric environment is an electrochemical process because corrosion involves the transfer of electrons between a metal surfaces and an aqueous electrolyte solution. It results from the overwhelming tendency of metals to react electrochemically with oxygen, water and other substances in the aqueous environment [6].

1.2 Economic Effects of Corrosion

The importance of corrosion studies is a threefold, the first area of significance is economical and the second area is improved safety and the third is conservation of metals [2].

The cost of corrosion has been estimated at $300 billion per year in the United States. The corrosion-related cost to the transmission pipeline industry is approximately $5.4 to $8.6 billion annually. This can be divided into the cost of failures, capital, and operations and maintenance (O&M) at 10, 38, and 52 percent, respectively [7].

The people working in the field of corrosion frequently try to point out how much it costs as percentage of a nation economy. The approximate annual cost of corrosion in the United States was first estimated in 1949 to be $5 billion, 2.1 % of Gross National Product (GNP) [2].

In the United the estimated cost of corrosion had risen to $70 billion, 2.4 % of GNP. In December 1979 the city of Westminster, London reported that it had a problem with falling lampposts. It was suggested that the main culprits for the corrosion that had occurred at the base of the posts were dogs. The city’s Pets were daily depositing about 2,000 liters of urine, mostly at the base of the city lampposts and this caused a great increase in the rate of corrosion. One of many problems experienced with the Charing Cross railway bridge in central London was also attributable to this surpassing cause. Repeated visits from dogs had caused severe crevice corrosion in a part of the structure that was impossible to maintain [3].

In this work two organic amine inhibitors (Ethylene diamine and Diethanol amine) were used. These are nitrogen-bearing organic compounds which demonstrated inhibitive action against corrosion processes [8].

Formaldehyde is available from commercial sources in 37-40 % aqueous solution, containing small amounts of methanol and known as formalin which is considered adsorption type inhibitor. In such solutions, it exists primarily as a number of low-molecular-weight polymers of the type $H(OCH_2)_nOH$. And it may also be obtained as a stable solid known as paraformaldehyde, composed of high-molecular-weight polymers of the same type [9].

Thiourea and its derivatives are widely used as acid inhibitors in industrial operations, such as pickling, descaling, cleaning, and acidization of oil wells, to protect metals and alloys. The corrosion inhibitor acts as a protective film and is superior to amine-based inhibitors in acidic media. This kind of inhibitor simultaneously acts on both anodic and cathodic areas. The organic substances belonging to this group contain mainly oxygen, sulfur, nitrogen atoms, and multiple bonds in the molecules that facilitate the adsorption on the metal surface are strongly polar [10].

1.3 Scope of Present Work

This work aims to investigate the performance of some corrosion inhibitors which are (Thiorea, Ethylene diamine, Diethanol Amine and Formaldehyde) under static and flow conditions in order to assess the influence of temperature, concentration and type of inhibitor. Also the purpose is to investigate the effect of Reynolds number on the corrosion rate of carbon steel in aerated HCl (0.1 N) and on the inhibitive action of these inhibitors.

CHAPTER TWO

Corrosion Inhibition in Acids

2.1 Classification of Corrosion

Corrosion has been classified in many different ways. One method divides corrosion into low-temperature and high-temperature corrosion. Another Separates corrosion into direct combination (or oxidation) and electrochemical corrosion. The preferred classification is (1) wet corrosion and (2) dry corrosion [4].

There are several types of corrosion that can occur. All are identical in the chemical process of corrosion. They differ in how and where they attack the metal [11]:

- **Immunity**: is the lack of measurable attack on a metal when exposed to operational environments.
- **Galvanic Corrosion:** is the corrosion that is caused or accelerated through the electrical coupling of two or more dissimilar metals that are both immersed in an electrolyte.
- **Pitting Corrosion:** Pitting is the attack of a metal where the corrosion rate is substantially higher at some exposed areas than at others. When the maximum penetration due to corrosion is less than two times the average rate the corrosion is considered to be uniform, when it is greater than two times the average rate, the attack is considered to be pitting.
- **Concentration Cell Corrosion**: Concentration cell corrosion is corrosion that is accelerated by differences in environment between separated areas on a single metal.
- **Dealloying:** It is the selective corrosive attack of one or more constituent of a metallic alloy.

- **Intergranular Corrosion**: Intergranular corrosion is a selective attack of a metal at or adjacent to grain boundaries.
- **Stress Corrosion Cracking**: Stress corrosion cracking is the intergranular or transgranular cracking of a material due to the combined action of tensile stress and a specific environment.
- **Hydrogen Embrittlement:** Hydrogen embrittlement is the severe loss of ductility of a metal when hydrogen has been introduced into the metal structure.
- **Corrosion Fatigue:** Corrosion fatigue is the reduced ability of a metal to withstand repeated stress when exposed to the combined action of stress and a corrosive environment as compared to the effects of stress alone.
- **Erosion Corrosion:** Corrosion accelerated by the high velocity flow of a liquid, or a suspension of solid particles in a liquid is known as erosion corrosion.
- **Cavitations Corrosion:** Cavitations corrosion is corrosion that is enhanced through the formation and collapse of gas or vapor bubbles at or near the metal surface.
- **Fretting Corrosion:** Fretting corrosion is an attack that is accelerated by the relative motion of contacting surfaces.
- **Uniform Corrosion:** Uniform attack or general corrosion occurs on the surface of a metal in the following way. If a metal is in contact with a conductive solution, some areas may become either anodic or cathodic sites. On the anode, oxidation of the metal will occur, and the electrons supplied will be taken up at the cathode through the metal itself. Small currents will then flow from one to the other. The ions produced at the anode will migrate through the solution towards the

cathode, where they will form an oxide film with the products of the oxygen reduction.

The location of the anode and the cathode changes all the time, which makes the whole surface of the metal corrode. Figure 2.1 gives an example of uniform attack occurring on the iron [12].

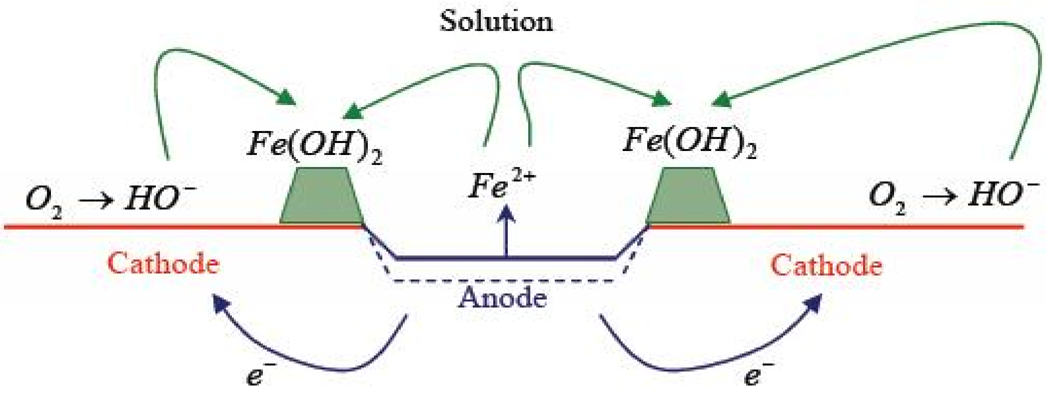

Figure 2-1: Uniform Corrosion Process (Example with Iron) [12].

2.2 Factors Affecting Corrosion Rate

2.2.1 Solution pH

The relationship between pH and corrosion rates tends to follow one of three general patterns:

i. Acid-soluble metals such as iron have a relationship as shown in figure 2.2. In the middle pH range (≈ 4 to 10), the corrosion rate is controlled by the rate of transport of oxidizer (usually dissolved O_2) to the metal surface. At very high temperature such as those encountered in boilers, the corrosion rate increases with increasing basicity as shown by the dashed line [13].

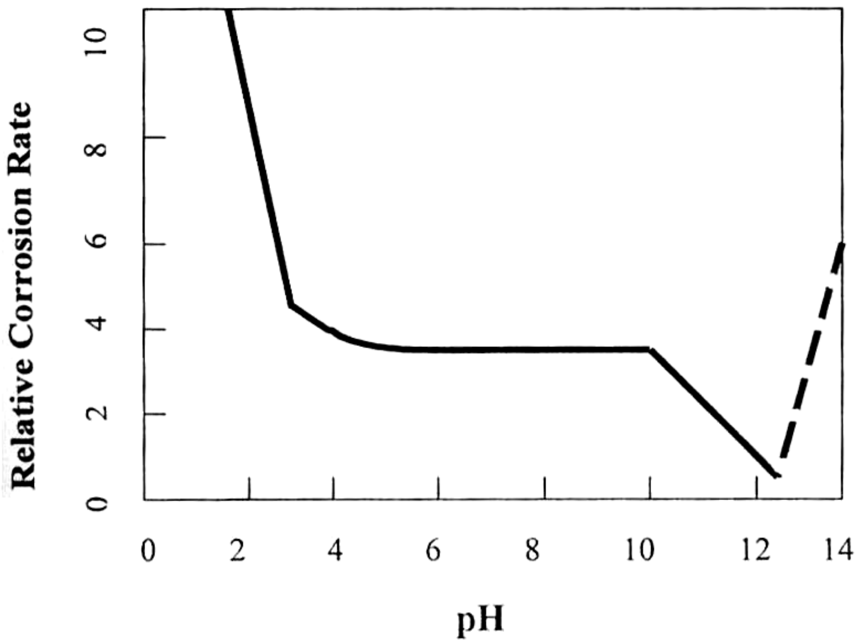

Figure 2-2 Effect of pH on Corrosion Rate of Iron [13].

ii. Amphoteric metals such as aluminum and zinc have a relationship as shown in figure 2.3. These metals dissolve rapidly in either acidic or basic solutions.

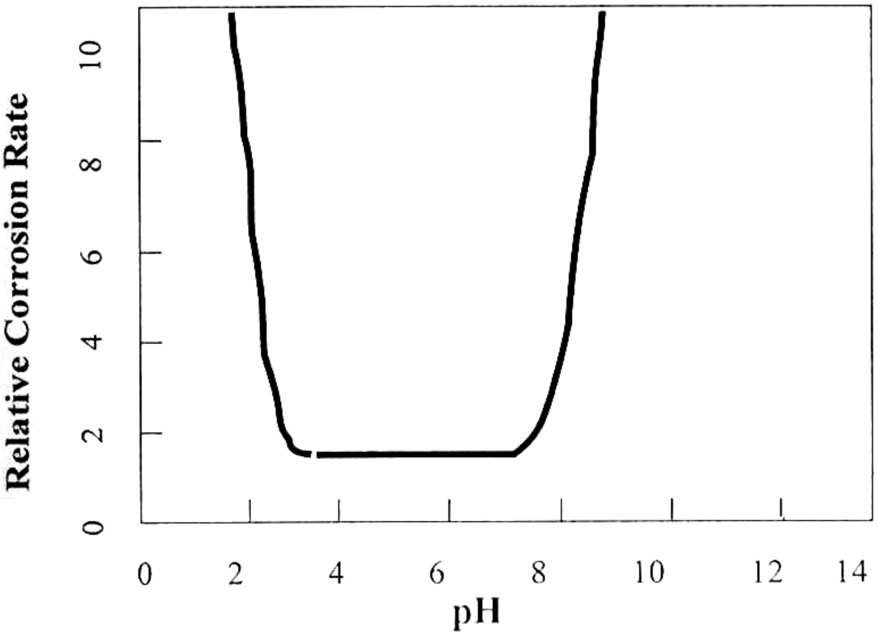

Figure 2-3 Effect of pH on the Corrosion Rate of Amphoteric Metals (Aluminum and Zinc) [13].

- iii. Noble metals such as gold and platinum are not appreciably affected by pH as shown in fig.2.4.

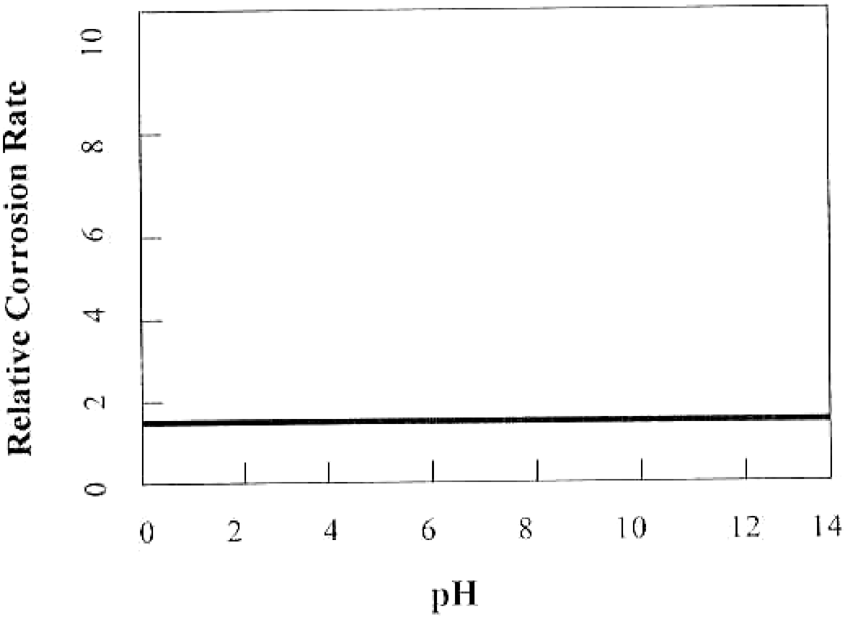

Figure 2-4 Effect of pH on the Corrosion Rate of Noble Metals [13].

2.2.2 Effect of Temperature

Temperature increases the rate of almost all chemical reactions. When the rate-determining step is the activation process, the temperature change has the greatest effect. In general, if diffusion rates are doubled for a certain increase in temperature, activation process may be increased by 10-100 times, depending on the magnitude of the activation energy [14].

In solutions, when the process is under activation control, the main effect of increasing the temperature is to increase the exchange current. Conway, Beatty and Maine [15] found that for nickel, the exchange current increased by 100 times when the temperature is changed from 10 to 75 °C while for concentration polarization, the diffusion coefficient for hydrogen ions would increase only twice over the same temperature range.

The corrosion process governed by the cathodic reduction of dissolved oxygen might be expected to be wholly controlled by concentration polarization because of low solubility of oxygen, especially in concentrated salt solutions. Temperature is complex in that the diffusivity of oxygen increases, but solubility decreases with temperature increase. Data are scarce for these effects [16, 14, and 17].

2.2.3 Fluid Velocity

Velocity primarily affects corrosion rate through its influence on diffusion phenomena. It has no effect on activation controlled processes. The manner in which velocity affects the limiting diffusion current is a marked function of the physical geometry of the system. In addition, the diffusion process is affected differently by velocity when the flow conditions are laminar as compared to a situation where turbulence exists. For most conditions the limiting diffusion current can be expressed by the equation:

$$i_L = k\,u^n \qquad \ldots (2\text{-}1)$$

where k is a constant, u is the velocity of the environment relative to the surface and n is a constant for a particular system. Values of n vary from 0.2 to 1. Figure 2.5 shows the effect of velocity on the limiting current density [18, 19].

The effect of velocity on corrosion rate, like the effect of oxidizer addition, complex and depends on the characteristics of the metal and the environment to which it is exposed. Figure 2.6 shows the typical observations when agitation or solution velocity is increased.

For corrosion processes which are controlled by activation polarization, agitation and velocity have no effect on the corrosion rate as illustrated in curve B. If corrosion process is under cathodic control, then agitation or velocity increases the corrosion rate as shown in curve A, section 1. This effect generally occurs when an oxidizer presents in very small amounts as in the case of dissolved oxygen in acids or water. If the process is under diffusion control and the metal is readily passivated, then the behavior corresponding to curve A, section 1 and 2, will be observed. Some metals owe their corrosion resistance in certain medium to the formation of massive bulk protective films on their surface. When materials such as these are exposed to extremely high corrosive velocities, mechanical damage or removal of these films can occur, resulting in accelerated attack as shown in curve C. this is called erosion-corrosion [4].

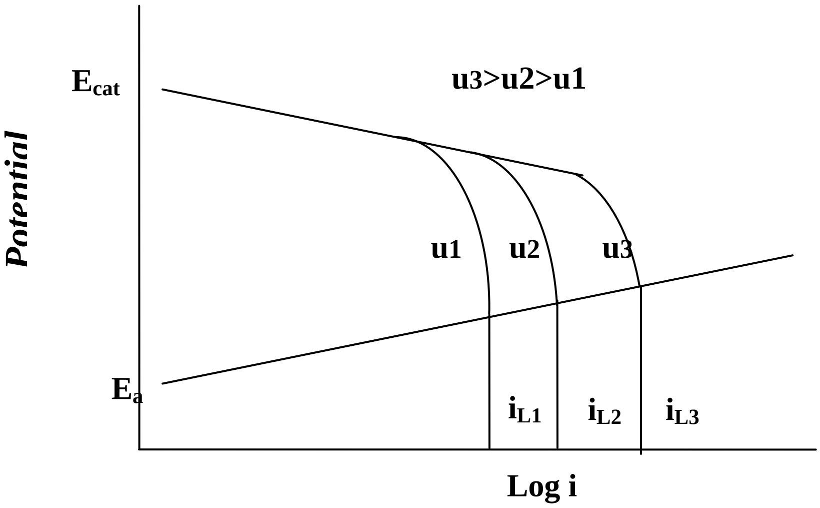

Fig. 2-5 Effect of Velocity on i_L [19].

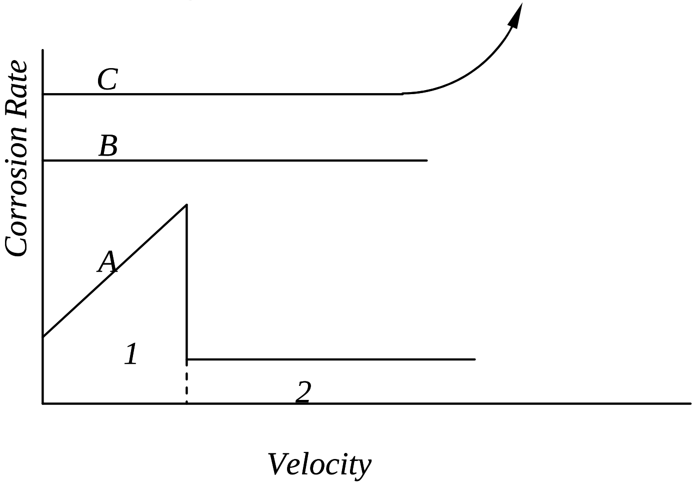

Fig.2-6 Effect of Velocity on the Corrosion Rate [4].

2.2.4 Effect of Salt Content and Chloride Ion

Chlorides have probably received most consideration in relation to their effect on corrosion. The effect of sodium chloride concentration on the corrosion of iron in air saturated water at room temperature was found to increase the corrosion rate. The corrosion rate in air saturated water at room temperature was found to increase with the increase of sodium chloride solution concentration reaching maximum at about 3% NaCl (seawater concentration), and then decreases, the value falling below that of distilled water when saturation is reached (26 % NaCl). To understand this behavior, oxygen solubility in water decreases continuously with an increase in sodium chloride concentration, explaining the falling off of corrosion rate at higher sodium chloride concentration. The initial rise appears to be related to a change in the protective nature of the barrier rust film that forms on the corroding metal. On the other hand, chlorides increase the electrical conductivity of the water so that the flow of corrosion currents will be facilitated [16, 2].

Later, Kolman et. al. [20] found the corrosion potential becomes more negative with increasing NaCl concentration.

Recently, Bahar [21] showed that, in stationary aerated water, the limiting current density increases with increasing NaCl concentration up to 3.5%, and the corrosion potential becomes more negative.

2.3 Polarization

Polarization is the shift in electrode potential resulting from the effects of current flow, measured with respect to the zero flow (reversible) potential, i.e., the counter emf caused by the products formed or concentration changes in the electrolyte.

When current flows to / or from an electrode, it is no longer at equilibrium. The measured potential of such an electrode is altered to an extent that depends on the magnitude of the external current and its direction. The direction of potential change always opposes the shift from equilibrium and hence opposes the flow of current, therefore, the anode becomes more cathodic in potential and the cathode becomes more anodic, and the difference of potential becomes smaller. As the degree of polarization increases, the rate of corrosion decreases. The polarization on the anode may be less than or greater than that on the cathode. The polarization value will vary with the nature of the electrode, the corrosion of its surface and with the content, temperature and concentration of the electrolyte as well as with the rate at which the reactions proceeding.

The corrosion reaction is said to be anodically controlled if the polarization occurs at the anode where the corrosion potential is close to the open circuit potential of the cathode fig. 2.7-a.

The corrosion reaction is said to be cathodically controlled if the polarization occurs at the cathode where the corrosion potential is near the open circuit potential of the anode fig. 2.7-b.

Resistance control occurs when the electrolyte resistance is so high that the resultant current is not sufficient to appreciably polarize anodes or cathodes fig. 2.7-c. It is common for polarization to occur in some degree at both anodes and cathodes; this situation is described as mixed control fig. 2.7-d [2, 22].

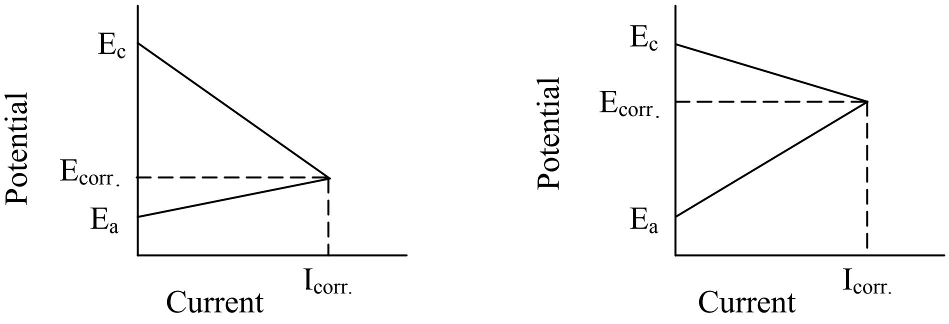

Cathodic Control Anodic Control

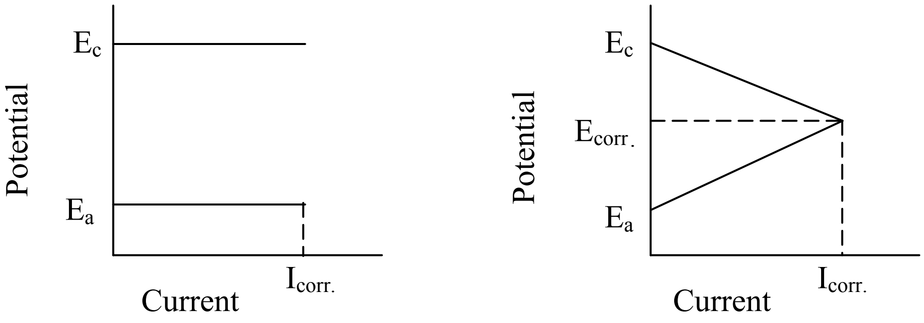

Resistance Control Mixed Control

Figure 2-7 Types of Corrosion Control [16].

2.3.1 Activation Polarization

Polarization refers to an electrochemical process, which is controlled by the reaction sequence at the metal-electrolyte interface or stated in another way the reaction at the electrode requires activation energy in order to go. Activation polarization is usually the controlling factor during corrosion in media containing a high concentration of active species (e.g., concentrated acids). This is easily illustrated by considering hydrogen evolution reaction on zinc during corrosion in acid solution; figure 2.8 shows some of the possible steps in hydrogen reduction on a zinc surface as [23]:

- It occurs rapidly and the species must be adsorbed or attached to the surface before the reaction.
- Electron transfer (resulting in a reduction of the species) to H^+ discharge.
- Two hydrogen atoms then combine to form hydrogen molecule.
- Hydrogen bubbles are formed.

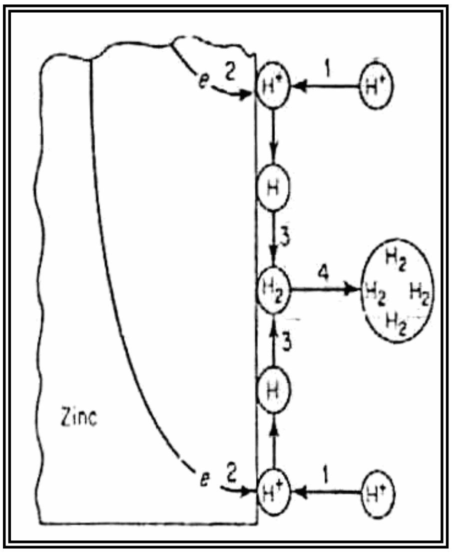

Figure 2-8 Hydrogen-Reduction Reaction under Activation Control [23].

Controlling slow step of H^+ discharge is not always the same, but varies with metal, current density, and environment [2].

Activation polarization is a function of the nature and concentration of the species being reduced, surface roughness and composition, and temperature. In addition it is sensitive to traces of reducible impurities in the system [19].

The activation overpotential, and hence the activation energy varies exponentially with the rate of charge transfer per unit area of electrode surface, as defined by the well-known ***Tafel*** equation [4, 16]:

$$\eta^A = a + b \log i \qquad ...(2.2)$$

where a and b are the ***Tafel*** constants which vary with the nature of the electrode process and with the nature of solution.

Thus η^A will be linearly related to log i at overpotentials greater than 0.01 V and the position and slope of the curve will be dependent on the magnitudes of a and b, which are in turn dependent on the equilibrium exchange current density i_o, the transfer coefficient α and the number of electrons z involved in one act of the rate-determining step. The total equation for cathodic process can be expressed in the form

$$\eta_c^A = \frac{RT}{\alpha_c zF} \ln i_o - \frac{RT}{\alpha_c zF} \ln i_c \qquad \ldots (2.3)$$

and since 2.303 RT/F ln x=0.059 log x at 25 °C.

$$\eta_c^A = \frac{0.059}{\alpha_c Z} \log i_o - \frac{0.059}{\alpha_c Z} \log i_c \text{ at } 25\ ^oC \qquad \ldots (2.4)$$

where η_c^A is the activation overpotential of the cathodic process. Similarly the activation over potential of the anodic process is given by [16]:

$$\eta_a^A = \frac{0.059}{\alpha_a Z} \log i_a - \frac{0.059}{\alpha_a z} \log i_o \qquad \text{at } 25\ ^oC \qquad \ldots (2.5)$$

The overpotential is displacement of the potential from its reversible value, i.e.

$$\eta = E_p - E_r \qquad \ldots (2.6)$$

since $E_{p,c} < E_{r,c}$ (more negative)

$$\eta_c = E_{p,c} - E_{r,c} < 0 \qquad \ldots (2.7)$$

hence, the cathode overpotential is always negative. Since $E_{p,a} > E_{r,a}$ (more positive), then

$$\eta_a = E_{p,a} - E_{r,a} > 0 \qquad \ldots (2.8)$$

The anode overpotential is always positive [16].

Eq. (2.2) can be written in the following form [4]:

$$\eta = \pm\beta \log \frac{i}{i_o} \qquad \text{... (2.9)}$$

where β is constant and is frequently termed β-slope or ***Tafel*** constant.

It is generally accepted that the activation polarization is the controlling factor during metal reactions [4, 24].

2.3.2 Concentration Polarization η^c

Concentration polarization refers to electrochemical reactions, which are controlled by the diffusion in the electrolyte. It is the slowing down of a reaction due to an insufficiency of the desired species or an excess of the unwanted species at the electrode. This type of polarization occurs at the cathode when reaction rate or the cathode current is so large that the substance being reduced cannot reach the cathode at a sufficiently rapid rate. Since the rate of reaction is determined by the slowest step, the diffusion rate will be the rate determining step. [17]

Concentration polarization generally predominates when the concentration of the reducible species is a small (e.g., dilute acids, aerated salt solutions). In most instances concentration polarization during metal dissolution is usually small and can be neglected; it is only important during reduction reactions. The hydrogen evolution reaction was considered to illustrate the phenomenon of concentration polarization. As shown in figure 2.9, at low reduction rates the distribution of hydrogen ions in the solution adjacent to the electrode surface is relatively uniform. At very high reduction rates, the region adjacent to the electrode surface will become depleted of ions. If the reduction rate is increased further, a limiting rate will be reached which is determined by the diffusion rate of hydrogen ions to the electrode surface. This limiting rate is the limiting diffusion current density iL. It represents the maximum rate of reduction possible for a given system; the expressing of this parameter is [4]:

$$i_l = \frac{DnFC_B}{\delta} \qquad \text{… (2.10)}$$

Equation (2.10) shows that the limiting diffusion current is a function of the diffusion coefficient, the concentration of the reacting ions in solution, and the thickness of the diffusion layer.

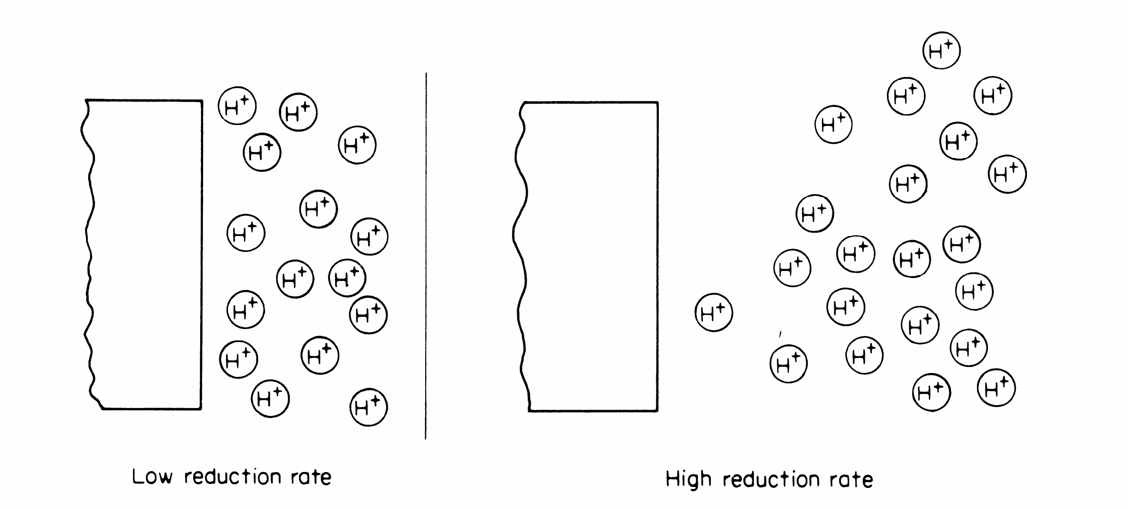

Figure 2-9 Concentration Gradients during Hydrogen Evolution [4].

By combining the laws governing diffusion with ***Nernest*** equation [4]:

$$E = E_o + 2.3\frac{RT}{nF}\log\frac{a_{oxid}}{a_{red}} \qquad \text{... (2.11)}$$

The following expression can be developed [4, 11]

$$E_i - E = \eta^c = \frac{2.303RT}{nF}\log\left(1-\frac{i}{i_l}\right) \qquad \text{… (2.12)}$$

This equation is shown in figure (2.9). For the case of hydrogen evolution, any change in the system which increases the diffusion rate will decrease the effects of concentration polarization and hence increases reaction rate. Thus, increasing the velocity or agitation of the corrosive medium will increase rate only if the cathodic process is controlled by concentration polarization, agitation will have no influence on corrosion rate [4] (Fig.2.7).

2.3.3 Combined Polarization

Both activation and concentration polarization usually occur at an electrode. At low reaction rates activation polarization usually controls, while at higher reaction rates concentration polarization becomes controlling. The total polarization of an electrode is the sum of the contribution of activation polarization and concentration polarization [4]:

$$\eta_T = \eta^A + \eta^c \qquad \text{... (2.13)}$$

During reduction process such as hydrogen evolution or oxygen reduction, concentration polarization is important as the reduction rate approaches the limiting diffusion current density. The overall reaction for activation process is given by [4]:

$$\eta_{red} = -\beta_c \log\frac{i_c}{i_o} + \frac{2.303RT}{nF}\log\left(1-\frac{i}{i_l}\right) \qquad \text{... (2.14)}$$

This case can be shown in fig.2-10 [4].

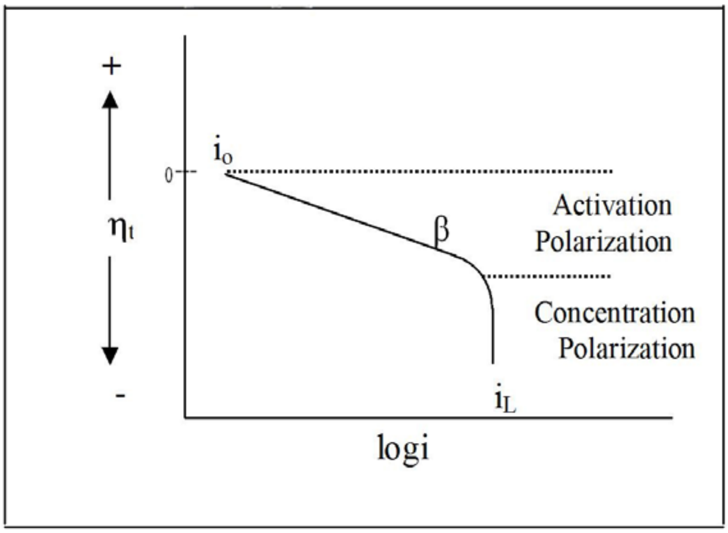

Figure 2-10 Combined Polarization Curves [4].

2.4 Corrosion Inhibitors

2.4.1 Definition

An inhibitor is a substance, which retards or slows down rate of electrochemical reaction. Thus, a corrosion inhibitor is a substance which, when added to an environment, decreases the rate of attack by the environment on a metal.

Corrosion inhibitors are usually added in small amounts to acids, cooling waters, steam, and other environments, either continuously or intermittently to prevent serious corrosion.

The efficiency of an inhibitor is thus expressed by the following equation:

$$\text{Inhibitor efficiency (\%)} = 100\,(CR_{\text{uninhibited}} - CR_{\text{inhibited}}) / CR_{\text{uninhibited}}$$

where $CR_{\text{uninhibited}}$ is the corrosion rate of the uninhibited system, and $CR_{\text{inhibited}}$ is the corrosion rate of the inhibited system [25, 26].

2.4.2 Classification of Corrosion Inhibitors

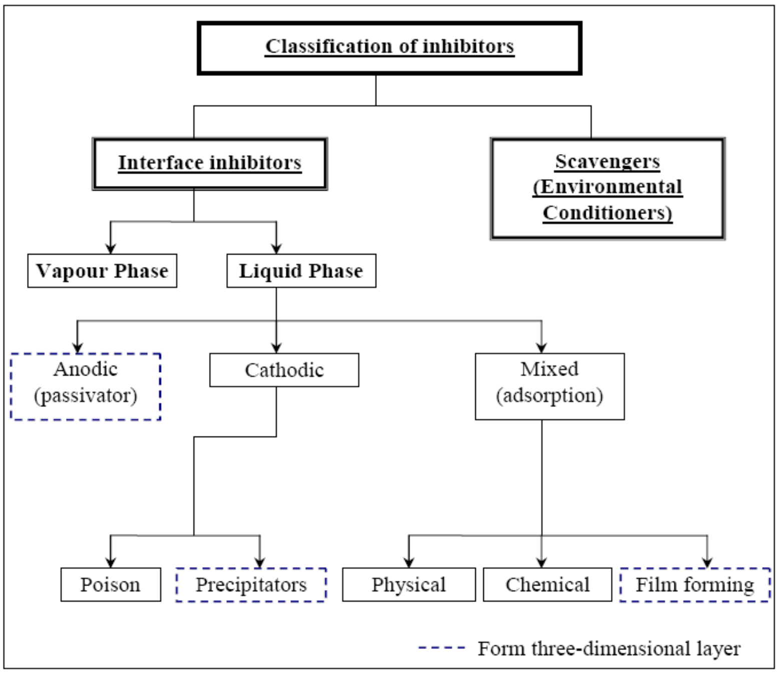

Figure 2-11 Diagram Representation the Classification of Inhibitors [27].

Inhibitors have been classified differently by various authors. Some authors, for example, prefer to group inhibitors by their chemical functionality. However, by far the most popular organization scheme consists in regrouping corrosion inhibitors in a functionality scheme as follows [28]:

- Passivating inhibitors.
- Organic inhibitors.
- Precipitation inhibitors.
- Volatile corrosion inhibitors.
- Cathodic inhibitors.
- Anodic inhibitors.
- Mixed inhibitors.

The range of inhibitors is wide and a way to classify them is to consider their mechanism action and their composition:

- Adsorption type inhibitors.
- Hydrogen-evolution poisons.
- Scavengers.
- Oxidizers.
- Vapor-phase inhibitors.

2.5 Adsorption Type Inhibitors

The largest class comprises the adsorption-type inhibitors (or interface inhibitors). They are usually organic compounds and are adsorbed on the surface of the metal. In this way, the metal dissolution and the reduction reaction are suppressed. Inhibitors act on both the anodic and cathodic processes, but usually with an unequal effect. Typical of this class of inhibitors are the organic amines [4].

The use of inhibitors to protect metals from corrosion is, often associated with chemical adsorption, involving a variation in the charge of the adsorbed substance and a transfer of charge from phase to the other. Therefore, the molecular structure of the inhibitors has special significance. The electron density at atoms of functional groups constituting a reaction center affects the strength of the adsorption bond. In addition the strength of the bond also depends on the properties of the metals. As well as on the polarizability of the functional group. Most organic inhibitors contain at least one polar group with an atom of nitrogen, sulfure, oxygen, or in some cases selenium or phosphorus. Comprehensive studies carried out by Hackerman and his co-workers, which formed the basis for an adsorption theory of organic inhibitors. According to this theory, the inhibiting properties of many compounds are determined by the electron density at the atom constituting the main reaction center. With an increase in the electron density at the reaction center, the chemisorption bonds between the inhibitor and the metal are strengthened [29].

Adsorption type inhibitors may obey one of the following isotherms:

i. The Langmuir Isotherm:

The model for the Langmuir isotherm is a set of uniform adsorption sites and many cases of strong adsorption do not fit this isotherm [30]. Mathematically, this isotherm is given as:

$$\log [\theta/1-\theta]=\log A+ \log C+q/2.303\ RT \qquad \text{... (2.15)}$$

where:

A = Constant for a given system.

This isotherm is usually plotted as log $[\theta/1-\theta]$ against log C [31].

A correlation between θ and C, the concentration of inhibitor in the electrolyte, can be achieved with Langmuir adsorption isotherm expressed mathematically as follows:

$$\theta=KC/(1+KC) \qquad \ldots (2.16)$$

or

$$C/\theta=1/K+C \qquad \ldots (2.17)$$

where:

K = is the adsorption constant [32].

ii. The Freundlich Isotherm [33]:

This isotherm is expressed as:

$$\theta=K\,C^{n} \qquad \ldots (2.18)$$

where, K and n are constant for a given system at a given temperature.

This isotherm can be written as:

$$\mathrm{Log}\,\theta=\log K+n\log C \qquad \ldots (2.19)$$

And is usually plotted as log θ against log C.

iii. The Temkin Isotherm [34]:

This isotherm is expressed mathematically as:

$$\theta=RT/q_{o}\alpha \ln(A_{o}C) \qquad \ldots (2.20)$$

Where

$$q_{o}=q/1-\theta \qquad \ldots (2.21)$$

α and A_o are constants for a given system at constant temperature.

This isotherm is usually plotted as θ versus log C.

2.6 Thiourea Inhibitor

Sulphur bearing organic compounds, such as thiourea, are good corrosion inhibitors for steel under acidic conditions, because sulphur atom is easily protonated in acidic solution and a stronger electron donor than nitrogen. Therefore sulfur atom is more strongly adsorbed to the metal surface. Moreover, the adsorption mainly depends on the presence of π-electrons and heteroatom, which induce greater adsorption of the inhibitor molecules onto the surface of the metal [35, 36].

All thiourea derivatives suppressed H_2 pickup by blocking the active sites on the steel surface [37].

Kuznetzov studied the mechanism of action of inhibitors considers that most chemical reactions can be treated as acid-base interactions. Based on this concept, thiourea would act as a rather strong base due to its sulphur, which serves as an electron donor. On the other hand, Fe^{3+}, Fe^{2+} and metallic Fe would behave like acids. Herein, they act as electron acceptors, with higher acidity corresponding to higher oxidation state. This interaction with the inhibitor would proceed mainly due to the presence of long-range electrostatic forces [38].

2.7 Formaldehyde Inhibitor

Formaldehyde (CH_2O) is a simple organic chemical made of hydrogen, oxygen and carbon. is also known as formalin, embalming fluid, or formol, is a colorless gas with a pungent odor were used in the manufacture of melamine and it is considered as a preservative and a disinfectant and it is also used as a corrosion inhibitor (adsorption type inhibitor). The family of formaldehyde chemicals is used in pressed wood products, urea-formaldehyde (UF) foam insulation, embalming fluids, carpets, combustion appliances, clothing, tobacco, and other uses. It is soluble in ethanol, ether, acetone and water forming in the latter methylene glycol and low molecular mass poly(oxymethylene)glycols $HO(CH_2O)nH$ (n = 1-8). It has a measured vapor pressure of 220 kPa at 0°C [39, 40, 41, and 42].

2.8 Organic Amine Inhibitors

These are nitrogen-bearing organic compounds, which demonstrated inhibitive action against corrosion processes. Their inhibition efficiency is determined, basically, by comparing the extent of corrosion in their presence and in their absence. The properties of corrosion inhibitors which were used are presented in table B-1 in appendix B [13].

2.8.1 Inhibition Mechanisms

Although different inhibition mechanisms have been identified (either directly or by studying their effect) for inhibitors in general, several of these mechanisms could occur simultaneously. These mechanisms can be broadly classified into two main types, Interface Inhibition and Interphase Inhibition [43].

Interface Inhibition: In this type of inhibition, the inhibitor is directly adsorbed on the metal surface, forming a thin two-dimensional (2-D) film [44]. This type can be further subdivided into non-selective and selective physisorption and chemisorption. In non-selective physisorption, which is also called geometrical blocking or screening the adsorption, is rapid and reversible, and the inhibitor that is indifferent to the nature of the adsorbent interacts with the surface via Van der Waal or electrostatic forces that lead to a relatively high degree of coverage [44, 45]. Selective physisorption, also called deactivating coverage, involves selective blockage of active sites at the metal surface by an indifferent inhibitor at relatively low coverages [44, 46]. Chemisorption, also called reactive coverage, is characterized by a specific and slow adsorption that is not completely reversible and involves charge sharing or transfer [43, 45, and 46].

Interphase Inhibition: A three-dimensional (3-D) layer emerges on the metal surface resulting from, for example, the chemical reaction of an inhibitor with corrosion products to form organometallic complexes [44, 47].

2.8.2 Factors Influencing Inhibitor Efficiency

Several structural and chemical factors determine the effectiveness of an inhibitor. For organic amines as inhibitors the following characteristics were identified.

- If chemisorption is involved in the inhibition process its contribution to the inhibition efficiency will increase as the electronic density or electron donation ability of the reaction center, nitrogen, increases [48].
- An increase in the carbon chain length of an amine inhibitor will enhance the inhibition efficiency [49]. This could be attributed to an increase in the electronic density at nitrogen due to inductive effects, an increase in the coverage ability, hydrophobicity, and polarizability and a decrease in the solubility of the inhibitor [43, 49, and 50].
- Inhibition efficiency will be affected by the degree of overlap between the inhibitor molecular orbital and the metal d-orbital, and the ability of the inhibitor to complex with the metal itself or the corrosion products [51, 52, and 53].
- The formation of a compact layer, [52] e.g. cross-linking, enhances inhibitor performance.

2.9 Literature Review

The corrosion of metals remains a world-wide scientific problem as it affects the metallurgical, chemical and oil-industries. The increasing interest in the manufacture of hydrochloric acid has created the need for obtaining information on the corrosion resistance of mild steel to hydrochloric acid attack. Of particular importance also is the need to introduce certain organic compounds as inhibitors into the mild steel – corrodent system to prevent corrosion of the mild steel. Mild steel corrosion in acid solution has been effectively controlled by the use of organic substances containing nitrogen, oxygen, or sulphur in the conjugated system as inhibitors. The corrosion of mild steel in HCl solution is a heterogeneous one, comprising of anodic and cathodic reactions [54].

Most corrosion reactions are electrochemical. An example illustrating the electrochemical nature of corrosion is the attack of iron, which is the most commonly, used industrial metal, in hydrochloric acid. The reaction is:

$$Fe + 2HCl \longrightarrow Fe\,Cl_2 + H_2 \qquad \ldots (2.22)$$

Noting that the chloride ion is not involved in the reaction, this equation can be written in the simplified form: -

$$Fe + 2H^+ \longrightarrow Fe^{2+} + 2e \qquad \ldots. (2.23)$$

Equation (2. 23) can be conveniently divided into two reactions:

Oxidation (anodic reaction): $Fe \longrightarrow Fe^{2+} + 2e$

Reduction (cathodic reaction): $2H^+ + 2e \longrightarrow H_2$

Both the oxidation reaction and the reduction reaction proceed at the same rate during electrochemical corrosion. Any changes in the system, which affect the rate of one, must of necessity affect the other. Thus, attempts at reducing corrosion rate may be directed toward changing either local oxidation or local reduction rate [55].

Soror, et al. (1999) [56] studied the corrosion inhibition of carbon steel in 5% hydrochloric acid (HCl) solution by two organic inhibitors [N, N'-dibenzyl ethane diammonium chloride (I) Cl-ph- CH_2-NH_2- $(CH_2)_2$-NH_2-CH_2ph-CL and dibenzyl butane diammonium chloride (II) Cl-ph- CH_2-NH_2-$(CH_2)_4$-NH_2-CH_2ph-Cl] at the temperature range of 30- 90°C . The objective of that study was to study the inhibition effect of two cationic surfactants as corrosion inhibitors for carbon steel in HCl media through weight loss method, open circuit potential, and linear polarization technique, they found that

- The dissolution of carbon steel in 5% HC1 in the temperature range 30-90°C was inhibited by two organic compounds (I) and (II).
- The best results, even at higher temperatures were obtained for (II). This is due to the chain length in compound II.
- The inhibitors I and II were able to inhibit the corrosion even at higher acid strength (5~10%).
- The electrochemical studies for the influence of organic compounds on the corrosion behavior of the steel showed that the polarization resistance *(R_p)* values increased with an increase in the concentration of the inhibitor, also the corrosion current decreased and higher inhibition efficiency was obtained.
- The compounds acted through a chemisorption mechanism. However the Cl^- ions produced as a result of the dissociation of organic cation salt in acid media were adsorbed onto the surface and decreased the positive charge of the carbon steel facilitating the adsorption of organic cations.

- The two compounds I and II were shown to be efficient inhibitors for the corrosion of carbon steel in acid pickling and cleaning operations.

Bentiss, et al. (1999) [57] studied the corrosion of mild steel in acid baths (1M HCl and 0.5 M H_2SO_4) by various corrosion monitoring techniques, such as corrosion weight loss tests and electrochemical impedance spectroscopy. The aim of that paper was to study the inhibition action of a new organic compound containing nitrogen, sulfur and aromatic rings, which was namely, 3,5-bis(2-thienyl)-4-amino-1,2,4-triazoles (2-TAT). They had found that the electrochemical study reveals that this compound is an anodic inhibitor. Changes in impedance parameters (R_{ct} and C_{dl}) are indicative of the adsorption of 2-TAT on the metal surface, leading to the formation of a protective film which grows with increasing exposure time. 2-TAT is able to reduce the steel corrosion more effectively in 1M HCl than in 0.5M H_2SO_4. The adsorption of this inhibitor is also found to obey the Langmuir adsorption isotherm in both acids. 2-TAT is considered as a non-cytotoxic substance.

Harek and Larabi (2004) [58] studied the inhibition effect of oxalic N-phenylhydrazideN-phenylthiosemicarbazide (OPHPT) for the corrosion inhibition of mild steel in 1 mol dm^{-3} HCl by mass loss, potentiodynamic and polarization resistance measurements. They had found that the inhibiting effect of OPHPT increases with increase of inhibitor concentration and attains approximately 93 % at 5×10^{-4} mol dm^{-3} and 55°C, and results showed that the rate of corrosion of mild steel increased with increasing temperature over the range 25 – 55°C, both, in the presence of inhibitor and in its absence. It was also found that, the presence of inhibitor in the solution induces an increase of the activation energy of the corrosion process. And also found that the inhibition is due to adsorption of the inhibitor molecules on the steel surface according to the *Langmuir and Temkin adsorption isotherms.* The substance is adsorbed through the S-atom which is the adsorption center. Polarization curves indicate that OPHPT acts as a mixed type inhibitor. The corresponding results suggest that the presence of iodide ions in the solution stabilized the adsorption of OPHPT molecules on the metal surface and, therefore, improved the inhibition efficiency of OPHPT.

Sorkhabi1, et al. (2006) [59] studied the inhibition of steel corrosion in hydrochloric acid solution by juice of Prunus cerasus, two electrochemical measurements was used to evaluate the inhibition efficiencies, linear polarization and electrochemical impedance spectroscopy. This inhibitor contains different organic compounds such as proteins, organic acids (such as ascorbic acid), vitamins, lipids, carbohydrates, pigments, and some inorganic ions which some of these organic compounds have been used as organic corrosion inhibitors for metals. The aim of that study was to investigate the inhibition effect of Prunus cerasus juice as a cheap, raw and non-toxic corrosion inhibitor on steel corrosion in hydrochloric acid. Results obtained from both electrochemical methods showed that the *Prunus cerasus* juice acts as an inhibitor for corrosion of steel in hydrochloric acid media. Corrosion inhibition action of *Prunus cerasus* juice increased as its concentration increases. Inhibition of steel in HCl solution by *Prunus cerasus* juice is attributed to adsorption of the phytochemical compounds in this juice. The authors reasoned the reduction of corrosion inhibition efficiencies by increasing the temperature, may be due to thermal degradation of its organic content especially degradation of anthocyanine pigments.

Jeyaprabha, et al. (2006) [60] studied the inhibition effect of halide ions such as iodide, bromide and chloride ions on the corrosion of iron in 0.5 mol L^{-1} H_2SO_4 and the adsorption behaviour of these ions on the electrode surface by using polarization and impedance methods. The authors reported that, the aggressive anions like Cl^-, Br^- and I^- are found to catalyze the iron dissolution reaction in higher concentrations. But some studies have shown that halide ions in lower concentrations inhibit the corrosion of iron in sulphuric acid. They found that the inhibition of nearly 90% was observed for iodide ions at $2.5 * 10^{-3}$ mol L^{-1}, for bromide ions at $10 * 10^{-3}$ mol L^{-1} and 80% for chloride ions at $5 * 10^{-3}$ mol L^{-1}. The inhibition effect is increased with increase of halide ions concentration in the case of I^- and Br^- ions, whereas it has decreased in the case of Cl^- ion at concentrations higher than $5 * 10^{-3}$ mol L^{-1}.

Cathodic polarization studies on the effect of addition of chloride and iodide ions on iron dissolution in H_2SO_4 solutions have revealed that the adsorbed halide ions inhibit the hydrogen evolution reaction predominantly. The mechanism of inhibition of iron dissolution in sulphuric acid solution by halide ions is mainly due to blocking of surface by adsorption [61, 62].

The authors concluded that the halide ions are found to inhibit the corrosion of iron in 0.5 mol L^{-1} H_2SO_4 to the extent of 80 to 90% at concentrations less than $5 * 10^{-3}$ mol L^{-1}. The order of inhibition is $I^- > Br^- > Cl^-$. The inhibition of halide ions is mainly due to adsorption on iron surface at the corrosion potential.

Shetty, et al. (2006) [63] studied the inhibiting effect of *N*-furfuryl-*N'*-phenyl thiourea (FPTU) on the corrosion of mild steel in aqueous solutions of 0.05 and 0.1M HCl, as well as 0.025 and 0.05M H_2SO_4 was investigated using the potentiodynamic polarization technique. very high inhibition efficiency was evidenced in both acid solutions and it was found to vary with the concentration of the inhibitor and temperature, where from the results, the inhibition efficiency (IE) increases with increasing concentration of inhibitor and decreasing the temperature, and decreases for all temperatures with concentration above $3*10^{-4}$ mol.L^{-1}.

They had found also that:

- FPTU acts as an efficient anodic inhibitor for the corrosion of mild steel in both HCl and H_2SO_4 acid solutions.
- FPTU inhibits the corrosion of mild steel by adsorption on the metal surface.
- The inhibitive ability of FPTU in reducing corrosion loss of mild steel in HCl is comparatively higher than in H_2SO_4 medium.
- FPTU forms a chemisorbed film on the mild steel surface in HCl medium, whereas in H_2SO_4, the inhibition is governed by the physisorption or mixed adsorption mechanism.

Olorunniwo, et al. (2006) [64] presents the investigation of sodium chromate and diethylene amine as inhibitors of corrosion of a mild steel in cassava fluid. The inhibition study was carried out using the weight loss immersion technique. The inhibitive potentials of the two inhibitors was evaluated based on a determination of the corrosion rates in the presence and absence of the inhibitors, determination of the pH of various cassava fluids and a calculation of the inhibition efficiencies of the two inhibitors at different levels of concentrations. The results of that study showed that diethylene amine is a much better inhibitor of the corrosion of mild steel in cassava fluid than sodium chromate. The inhibition efficiencies by diethylene amine are higher than 85% for the 0.5, 1.0 and 1.5 M concentrations investigated. In the case of sodium chromate, inhibition efficiencies only become significant for 1.0 M and 1.5 M concentrations. Generally, the pH of all cassava fluid with and without inhibitors increased with duration of exposure and the corrosion rates of the mild steel decreased with increase in the pH of the cassava fluid.

James, et al. (2007) [54] studied the action of *Pyridoxal hydrochloric* (PXA) and *Pyridoxol hydrochloride* (PXO) inhibitors on the corrosion of mild steel in 2M HCl solution using weight loss and gasometry methods. The objective of that study was to explore the inhibitory properties of PXA and PXO on mild steel in HCl solution. They found, from weight loss measurements, that PXO inhibits corrosion processes more strongly than PXA, where the inhibition efficiency increases with increasing concentration of the inhibitor and decreasing temperature of the HCl-inhibitor systems and reaches a maximum value which depends on the inhibitor for example, at the 0.01 M inhibitor concentration, values of 71.9% and 58.2% were obtained for PXO and PXA respectively. In addition, they concluded that the difference in the inhibitory properties of the two inhibitors was closely related to the difference in the availability of electrons in the molecules of the inhibitors.

Abderrahim, et al. (2007) [65] studied the inhibition effect of Pyrazolo [3, 4-b] Pyridine on corrosion of stainless steel in 1M HCl solutions. Most of the well known acid inhibitors to inhibit the corrosion of stainless steel are organic compounds containing N and O atoms, where a Pyrazolo [3-4-b] pyridine have been chosen as good organic inhibitor. From electrochemical impedance spectroscopy (EIS) measurements, it is found that, as the inhibitor concentration increases, the charge transfer resistance (R_{ct}) increases, but the double layer capacitance (C_{dl}) values tend to decrease, the decrease in the C_{dl} values is due to the adsorption of inhibitor on the metal surface. From weight loss measurements, it is clear that the inhibition efficiency increased with increasing inhibitor concentration. The electrochemical parameters determined from the polarization curves have been shown that the values of corrosion current density (I_{corr}) of stainless steel in the inhibited solutions were smaller than those for the inhibitor free solution. It was found that the adsorption of inhibitor could prevent steel weight loss and the adsorption accorded with the *Langmuir adsorption*, the corrosion protection was explained by the adsorption of inhibitor and formation of a protective layer attached to the metal surface.

Arora, et al. (2007) [66] studied the corrosion inhibition of aluminium by *Capparis decidua* in acidic media (HCl and H_2SO_4 solutions) by using weight loss tests and electrochemical technique. Organic compounds containing nitrogen have been found to function as very effective corrosion inhibitors. The efficiency of these compounds as corrosion inhibitors can be attributed to the number of mobile electron pair present, the orbital character of free electrons and electron density around the nitrogen atoms. In this study, the inhibitive effects have been evaluated of ethanolic extract of fruit, stem bark and root bark of *Capparis decidua*. This inhibitor has better inhibition efficiencies in HCl solution than in H_2SO_4 solution.

The inhibition efficiency (IE %) calculated from the mass loss measurement for hydrochloric acid and sulphuric acid in the presence of the inhibitor are given in tables. It is observed that the inhibition efficiency increases with increase in the concentration of inhibitor and decreases with increases in acid strength. The corrosion rate decreases with increases in concentration of inhibitor. The maximum effeciency was obtained in low acid concentration.

From this study, the following conclusions can be drawn:

- The rate of corrosion of mild steel and aluminum in hydrochloric acid and sulphuric acid is a function of the concentration of *Capparis decidua*.
- The inhibition increases with increased additive concentration.
- *Capparis decidua* ethanolic extract is a corrosion inhibitor and can replace toxic chemicals.

Atul Kumar (2007) [67] studied the effect of sodium lauryl sulfate (SLS), a surfactant on corrosion of mild steel in 1M hydrochloric acid by using three techniques: weight loss, electrochemical polarization and metallurgical research microscopy. Results obtained reveal that SLS is good inhibitor and shows very good corrosion inhibition efficiency (IE). And he had found that the (IE) of SLS increases with increase in concentration of this inhibitor, and from weight loss measurements, the IE increases with temperature up to 35ºC and after that it decreases at higher temperature due to desorption of inhibitor. Corrosion inhibition of mild steel in 1M HCl solutions by SLS is under anodic control, this revealed by electrochemical polarization result.

Srisuwan, et al. (2008) [68] studied the variation of carbon steel corrosion rate in the presence of an inhibitive formulation, which was composed of fatty amines (FA) in association with phosphonocarboxylic acid salts (PCAS), which was evaluated from impedance data and polarization curves for different electrode rotation rates. The corrosive medium was a 200 mg L^{-1} NaCl solution (reagent grade) in contact with air maintained at 25ºC. It was shown that PCAS acts as anodic inhibitors whereas a mixed action was seen for FA. A synergistic effect was observed for the mixture containing 200 mg L^{-1} PCAS + 50 mg L^{-1} FA. X-ray photoelectron spectroscopy revealed that the inhibitive film was composed of an iron oxide/hydroxide mixture incorporating the organic molecules.

It was shown from the impedance results that the variation of I_{corr} was non-monotonic. This behaviour was explained by taking into account both the steady-state results and the presence of the two layers on the electrode surface and was attributed to the variation of the ratio between the two layers, which each have different intrinsic protective properties. From the polarization curves plotted under the same conditions, the non-monotonic variation was not shown. Independently of the electrode rotation rate, the corrosion current densities remained low. A similar study with only the PCAS compound could be considered because it was seen that PCAS only has an anodic action and thus it might be responsible for the variation observed in I_{corr}.

Abida Begum**,** et al. (2008) [69] studied the enhancement of the inhibitor efficiency of atropine methochloride (amci) in corrosion control of mild steel in sulphuric acid. The inhibition efficiency and synergistic behavior of 10^{-4} M (amci) was carried out using mass loss and polarization methods in the presence of (i) metal ions, Ni^{2+} and Cu^{2+} between 10^{-2}M to 10^{-6}M concentrations, (ii) different concentrations of metal ions and 10^{-3}M I^{-}, 10^{-3}M Cl^{-} and 10^{-3}M Br^{-} solutions and (iii) different metal ions, 10^{-3}M I^{-} and at three different temperatures.

The investigations of the study of **“**Synergistic effect of metal ions and halides on corrosion inhibition of mild steel in the presence of atropine methochloride in acidic medium” reveal that;

- As the concentration of AMCI increased, the inhibition efficiency (IE) also increased, which was maximum at 10^{-2} M in 5 hours of immersion period.
- Halide ions decreased the corrosion rate of mild steel in sulphuric acid. A steady decrease in corrosion rate is observed by increasing the concentration of iodide, chloride and bromide ions. The decrease is maximum with iodide ions. Enhancement of inhibition efficiency (IE) of 10^{-4}M AMCI in the presence of different cations with 10^{-3}M iodide ion and at higher temperature was found to be maximum.
- As the temperature increased from 298K to 308K, the inhibition efficiency gradually decreased. The inhibitor was found to be effective up to 303K.

Saliyan and Adhikari (2008) [70] studied the inhibition effect of a N′-benzylidene-3-(quinolin-4 ylthio) propanohydrazide (DHBTPH) as a corrosion inhibitor for mild steel in HCl (1 M, 2 M) and H_2SO_4 (0·5 M, 1 M) solutions using weight-loss method, electrochemical impedance spectroscopy (EIS) and potentiodynamic polarization methods. They had found that:

- The inhibition efficiency in different acid media was found to be in the decreasing order 0·5 M H_2SO_4 > 1 M HCl > 1 M H_2SO_4 > 2 M HCl.
- Reasonably good agreement was observed between the data obtained from the weight loss, electrochemical impedance spectroscopy and potentiodynamic polarization techniques.

- DHBTPH suppressed the anodic reaction to greater extents than the cathodic one; these observations suggest that DHBTPH behaves mainly as anodic inhibitor in the studied acid.
- The inhibition efficiency increases with increasing inhibitor concentration and with increasing temperature.
- The thermodynamic parameters reveal that the inhibition of corrosion by DHBTPH is due to the formation of a chemisorbed film on the metal surface.
- Adsorption of DHBTPH was found to follow the Langmuir's adsorption isotherm.

Elewady (2008) [71] studied the inhibition effect of 4,6-Dimethylpyrimidine-2-amine(I),N-Benzylidene-4,6-dimethylpyrimidine-2-amine(II) and 2-[(3,6-Dimethylpyridimine-2-ylimino)methyl]-4-nitrophenol(III) on the corrosion of carbon-steel (C-steel) in 2M HCl solution using electrochemical impedance spectroscopy (EIS) and weight loss techniques. All the examined pyramiding derivatives are effective corrosion inhibitors for C-steel in 2M HCl solution.

Double layer capacitance (C_{dl}), and charge transfer resistance (R_{ct}), values were derived from Nyquist and Bode plots obtained from A.C. impedance studies. Changes in impedance parameters are indicative of the adsorption of these inhibitors on the iron surface. He found that the inhibition efficiency mainly depends on the nature of the investigated compounds. And also observed from the weight loss measurements that the order of inhibition efficiency for the used inhibitors is II > III > I which is in good agreement with those obtained from EIS technique. The investigated compounds inhibit corrosion by adsorption mechanism and the adsorption of these compounds on the C-steel surface was found to obey Langmuir adsorption isotherm.

Abdallah, et. al. (2008) [72] studied the inhibitive action of some newly prepared mono azo dye compounds toward the corrosion of C-steel in 2M hydrochloric acid solution using weight loss, and galvanostatic polarization techniques. Moreover, the effect of temperature on the dissolution of carbon steel, as well as, on the inhibition efficiency of the studied compounds was also investigated and some thermodynamic parameters were computed.
They had found that:

- The inhibition efficiency was found to increase with increasing inhibitor concentration (or increasing the electron donor characteristic of the substituted groups) and decreasing temperatures.
- The inhibition action of these compounds is attributed to adsorption of stable insoluble complex on the metal surface.
- The adsorption of azo dye compounds on the carbon steel surface at different temperature was found to obey the Langmuir adsorption isotherm.
- The stiochiometry of the expected Fe-azo dye compounds complexes was estimated by conductometric titration.

CHAPTER THREE

Experimental Work

The inhibitive action of Formaldehyde, Thiourea, Ethylene diamine and Diethanol amine as adsorption type inhibitors on the corrosion behavior of carbon steel in 0.1 N HCl aerated acid solutions, for temperature 35, 45, 60°C and 500, 1000 and 2000 ppm inhibitor concentration, was investigated using weight loss measurements in free corrosion system at a range of rotating speeds for specimens of 0, 400, 700, 1000 and 1400 rpm.

3.1 The Electrolyte

The electrolyte is composed of:

- The corrosive solution used in this work was hydrochloric acid of concentration 37%, supplied by *Rayon State Establishment, Saddat AL-Hindiyah*, which has a molecular weight of 36.64 g/gmol and density of 1180 gm/cm^3.The concentrated acid was diluted by distilled water to obtain the required normality of 0.1 N HCl.
- The inhibitors used were Formaldehyde, Thiourea, Ethylene diamine and Diethanol amine.
- Distilled Water.

3.2 Solvents Used

These were used to clean the metal specimens.

- Acetone**:** C_3H_6O of concentration ≅ 99% supplied by FLUKA.
- Ethanol **:** C_2H_4O of concentration ≅ 99% supplied by FLUKA

3.3 Apparatus

- Thermometers**:** They are made of glass to measure temperature up to 100°C.
- PH-meter**:** A digital pH-meter, type CHEMTRIX, was used to measure and monitor the PH of the working solution during the test run. The pH-meter was calibrated using buffer solutions of pH 4, 7, and 9.
- Water bath**:** Water bath with temperature controller was used, type Gkeenfield.NR.Oldha. Voltage=200/20, power = 1000 Watt.
- Electronic Balance**:** High accuracy digital balance with 4 decimal points of type (METTLER AE260) was used for weight loss determination. The balance has 0.1 mg accuracy.
- Desiccator**.**
- Motor for rotating the specimens**.**
- Beakers (2and 3 liters)**.**
- Teflon rod**.**
- Teflon washers and Teflon cap.

The details of the rotating holder are shown in figure 3.1:

(1)Motor for rotating the specimens (2) Teflon rod (3) cylindrical specimen (4) Teflon washer (5) Teflon cap (6) Beaker (7) Water bath (8) Stand to hold the motor (9) Thermometer.

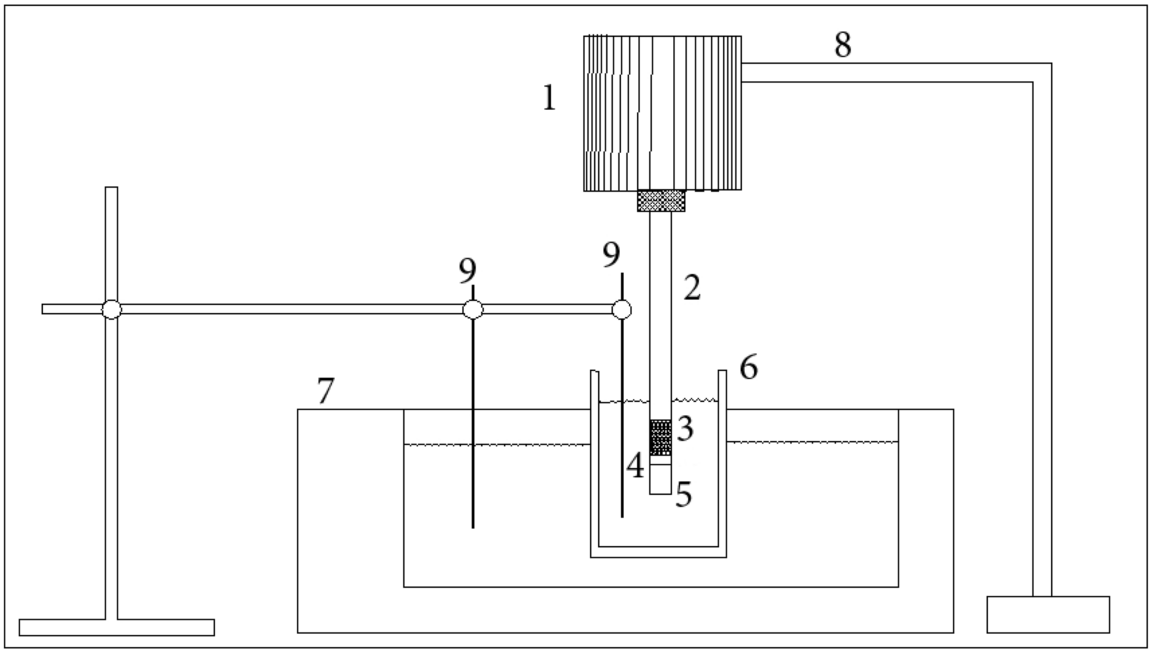

Fig 3-1 Simple Sketch Showing the Details of the Rotating Holder.

Fig 3-2 System Used for the Weight Loss Technique.

3.4 Materials

Carbon steel (CS) pipe was used as a working electrode in a cylindrical shape for weight loss measurements with a length of 30 mm, outside diameter of 25 mm and inside diameter of 20 mm.

The carbon steel was analyzed by the *Specialized Institute of Engineering Industries* as follows:

Table 3-1 Composition of the Studied Carbon Steel Specimen.

Element	C	Mn	P	S	Fe
Weight (%)	0.1649	0.5027	0.0020	0.0068	Rest

3.5 Weight Loss Measurements

Cylindrical specimens of area $\pi * 0.025 * 0.03$ m^2 and wall thickness of 0.005 m were immersed in a solution of HCl of a strength 0.1N. In order to assess the corrosion rates by weight loss technique, before each experimental run, the metal specimen was washed by tap water followed by distilled water, dried with clean tissue, immersed in analar ethanol for 5 minutes, rinsed with clean acetone and dried with clean tissue. The specimens were then stored in a desiccator over highly active silica gel for 1.5 hour before use, and then they were weighed and directly exposed to the corrosion environment [4, 73,74 and 75]. For these measurements the metal samples were completely immersed in 2 liters corrosive solution contained in 2.5 liters volume beaker. They were exposed for period of 2 hours at specified temperature, concentration of inhibitor and rotational velocity.

After the exposure to the corrosion environment, the specimen was washed by tap water then brushed by smooth brush under running tap water to remove non-adherent corrosion products. After that the specimen was washed by tap water, distilled water, dried with clean tissue, and kept in desiccator for 1.5h, and then weighed [4, 76, and 77]. Each run was repeated twice with a third run when reproducibility was in doubt. The above procedure was repeated for a specimen in absence and presence of inhibitor for the whole investigated range of rotational velocity and temperature.

CHAPTER FOUR

Results and Interpretations

Tables 4-1 through 4-45 show the values of experimental results for the whole investigated range of velocity (or Re), temperature, and inhibitors concentration.

Tables 4-1 through 4-3 show the experimental results for corrosion rate without inhibitor at 35, 45, and 60°C. It is clear from these tables that corrosion rate increases with increasing Re at constant temperature.

Table 4-1 Results of Corrosion Rate at 35°C without Inhibitor.

U(rpm)	Re	CR(gmd)	CR(mm/y)
0	static	175.7504	8.15025
400	5729	201.3369	9.3368
700	10025.78	232.3151	10.7734
1000	14322.55	270.8047	12.5583
1400	20051.58	377.1662	17.4907

Table 4-2 Results of Corrosion Rate at 45°C without Inhibitor.

U(rpm)	Re	CR(gmd)	CR(mm/y)
0	static	239.4582	11.1046
400	6887.8	327.5282	15.1888
700	12053.77	377.4623	17.5044
1000	17219.67	412.68	19.1376
1400	24107.54	566.2837	26.2608

Table 4-3 Results of Corrosion Rate at 60°C without Inhibitor.

U(rpm)	Re	CR(gmd)	CR(mm/y)
0	static	476.7006	22.1065
400	8734.89	874.3937	40.5491
700	15286.07	1074.715	49.8388
1000	21837.24	1190.9536	55.2293
1400	30572.139	1211.5137	56.1827

Tables 4-4 through 4-12 show the experimental results of corrosion rate in the presence of formaldehyde, ethylene diamine, and diethanol amine inhibitors at concentration of 500, 1000, and 2000 ppm respectively and a temperature of 35°C. It is clear that corrosion rate decreases with increasing the concentration of these inhibitors for the whole range of rotational velocity. It is also observed that the inhibition efficiency increases with increasing the concentration of inhibitors. But this increase is not so pronounced.

Table 4-4 Formaldehyde Inhibitor at 35°C and 500 ppm.

U(rpm)	Re	CR without Inhibitor(gmd)	CR with Inhibitor(gmd)	CR(mm/y)	η %
0	static	175.7504	110.5042	5.1242	37.12
400	5729	201.3369	167.7942	7.4075	16.66
700	10025.78	232.3151	214.1788	9.9323	7.81
1000	14322.55	270.8047	251.2797	11.3161	7.21
1400	20051.58	377.1662	365.0408	16.9284	3.21

Table 4-5 Formaldehyde Inhibitor at 35°C and 1000 ppm.

U(rpm)	Re	CR without Inhibitor(gmd)	CR with Inhibitor(gmd)	CR(mm/y)	η %
0	static	175.7504	104.5042	4.8463	40.54
400	5729	201.3369	132.7414	7.0522	34.47
700	10025.78	232.3151	171.2407	7.9411	26.3
1000	14322.55	270.8047	223.5785	10.3682	17.44
1400	20051.58	377.1662	357.9641	16.6002	5.09

Table 4-6 Formaldehyde Inhibitor at 35°C and 2000 ppm.

U(rpm)	Re	CR without Inhibitor(gmd)	CR with Inhibitor(gmd)	CR(mm/y)	η %
0	static	175.7504	70.8098	3.2837	59.71
400	5729	201.3369	101.5745	4.71	49.55
700	10025.78	232.3151	131.5833	6.102	43.36
1000	14322.55	270.8047	184.739	8.567	31.78
1400	20051.58	377.1662	268.4292	12.448	28.83

Table 4-7 Ethylene diamine Inhibitor at 35°C and 500 ppm.

U(rpm)	Re	CR without Inhibitor(gmd)	CR with Inhibitor(gmd)	CR(mm/y)	η %
0	static	175.7504	73.077	3.3889	58.42
400	5729	201.3369	121.3659	8.8094	39.72
700	10025.78	232.3151	189.964	8.9176	18.23
1000	14322.55	270.8047	229.8049	10.4062	15.14
1400	20051.58	377.1662	322.8543	13.0495	14.4

Table 4-8 Ethylene diamine Inhibitor at 35°C and 1000 ppm.

U(rpm)	Re	CR without Inhibitor(gmd)	CR with Inhibitor(gmd)	CR(mm/y)	η %
0	static	175.7504	59.509	2.7597	66.14
400	5729	201.3369	102.9656	4.775	48.85
700	10025.78	232.3151	151.2604	7.0145	34.89
1000	14322.55	270.8047	189.2243	8.7751	30.13
1400	20051.58	377.1662	269.5229	12.498	28.54

Table 4-9 Ethylene diamine Inhibitor at 35°C and 2000 ppm.

U(rpm)	Re	CR without Inhibitor(gmd)	CR with Inhibitor(gmd)	CR(mm/y)	η %
0	static	175.7504	42.76	1.983	75.67
400	5729	201.3369	89.4338	4.1474	55.58
700	10025.78	232.3151	107.376	4.9795	53.78
1000	14322.55	270.8047	141.6309	6.567	47.7
1400	20051.58	377.1662	227.1672	10.5347	39.77

Table 4-10 Diethnol amine Inhibitor at 35°C and 500 ppm.

U(rpm)	Re	CR without Inhibitor(gmd)	CR with Inhibitor(gmd)	CR(mm/y)	η %
0	static	175.7504	85.0808	3.9455	51.59
400	5729	201.3369	151.7476	7.037	24.63
700	10025.78	232.3151	198.9546	9.226	14.36
1000	14322.55	270.8047	235.7084	10.8297	12.96
1400	20051.58	377.1662	343.5229	15.9304	8.92

Table 4-11 Diethnol amine Inhibitor at 35°C and 1000 ppm.

U(rpm)	Re	CR without Inhibitor(gmd)	CR with Inhibitor(gmd)	CR(mm/y)	η %
0	Static	175.7504	80.5639	3.739	54.16
400	5729	201.3369	109.2454	5.066	45.74
700	10025.78	232.3151	153.6764	7.1266	33.85
1000	14322.55	270.8047	202.6432	10.3254	25.17
1400	20051.58	377.1662	293.8502	13.627	22.09

Table 4-12 Diethnol Amine Inhibitor at 35°C and 2000 ppm.

U(rpm)	Re	CR without Inhibitor(gmd)	CR with Inhibitor(gmd)	CR(mm/y)	η %
0	Static	175.7504	62.7728	2.911	64.28
400	5729	201.3369	93.9035	4.3547	53.36
700	10025.78	232.3151	117.9928	5.4718	49.21
1000	14322.55	270.8047	155.3065	7.202	42.65
1400	20051.58	377.1662	247.157	11.4611	34.47

Tables 4-13 through 4-16 show the experimental results of corrosion rate in the presence of thiourea inhibitor at concentration of 100, 400, 1000, and 2000 ppm and temperature of 35°C. It is indicated that the inhibition efficiency increases with increasing the concentration of thiourea inhibitor for the whole range of temperature and rotational velocity.

Table 4-13 Thiourea Inhibitor at 35°C and 100 ppm.

U(rpm)	Re	CR without Inhibitor(gmd)	CR with Inhibitor(gmd)	CR(mm/y)	η %
0	static	175.7504	107.7525	4.997	38.69
400	5729	201.3369	128.2516	5.9475	36.3
700	10025.78	232.3151	167.3366	7.76	27.97
1000	14322.55	270.8047	217.1268	10.5327	19.82
1400	20051.58	377.1662	315.7737	14.6437	16.28

Table 4-14 Thiourea Inhibitor at 35°C and 400 ppm.

U(rpm)	Re	CR without Inhibitor(gmd)	CR with Inhibitor(gmd)	CR(mm/y)	η %
0	static	175.7504	62.532	7.4445	64.42
400	5729	201.3369	99.2389	4.6025	50.71
700	10025.78	232.3151	142.0607	6.5879	38.85
1000	14322.55	270.8047	182.3328	9.8372	32.67
1400	20051.58	377.1662	259.4903	11.423	31.2

Table 4-15 Thiourea Inhibitor at 35°C and 1000 ppm.

U(rpm)	Re	CR without Inhibitor(gmd)	CR with Inhibitor(gmd)	CR(mm/y)	η %
0	static	175.7504	52.8981	2.453	69.93
400	5729	201.3369	83.6353	3.8783	58.46
700	10025.78	232.3151	102.9853	4.7761	55.67
1000	14322.55	270.8047	132.5493	6.1468	51.05
1400	20051.58	377.1662	194.58	9.0235	48.41

Table 4-16 Thiourea Inhibitor at35°C and 2000 ppm.

U(rpm)	Re	CR without Inhibitor(gmd)	CR with Inhibitor(gmd)	CR(mm/y)	η %
0	static	175.7504	39.3857	1.8265	77.59
400	5729	201.3369	71.12	3.3079	64.57
700	10025.78	232.3151	87.7222	4.0536	62.24
1000	14322.55	270.8047	115.9586	5.3775	57.18
1400	20051.58	377.1662	168.706	7.8236	55.27

Tables 4-17 through 4-22 show the experimental results of corrosion rate in the presence of thiourea inhibitor at concentration of 400, 1000, and 2000 ppm and temperature of 45°C and 60°C respectively. It is evident from these tables that the inhibition efficiency decreases with increasing temperature of the corrosive solution for constant thiourea concentration and rotational velocity.

Table 4-17 Thiourea Inhibitor at 45°C and 400 ppm.

U(rpm)	Re	CR without Inhibitor(gmd)	CR with Inhibitor(gmd)	CR(mm/y)	η %
0	static	239.4582	112.6063	5.222	52.97
400	6887.8	327.5282	172.2448	7.9876	47.41
700	12053.77	377.4623	206.366	9.57	45.33
1000	17219.67	412.68	246.585	11.435	40.25
1400	24107.54	566.2837	367.3283	17.0345	35.13

Table 4-18 Thiourea Inhibitor at 45°C and 1000 ppm.

U(rpm)	Re	CR without Inhibitor(gmd)	CR with Inhibitor(gmd)	CR(mm/y)	η %
0	static	239.4582	82.4215	3.8224	65.58
400	6887.8	327.5282	158.5323	7.3517	51.59
700	12053.77	377.4623	188.6179	8.747	50.03
1000	17219.67	412.68	216.86	10.0567	47.45
1400	24107.54	566.2837	322.272	14.945	43.09

Table 4-19 Thiourea Inhibitor at 45°C and 2000 ppm.

U(rpm)	Re	CR without Inhibitor(gmd)	CR with Inhibitor(gmd)	CR(mm/y)	η %
0	static	239.4582	80.5734	3.7365	66.35
400	6887.8	327.5282	131.2733	6.0876	59.92
700	12053.77	377.4623	161.1764	7.4744	57.3
1000	17219.67	412.68	208.1145	9.6511	49.57
1400	24107.54	566.2837	320.3665	14.8566	43.43

Table 4-20 Thiourea Inhibitor at 60°C and 400 ppm.

U(rpm)	Re	CR without Inhibitor(gmd)	CR with Inhibitor(gmd)	CR(mm/y)	η %
0	static	476.7006	213.1951	9.8867	55.3
400	8734.89	874.3937	487.53	22.6	44.2
700	15286.07	1074.715	582.5764	27	45.8
1000	21837.24	1190.9536	708.77	32.8685	40.5
1400	30572.139	1211.5137	739.3125	34.2848	39

Table 4-21 Thiourea Inhibitor at 60°C and 1000 ppm

U(rpm)	Re	CR without Inhibitor(gmd)	CR with Inhibitor(gmd)	CR(mm/y)	η %
0	static	476.7006	170.4205	7.9031	64.25
400	8734.89	874.3937	444.28	20.603	49.19
700	15286.07	1074.715	549.716	25.4925	48.85
1000	21837.24	1190.9536	686.98	31.858	42.4
1400	30572.139	1211.5137	726.666	33.698	40.02

Table 4-22 Thiourea Inhibitor at 60°C and 2000 ppm.

U(rpm)	Re	CR without Inhibitor(gmd)	CR with Inhibitor(gmd)	CR(mm/y)	η %
0	static	476.7006	164.27	7.6178	65.54
400	8734.89	874.3937	409.566	18.9932	53.16
700	15286.07	1074.715	529.727	24.5657	50.71
1000	21837.24	1190.9536	619.7723	28.7413	47.96
1400	30572.139	1211.5137	711.6431	33.0017	41.26

Tables 4-23 through 4-25 show the experimental results of mass transfer coefficient of dissolved oxygen (K_{O2}), oxygen current (i_{O2}), and corrosion current of iron metal (i_{Fe}) which are increased with increasing the rotational velocity at three temperatures. Increasing the velocity has no appreciable effect on hydrogen evolution current (i_{H2}).

Table 4-23 Results of Corrosion Current at 35°C Without Inhibitor.

U(rpm)	Re	K_{O2} (m/sec)	i_{O2} (A/m^2)	i_{Fe} (A/m^2)	i_{H2} (A/m^2)
0	static	$5.88*10^{-6}$	0.47	7.0275	6.5575
400	5729	$2.54*10^{-5}$	2.0285	8.0505	6.0220
700	10025.78	$4.02*10^{-5}$	3.2097	9.2732	6.0630
1000	14322.55	$5.38*10^{-5}$	4.3002	10.7881	6.4879
1400	20051.58	$7.09*10^{-5}$	5.6665	15.0238	9.3573

Table 4-24 Results of Corrosion Current at 45°C Without Inhibitor.

U(rpm)	Re	K_{O2} (m/sec)	i_{O2} (A/m^2)	i_{Fe} (A/m^2)	i_{H2} (A/m^2)
0	static	$7.76*10^{-6}$	0.563	9.5952	9.0322
400	6887.8	$3.31*10^{-5}$	2.4039	13.0963	10.6924
700	12053.77	$5.24*10^{-5}$	3.8038	15.0963	11.2896
1000	17219.67	$7.02*10^{-5}$	5.0960	16.5016	11.4056
1400	24107.54	$9.25*10^{-5}$	6.7152	22.6434	15.9282

Table 4-25 Results of Corrosion Current at 60°C Without Inhibitor.

U(rpm)	Re	K_{O2}(m/sec)	i_{O2} (A/m^2)	i_{Fe} (A/m^2)	i_{H2} (A/m^2)
0	static	$1.14*10^{-5}$	0.62	19.0686	18.4486
400	8734.89	$4.76*10^{-5}$	2.5906	34.9613	32.3706
700	15286.07	$7.53*10^{-5}$	4.0992	42.9777	38.8785
1000	21837.24	$1.01*10^{-4}$	5.4918	48.2046	42.7128
1400	30572.139	$1.33*10^{-4}$	7.2367	48.3024	41.0657

Tables 4-26 through 4-34 show the experimental results of mass transfer coefficient of dissolved oxygen (K_{O2}), oxygen current (i_{O2}), and corrosion current of iron metal (i_{Fe}) at a temperature of 35°C. From these result is evident that increasing of rotational velocity leads to increase the value of K_{O2}, i_{O2}, and (i_{Fe}). Increasing the velocity has no appreciable effect on hydrogen evolution current (i_{H2}).Moreover, increasing the concentration for formaldehyde, ethylene diamine, and diethanol amine inhibitors leads to decrease the values of i_{Fe} and i_{H2} at constant temperature and velocity. While the values of K_{O2} and i_{O2} are not clearly affected by the inhibitor concentration.

Table 4-26 Results of Corrosion Current at 35°C and 500 ppm of Formaldehyde Inhibitor.

U(rpm)	Re	K_{O2}(m/sec)	i_{O2} (A/m^2)	i_{Fe} (A/m^2)	i_{H2} (A/m^2)
0	static	$5.88*10^{-6}$	0.47	4.4188	3.9488
400	5729	$2.54*10^{-5}$	2.0285	6.7093	4.6808
700	10025.78	$4.02*10^{-5}$	3.2097	8.5637	5.3539
1000	14322.55	$5.38*10^{-5}$	4.3002	10.0474	5.7473
1400	20051.58	$7.09*10^{-5}$	5.6665	14.5962	8.9297

Table 4-27 Results of Corrosion Current at 35°C and 1000 ppm of Formaldehyde Inhibitor.

U(rpm)	Re	K_{O2}(m/sec)	i_{O2} (A/m^2)	i_{Fe} (A/m^2)	i_{H2} (A/m^2)
0	static	$5.88*10^{-6}$	0.47	4.1786	3.7086
400	5729	$2.54*10^{-5}$	2.0285	5.3077	3.2792
700	10025.78	$4.02*10^{-5}$	3.2097	6.8471	3.6374
1000	14322.55	$5.38*10^{-5}$	4.3002	8.9398	4.6396
1400	20051.58	$7.09*10^{-5}$	5.6665	14.3134	8.6469

Table 4-28 Results of Corrosion Current at 35°C and 2000 ppm of Formaldehyde Inhibitor.

U(rpm)	Re	K_{O2}(m/sec)	i_{O2} (A/m^2)	i_{Fe} (A/m^2)	i_{H2} (A/m^2)
0	static	$5.88*10^{-6}$	0.47	2.8313	2.3613
400	5729	$2.54*10^{-5}$	2.0285	4.0615	2.033
700	10025.78	$4.02*10^{-5}$	3.2097	5.2614	2.0516
1000	14322.55	$5.38*10^{-5}$	4.3002	7.3870	3.0868
1400	20051.58	$7.09*10^{-5}$	5.6665	10.7332	5.0667

Table 4-29 Results of Corrosion Current at 35°C and 500 ppm of Ethylene diamine Inhibitor.

U(rpm)	Re	K_{O2}(m/sec)	i_{O2} (A/m^2)	i_{Fe} (A/m^2)	i_{H2} (A/m^2)
0	static	$5.88*10^{-6}$	0.47	2.922	2.452
400	5729	$2.54*10^{-5}$	2.0285	4.8528	2.8243
700	10025.78	$4.02*10^{-5}$	3.2097	7.5957	4.3860
1000	14322.55	$5.38*10^{-5}$	4.3002	9.1888	4.8886
1400	20051.58	$7.09*10^{-5}$	5.6665	12.9094	7.2429

Table 4-30 Results of Corrosion Current at 35°C and 1000 ppm of Ethylene diamine Inhibitor.

U(rpm)	Re	K_{O2}(m/sec)	i_{O2} (A/m^2)	i_{Fe} (A/m^2)	i_{H2} (A/m^2)
0	static	$5.88*10^{-6}$	0.47	2.3795	1.9095
400	5729	$2.54*10^{-5}$	2.0285	4.1171	2.0886
700	10025.78	$4.02*10^{-5}$	3.2097	6.0482	2.8384
1000	14322.55	$5.38*10^{-5}$	4.3002	7.5656	3.2654
1400	20051.58	$7.09*10^{-5}$	5.6665	10.7769	5.1104

Table 4-31 Results of Corrosion Current at 35°C and 2000 ppm of Ethylene diamine Inhibitor.

U(rpm)	Re	K_{O2}(m/sec)	i_{O2} (A/m^2)	i_{Fe} (A/m^2)	i_{H2} (A/m^2)
0	static	$5.88*10^{-6}$	0.47	1.7098	1.2398
400	5729	$2.54*10^{-5}$	2.0285	3.576	1.5475
700	10025.78	$4.02*10^{-5}$	3.2097	4.2934	1.0837
1000	14322.55	$5.38*10^{-5}$	4.3002	5.6631	1.3629
1400	20051.58	$7.09*10^{-5}$	5.6665	9.0833	3.4168

Table 4-32 Results of Corrosion Current at 35°C and 500 ppm of Diethanol amine Inhibitor.

U(rpm)	Re	K_{O2}(m/sec)	i_{O2} (A/m^2)	i_{Fe} (A/m^2)	i_{H2} (A/m^2)
0	static	$5.88*10^{-6}$	0.47	3.402	2.932
400	5729	$2.54*10^{-5}$	2.0285	6.0676	4.0391
700	10025.78	$4.02*10^{-5}$	3.2097	7.9552	4.7455
1000	14322.55	$5.38*10^{-5}$	4.3002	9.4248	5.1246
1400	20051.58	$7.09*10^{-5}$	5.6665	13.7358	8.0693

Table 4-33 Results of Corrosion Current at 35°C and 1000 ppm of Diethanol amine Inhibitor.

U(rpm)	Re	K_{O2}(m/sec)	i_{O2} (A/m^2)	i_{Fe} (A/m^2)	i_{H2} (A/m^2)
0	static	$5.88*10^{-6}$	0.47	3.2214	2.7514
400	5729	$2.54*10^{-5}$	2.0285	4.3682	2.3397
700	10025.78	$4.02*10^{-5}$	3.2097	6.1448	2.9350
1000	14322.55	$5.38*10^{-5}$	4.3002	8.1027	3.8025
1400	20051.58	$7.09*10^{-5}$	5.6665	11.7496	6.0832

Table 4-34 Results of Corrosion Current at 35°C and 2000 ppm of Diethanol amine Inhibitor.

U(rpm)	Re	K_{O2}(m/sec)	i_{O2} (A/m^2)	i_{Fe} (A/m^2)	i_{H2} (A/m^2)
0	static	$5.88*10^{-6}$	0.47	2.51	2.04
400	5729	$2.54*10^{-5}$	2.0285	3.7547	1.7262
700	10025.78	$4.02*10^{-5}$	3.2097	4.718	1.5082
1000	14322.55	$5.38*10^{-5}$	4.3002	6.2099	1.9098
1400	20051.58	$7.09*10^{-5}$	5.6665	9.8826	4.2161

Tables 4-35 through 4-44 show the experimental results of K_{O2}, i_{O2}, i_{Fe}, and i_{H2} for thiourea inhibitor with various concentration at 35, 45, 60°C respectively. It is clear that the values of K_{O2} and i_{O2} were not affected by the presence of corrosion inhibitors in the corrosive solution, but increases with increasing the rotational velocity and temperature of the corrosive solution. Whereas, the values of i_{Fe} increases with increasing the rotational velocity and temperature and decreases with increasing the concentration of thiourea inhibitor. In addition, it is also evident that the values of i_{H2} increases with increasing the temperature of the corrosive solution for the same concentration of thiourea inhibitor and decreases with increasing the concentration of thiourea inhibitor at constant temperature.

Table 4-35 Results of Corrosion Current at 35°C and 100 ppm of Thiourea Inhibitor.

U(rpm)	Re	K_{O2}(m/sec)	i_{O2} (A/m^2)	i_{Fe} (A/m^2)	i_{H2} (A/m^2)
0	static	$5.88*10^{-6}$	0.47	4.3085	3.8385
400	5729	$2.54*10^{-5}$	2.0285	5.1282	3.0997
700	10025.78	$4.02*10^{-5}$	3.2097	6.691	3.4812
1000	14322.55	$5.38*10^{-5}$	4.3002	8.6818	4.3816
1400	20051.58	$7.09*10^{-5}$	5.6665	12.6263	6.9598

Table 4-36 Results of Corrosion Current at 35°C and 400 ppm of Thiourea Inhibitor.

U(rpm)	Re	K_{O2}(m/sec)	i_{O2} (A/m^2)	i_{Fe} (A/m^2)	i_{H2} (A/m^2)
0	static	$5.88*10^{-6}$	0.47	2.5003	2.0303
400	5729	$2.54*10^{-5}$	2.0285	3.9681	1.9396
700	10025.78	$4.02*10^{-5}$	3.2097	5.6803	2.4706
1000	14322.55	$5.38*10^{-5}$	4.3002	7.2906	2.9904
1400	20051.58	$7.09*10^{-5}$	5.6665	10.3758	4.7093

Table 4-37 Results of Corrosion Current at 35°C and 1000 ppm of Thiourea Inhibitor.

U(rpm)	Re	K_{O2}(m/sec)	i_{O2} (A/m^2)	i_{Fe} (A/m^2)	i_{H2} (A/m^2)
0	static	$5.88*10^{-6}$	0.47	2.1146	1.6446
400	5729	$2.54*10^{-5}$	2.0285	3.3442	1.3157
700	10025.78	$4.02*10^{-5}$	3.2097	4.1179	0.9082
1000	14322.55	$5.38*10^{-5}$	4.3002	5.300	0.9988
1400	20051.58	$7.09*10^{-5}$	5.6665	6.6195	0.9531

Table 4-38 Results of Corrosion Current at 35°C and 2000 ppm of Thiourea Inhibitor.

U(rpm)	Re	K_{O2}(m/sec)	i_{O2} (A/m^2)	i_{Fe} (A/m^2)	i_{H2} (A/m^2)
0	static	$5.88*10^{-6}$	0.47	1.5748	1.1048
400	5729	$2.54*10^{-5}$	2.0285	2.8437	0.8152
700	10025.78	$4.02*10^{-5}$	3.2097	3.5076	0.2979
1000	14322.55	$5.38*10^{-5}$	4.3002	4.6366	0.3364
1400	20051.58	$7.09*10^{-5}$	5.6665	6.7484	1.0819

Table 4-39 Results of Corrosion Current at 45°C and 400 ppm of Thiourea Inhibitor.

U(rpm)	Re	K_{O2} (m/sec)	i_{O2} (A/m^2)	i_{Fe} (A/m^2)	i_{H2} (A/m^2)
0	static	$7.76*10^{-6}$	0.563	4.5026	3.9396
400	6887.8	$3.31*10^{-5}$	2.4039	6.8872	4.4833
700	12053.77	$5.24*10^{-5}$	3.8038	8.243	4.4392
1000	17219.67	$7.02*10^{-5}$	5.0960	9.8525	4.7565
1400	24107.54	$9.25*10^{-5}$	6.7152	14.6913	7.9761

Table 4-40 Results of Corrosion Current at 45°C and 1000 ppm of Thiourea Inhibitor.

U(rpm)	Re	K_{O2}(m/sec)	i_{O2} (A/m^2)	i_{Fe} (A/m^2)	i_{H2} (A/m^2)
0	static	$7.76*10^{-6}$	0.563	3.2956	2.7362
400	6887.8	$3.31*10^{-5}$	2.4039	6.3389	3.9350
700	12053.77	$5.24*10^{-5}$	3.8038	7.5418	3.7381
1000	17219.67	$7.02*10^{-5}$	5.0960	8.6645	3.5685
1400	24107.54	$9.25*10^{-5}$	6.7152	12.8861	6.1709

Table 4-41 Results of Corrosion Current at 45°C and 2000 ppm of Thiourea Inhibitor.

U(rpm)	Re	K_{O2}(m/sec)	i_{O2} (A/m^2)	i_{Fe} (A/m^2)	i_{H2} (A/m^2)
0	static	$7.76*10^{-6}$	0.563	3.2217	2.6587
400	6887.8	$3.31*10^{-5}$	2.4039	5.2439	2.84
700	12053.77	$5.24*10^{-5}$	3.8038	6.4447	2.6409
1000	17219.67	$7.02*10^{-5}$	5.0960	8.3215	3.2254
1400	24107.54	$9.25*10^{-5}$	6.7152	12.8099	6.0947

Table 4-42 Results of Corrosion Current at 60°C and 400 ppm of Thiourea Inhibitor.

U(rpm)	Re	K_{O2}(m/sec)	i_{O2} (A/m^2)	i_{Fe} (A/m^2)	i_{H2} (A/m^2)
0	static	$1.14*10^{-5}$	0.62	8.5246	7.9046
400	8734.89	$4.76*10^{-5}$	2.5906	19.4939	16.9033
700	15286.07	$7.53*10^{-5}$	4.0992	23.2944	19.1952
1000	21837.24	$1.01*10^{-4}$	5.4918	28.3403	22.8484
1400	30572.139	$1.33*10^{-4}$	7.2367	29.5615	22.3248

Table 4-43 Results of Corrosion Current at 60°C and 1000 ppm of Thiourea Inhibitor.

U(rpm)	Re	K_{O2}(m/sec)	i_{O2} (A/m^2)	i_{Fe} (A/m^2)	i_{H2} (A/m^2)
0	static	$1.14*10^{-5}$	0.62	6.8103	6.1903
400	8734.89	$4.76*10^{-5}$	2.5906	17.7673	15.1767
700	15286.07	$7.53*10^{-5}$	4.0992	21.9853	17.8861
1000	21837.24	$1.01*10^{-4}$	5.4918	27.47	21.9782
1400	30572.139	$1.33*10^{-4}$	7.2367	29.0645	21.8278

Table 4-44 Results of Corrosion Current at 60°C and 2000 ppm of Thiourea Inhibitor.

U(rpm)	Re	K_{O2} (m/sec)	i_{O2} (A/m^2)	i_{Fe} (A/m^2)	i_{H2} (A/m^2)
0	static	$1.14*10^{-5}$	0.62	6.5653	5.9453
400	8734.89	$4.76*10^{-5}$	2.5906	16.3781	13.7875
700	15286.07	$7.53*10^{-5}$	4.0992	21.1874	17.0882
1000	21837.24	$1.01*10^{-4}$	5.4918	24.7783	19.2865
1400	30572.139	$1.33*10^{-4}$	7.2367	28.4483	21.2116

Table 4-45 shows the experimental results K_{O2}, i_{O2}, i_{Fe}, and i_{H2} in the absence of corrosion inhibitor under static condition. It is evident from this table that all these values increase with increasing temperature of the corrosive solution.

Table 4-45 Results of Corrosion Current Without Inhibitor under Static Condition at Various Temperatures.

Temperature	K_{O2} (m/sec)	i_{O2} (A/m^2)	i_{Fe} (A/m^2)	i_{H2} (A/m^2)
35°C	$5.88*10^{-6}$	0.47	7.0275	6.5575
45°C	$7.76*10^{-6}$	0.563	9.5952	9.0322
60°C	$1.14*10^{-5}$	0.62	19.0686	18.4486

CHAPTER FIVE
Discussion

5.1 Introduction

Corrosion behavior of carbon steel in hydrochloric acid solution with and without inhibitor was studied under different conditions of temperature of 35-60ºC, rotational speed of 400-1400 rpm and different corrosion inhibitors, which are thiourea, ethylene diamine, diethanol amine and formaldehyde at concentration of 500-2000 ppm. A total of 110 runs were made by weight loss technique, 15 runs in an uninhibited solution at static and flow conditions and one temperature of 35 ºC. 45 run in inhibited solutions using formaldehyde, diethanol amine and ethylene diamine as inhibitors at one temperature and different rotation speeds. 50 runs in inhibited solutions using thiourea, 20 runs of these at 35ºC, 15 runs at 45ºC and 15 runs at 60ºC. All of these runs were curried out under static and different rotational speeds.

System consists of HCl solution and iron, such system is made of anodic and cathodic reactions as follows:

- Anodic reaction, which is the dissolution process of iron.

  $$(Fe \Rightarrow Fe^{+2} + 2e)$$

- Since the environment is acidic solution and not deaerated, so one of the cathodic reaction takes place is oxygen reduction expressed as: ($O_2 + 4H^+ + 4e \Rightarrow 2H_2O$).
- The other cathodic reaction takes place is hydrogen evolution reaction expressed as: ($2H^+ + 2e \Rightarrow H_2$)**.**

One can notice in table 5-1 that the difference between corrosion rate at 400 rpm and the corrosion rate at static condition (0 rpm) for example at 400 ppm and 35°C is equal to 36.7069 gmd. This difference increases with increasing the rotational velocity and this behavior can be observed for the same concentration of thiourea inhibitor and the remaining concentration for 45°C and 60°C, this increase results from the effect of flow only on the oxygen transport to the metal surface where it is considered as mass transfer controlled.

Table 5-1 Effect of Rotational Velocity on Oxygen Transfer in the Entire Ranges of Temperature and Thiourea Concentration.

Temperature	Inhibitor Concentration (ppm)	$CR_{rpm=0}$ (gmd)	$CR_{rpm=400}$ (gmd)	$CR_{rpm=400}$ $-CR_{rpm=0}$ (gmd)	$CR_{rpm=700}$ (gmd)	$CR_{rpm=700}$ $-CR_{rpm=0}$ (gmd)	$CR_{rpm=1000}$ (gmd)	$CR_{rpm=100}$ $-CR_{rpm=0}$ (gmd)	$CR_{rpm=1400}$ (gmd)	$CR_{rpm=1400}$ $-CR_{rpm=0}$ (gmd)
35°C	100	107.7525	128.2516	20.4991	167.3366	59.5841	217.1268	109.3743	315.7737	208.0212
	400	62.532	99.2389	36.7069	142.0607	79.5287	182.3328	119.8008	259.4903	196.9583
	1000	52.8981	83.6353	30.7372	102.9853	50.0872	132.5493	79.6512	194.58	141.6819
	2000	39.3857	71.12	31.7343	87.7222	48.3365	115.9586	76.5729	168.706	129.3203
45°C	400	112.6063	172.2448	59.6385	206.366	93.7597	246.585	133.9787	367.3283	254.722
	1000	82.4215	158.5323	76.1108	188.6179	106.1964	216.86	134.4385	322.272	239.8505
	2000	80.5734	131.2733	50.6999	161.1764	80.603	208.1145	127.5411	320.3665	239.7931
60°C	400	213.1951	487.53	274.3349	582.5764	369.3813	708.77	495.5749	739.3125	526.1174
	1000	170.4205	444.28	273.8595	549.716	379.2955	686.98	516.5595	726.666	556.2455
	2000	164.27	409.566	245.296	529.727	365.457	619.7723	455.5023	711.6431	547.3731

5.2 Corrosion Rate by Weight Loss

The corrosion rate (CR) was obtained by dividing the weight loss of the specimen during a specified time by the area (A) exposed to the corrosive solution, as follows:

Area of specimen exposed to corrosive solution:

$$A = \pi \; d \; L \qquad \dots (5.1)$$

Corrosion rate (CR) in g/m^2. day (gmd).

$$CR = \frac{\Delta W}{A \times t} \qquad \dots (5.2)$$

$$CR\left(mm \cdot y^{-1}\right) = \frac{CR\left(gmd\right)}{21.5638} \qquad \dots (5.3)$$

5.2.1 Effect of Temperature and Rotational Velocity

The effect of temperature on the inhibiting process is of a great importance in industry. Figure 5.1 shows the variation of corrosion rate with Reynolds number at three temperatures. It is evident that at a particular temperature, the corrosion rate increases with Re. This figure shows that under static conditions the corrosion rate at 35ºC is slightly lower than at 45ºC and the latter is markedly lower than at 60ºC. Under static conditions the corrosion rates at 35, 45 and 60ºC are equal to 175.75, 239.5 and 476.7 gmd respectively, were at the same Re the CR increased with increasing the temperature of the acid solution. This behavior can be explained as follows: Increasing temperature leads to change two variables that act in a conflicting way. Firstly, increasing temperature accelerates the reaction rate as dictated by Arrhenius equation. Moreover, diffusion rate of dissolved oxygen by increasing the molecular diffusion coefficient. Secondly, as the temperature increases the oxygen solubility decreases [14, 16 and 77].

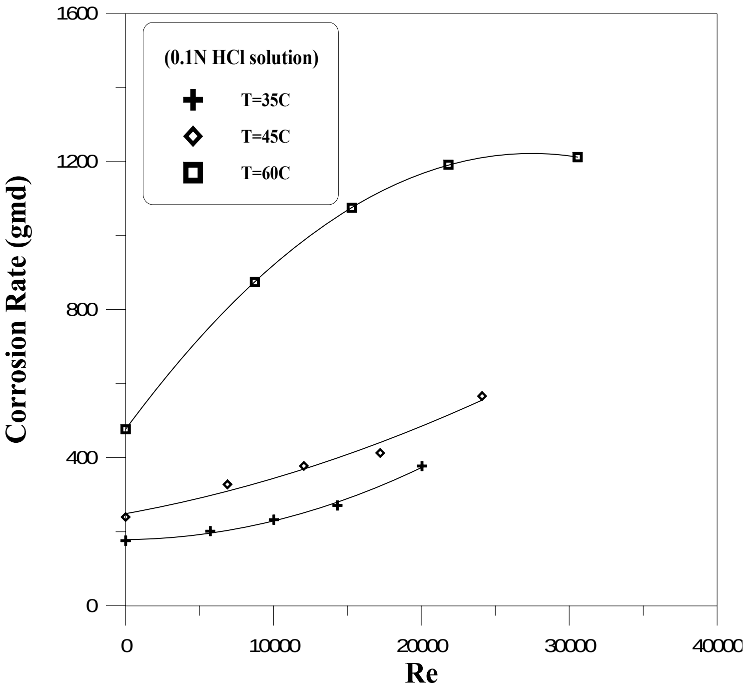

Figure 5-1 Corrosion Rate versus Reynolds Number

5.2.2 Effect of Inhibitor Concentration

Figures 5.2 through 5.5 show the relationship between the corrosion rate and Re in the presence of formaldehyde, diethanol amine, ethylene diamine and thiourea as inhibitors respectively at various concentrations of these inhibitors in 0.1N HCl solution at 35ºC. These figures show the influence of concentration of each inhibitor on the corrosion rate of the carbon steel metal. The variation of corrosion rate with Re at constant temperature of 35ºC as shown in figure 5.2 indicates that under static conditions the corrosion rates in 0.1N HCl solution and in presence of 500 ppm, 1000 ppm and 2000 ppm of formaldehyde as inhibitor are 175.75, 110.5 104.5, and 70.8 gmd respectively. At Re > 20,000 with constant temperature of 35ºC, the corrosion rates in 0.1N HCl solution and in presence of the same inhibitor are 377.16, 365, 357.96 and 268.4 gmd respectively. It is clear that CR increases with increasing Re for all values of formaldehyde concentration. This behavior is the same for the remaining inhibitors as shown in figures 5.3 through 5.5.

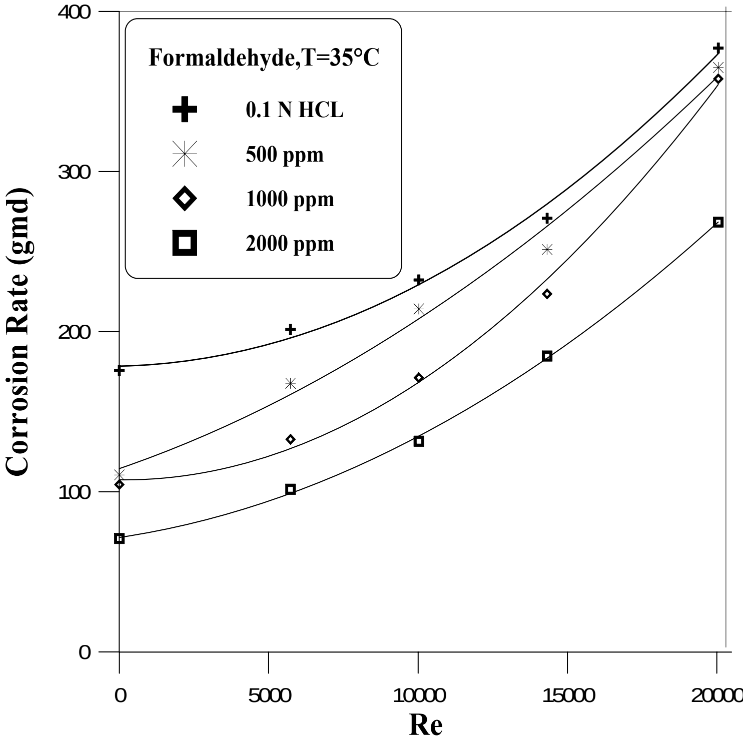

Figure 5-2 Variation of Corrosion Rate with Reynolds Number in the Presence of Formaldehyde Inhibitor at T= 35°C.

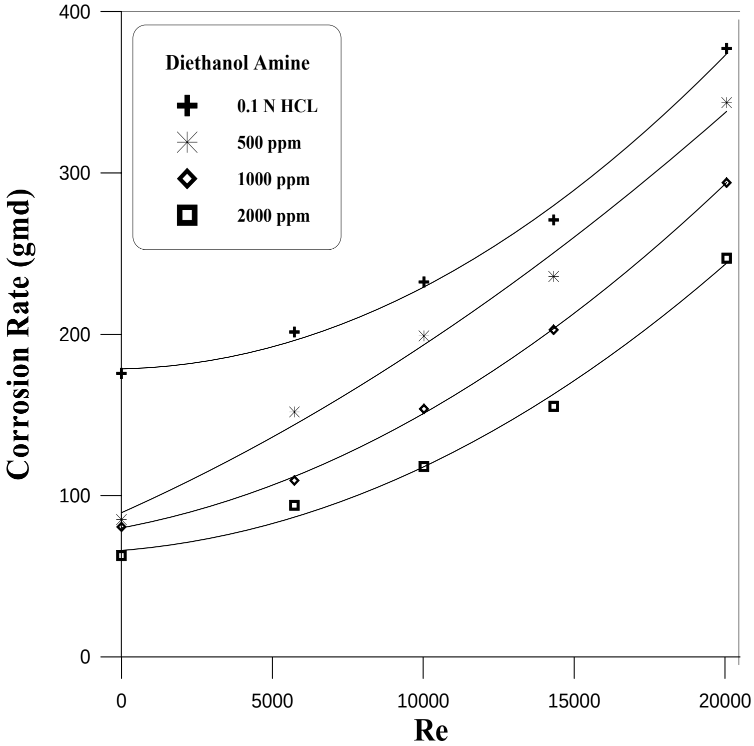

Figure 5-3 Variation of Corrosion Rate with Reynolds Number in Presence of Diethanol amine Inhibitor at T= 35°C.

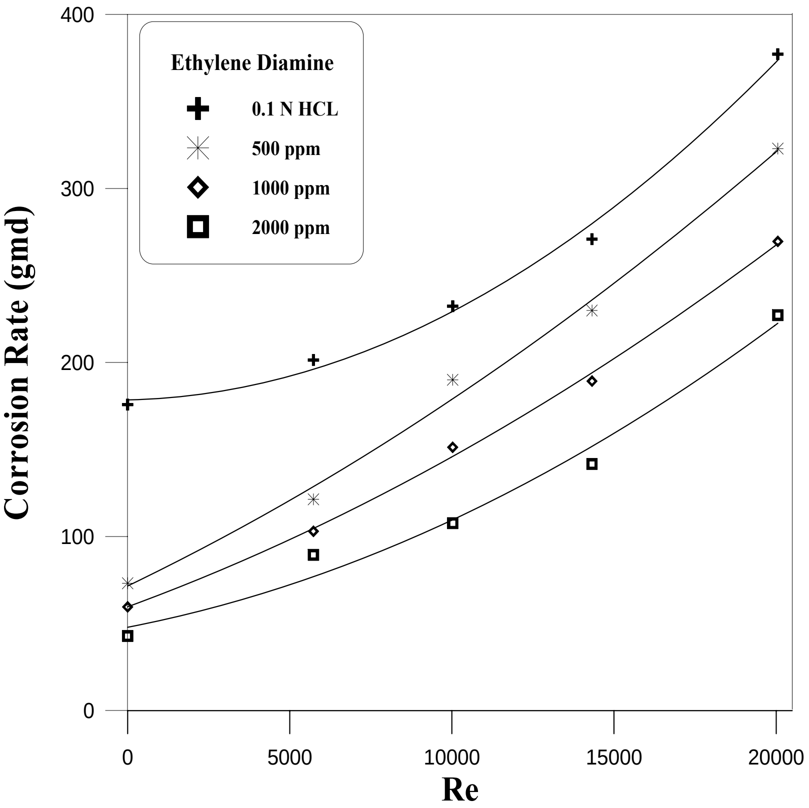

Figure 5-4 Variation of Corrosion Rate with Reynolds Number in Presence of Ethylene Diamine Inhibitor at T= 35°C.

Organic Amine Inhibitors decrease the corrosion rate by one of two ways: either adsorbed on the metal surface, forming a thin two-dimensional (2-D) film. This type can be further subdivided into non-selective and selective physisorption and chemisorptions or by forming three-dimensional (3-D) layer emerges on the metal surface resulting from, for example, the chemical reaction of an inhibitor with corrosion products to form organometallic complexes [44, 47].

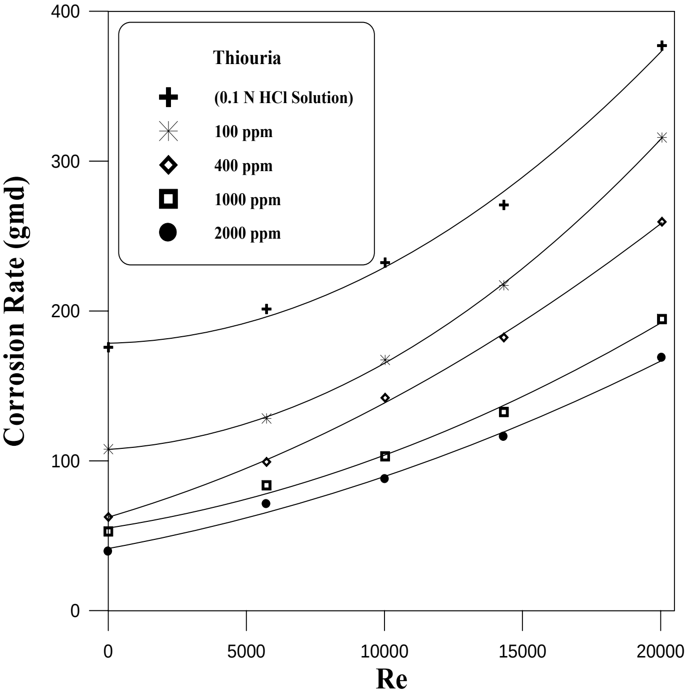

Figure 5-5 Variation of Corrosion Rate with Reynolds Number in Presence of Thiourea Inhibitor at T = 35°C.

Figures 5.6 through 5.8 show comparison among corrosion rates in the presence of formaldehyde, diethanol amine, ethylene diamine and thiourea as inhibitors used at 35ºC and inhibitor concentrations of 500 ppm, 1000 ppm and 2000 ppm respectively. It was found that the four inhibitors work for different degrees of inhibition. It is clear that the thiourea inhibitor inhibits the corrosion of carbon steel (CS) more than the others at the same concentration and temperature, followed by ethylene diamine, diethanol amine and formaldehyde respectively. These figures reveal that increasing inhibitor concentration decreases the corrosion rate of carbon steel. From figure 5.6 the recorded corrosion rates for the four inhibitors respectively under static conditions, T = 35ºC and in presence of 500 ppm inhibitor concentration, were 110.5, 85.08, 73.07 and 62.5 gmd. While the CR from figure 5.7 were 104.5, 80.5, 59.5 and 52.89 gmd under similar conditions but at 1000 ppm inhibitor concentration. Figure 5.8 shows corrosion rates to be

70.8, 62.77, 42.76 and 39.38 gmd under similar conditions at C_{inh} = 2000 ppm.

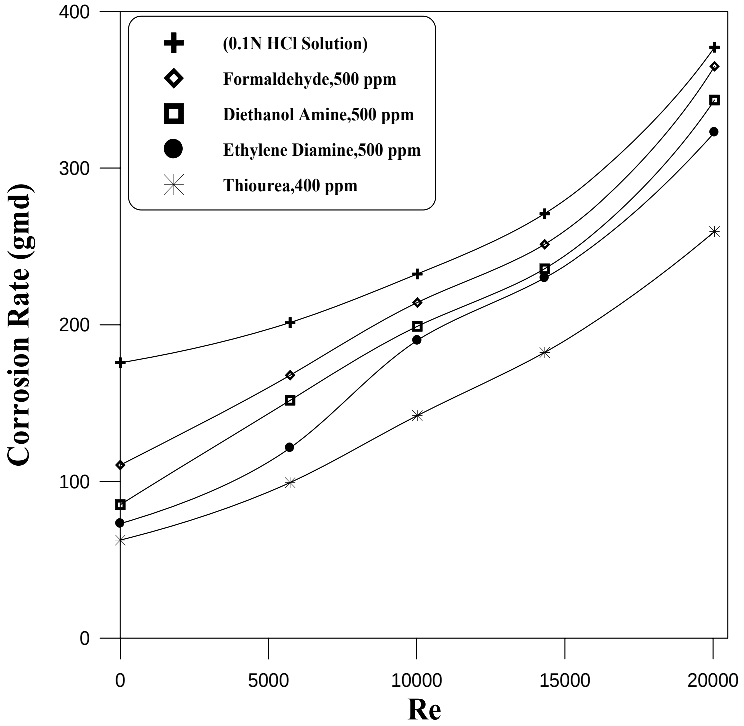

Figure 5-6 Comparison among Corrosion Rates in Presence of Various Inhibitors at T=35°C.

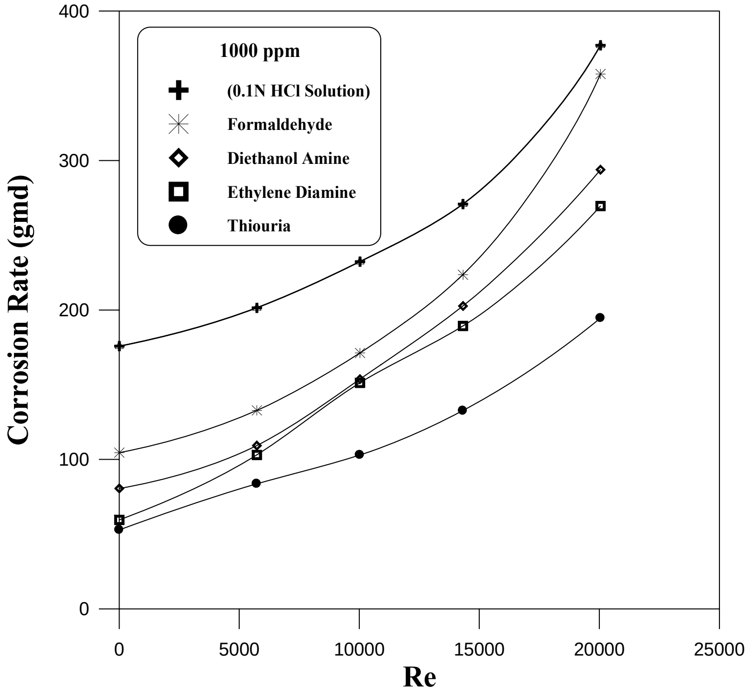

Figure 5-7 Comparison among Corrosion Rates in Presence of Various Inhibitors at T=35°C.

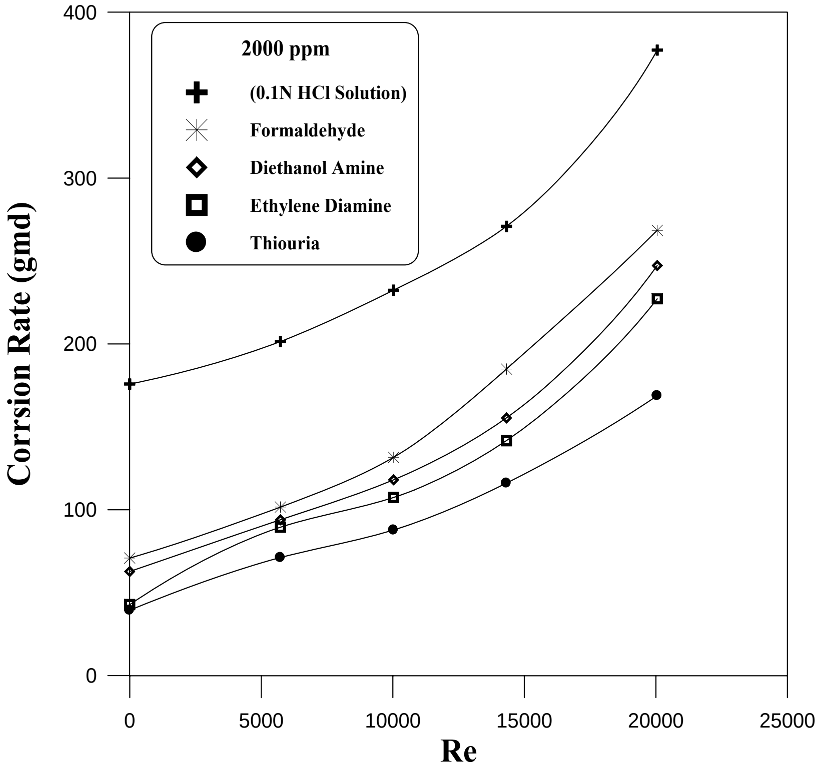

Figure 5-8 Comparison among Corrosion Rate of Inhibitors at T=35°C.

Yee [79], stated that Amines are cationic type inhibitors. They are often added to HCl-rich environments. When the system involved is ferrous metal, neutralizing amines work by the mechanism that modifies the pH of the electrolyte and thus inhibiting rust formation. Musa, et al. [80] demonstrated that the behavior of ethylenediaminetetra-Acetic acid di-sodium salt (EDTA di-sodium) and thiourea on the corrosion of mild steel in 1M hydrochloric acid solution are mixed-type inhibitors.

Figures 5.9 and 5.10 show variation of corrosion rate with Re in the presence of thiourea inhibitor at 45ºC and 60ºC respectively under the influence of various concentration of this inhibitor. It is clear that the values of corrosion rate increase with increasing temperature from 35ºC to 60ºC for the same concentration of thiourea inhibitor and rotation velocities (or Re).

The inhibition efficiency (η %) for the same concentration and Re decreases with increasing temperature as shown in table (5-2).

Table 5-2 Effect of Temperature and Thiourea Concentration on its Inhibition Efficiency.

Temperature	Reynolds number	Inhibition Efficiency (η %)		
		400 ppm	1000 ppm	2000 ppm
35ºC	static	64.42	69.93	77.59
	5729	50.71	58.46	64.57
	10025.78	38.85	55.67	62.24
	14322.55	32.67	51.05	57.18
	20051.58	31.2	48.41	55.27
45ºC	static	52.97	65.58	66.35
	6887.8	47.41	51.59	59.92
	12053.77	45.33	50.03	57.3
	17219.67	40.25	47.45	49.57
	24107.54	35.13	43.09	43.43
60ºC	static	55.3	64.25	65.54
	8734.89	44.2	49.19	53.16
	15286.07	45.8	48.85	50.71
	21837.24	40.5	42.4	47.96
	30572.139	39	40.02	41.26

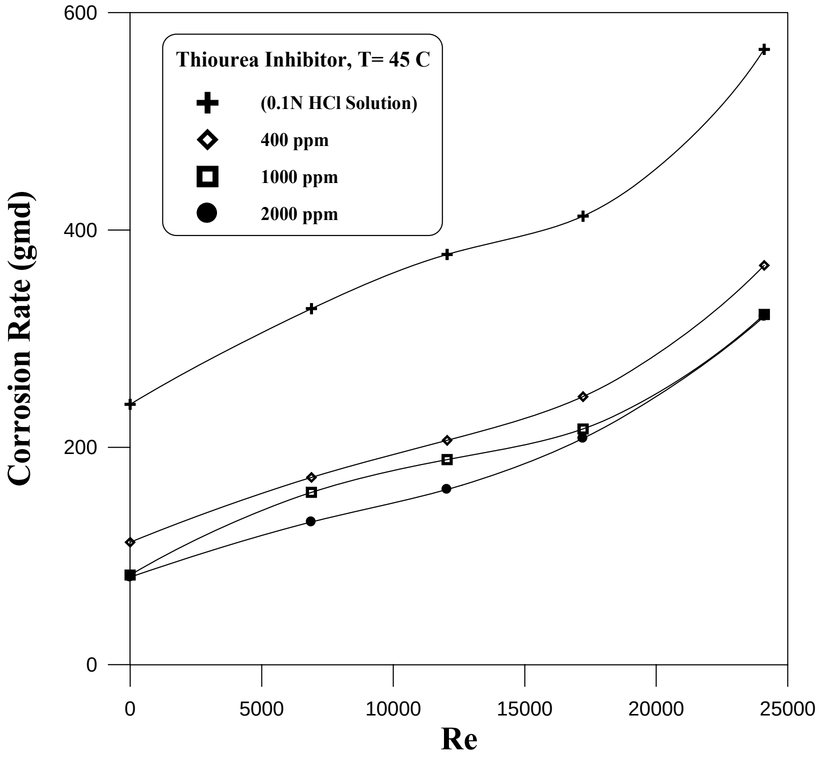

Figure 5-9 Variation of Corrosion Rate with Reynolds Number in Presence of Thiourea Inhibitor at T= 45°C.

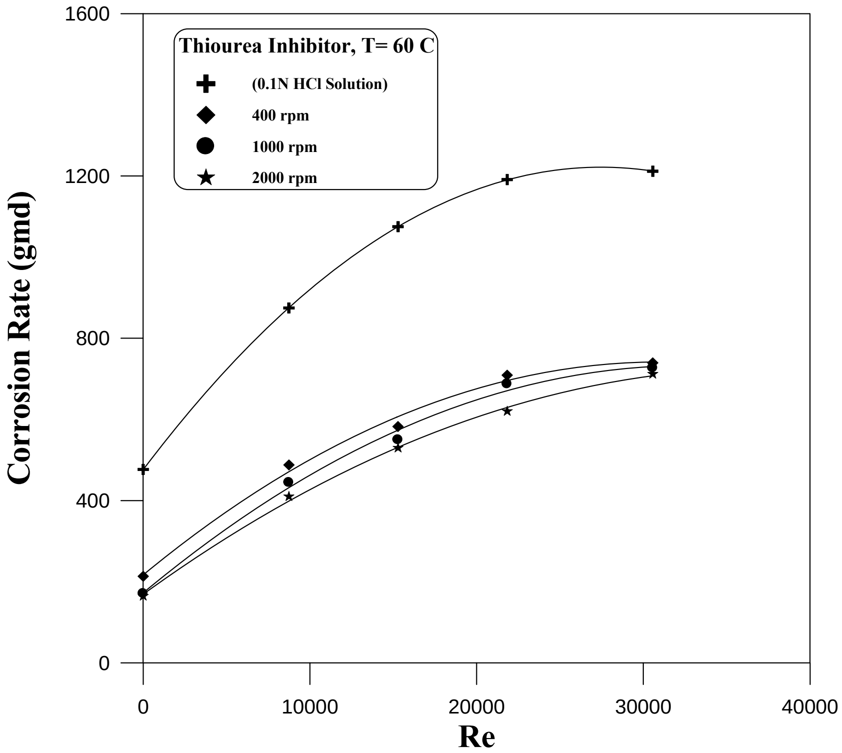

Figure 5-10 Variation of Corrosion Rate with Reynolds Number in Presence of Thiourea Inhibitor at T= 60°C.

Shetty, et al. [63] stated that thiourea and its derivatives decrease the corrosion rate of mild steel in aqueous solutions of HCl as well H_2SO_4, by forming adsorption layer on the metal surface to decrease the anodic reaction, i.e. it works as anodic inhibitor. While Shen, et al. [10] stated that thiourea simultaneously acts in both anodic and cathodic areas by decreasing the corrosion rate of mild steel (dissolution process of iron) in dilute HCl solution and decreasing the oxygen reduction and hydrogen evolution.

Figures 5.11 through 5.13 show the variation of corrosion rate with Re at three temperatures 35ºC, 45ºC and 60ºC and at constant thiourea concentrations of 400, 1000 and 2000 ppm respectively. It is clear from these figures that the corrosion rate increased with increasing temperature for the particular inhibitor concentration and Re. From figure 5.11, CR under static conditions at 35ºC, 45ºC and 60ºC are equal to 62.532, 112.6063 and 213.1951 gmd respectively. Similar behavior was observed in figure 5.12 and 5.13 where it is clear from these figures that for the same Re and temperature the CR decreases with increasing concentration of thiourea inhibitor; for Re = 6887.8 (u = 400 rpm), at 45ºC and 400 ppm is equal to 172.245 gmd while CR for the same Re and temperature but at 1000 and 2000 ppm is equal to 158.53 and 131.27gmd respectively.

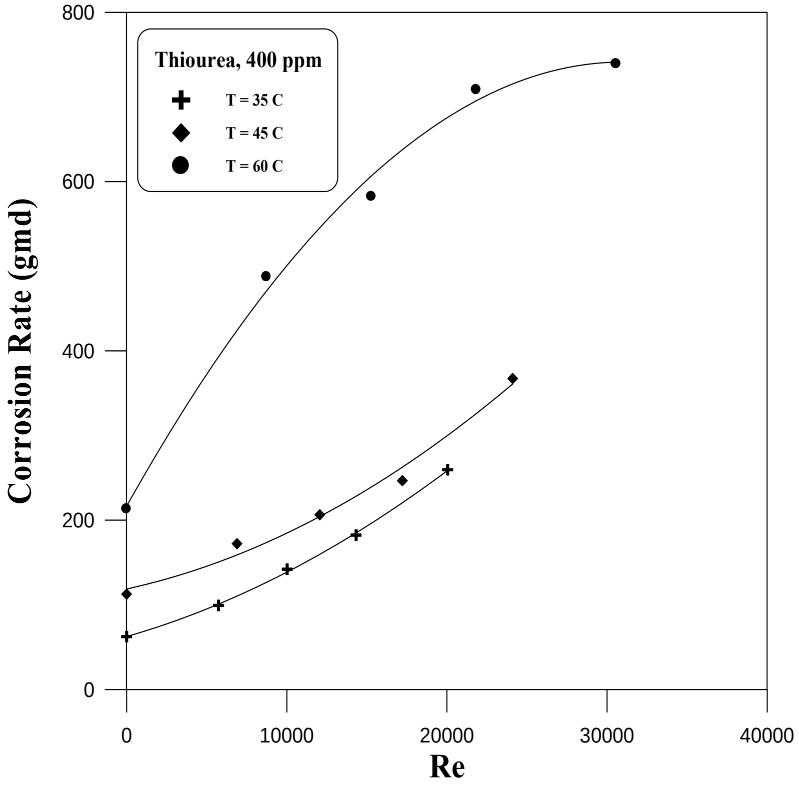

Figure 5-11 Corrosion Rate versus Reynolds Number in Presence of Thiourea Inhibitor at Concentration of 400 ppm.

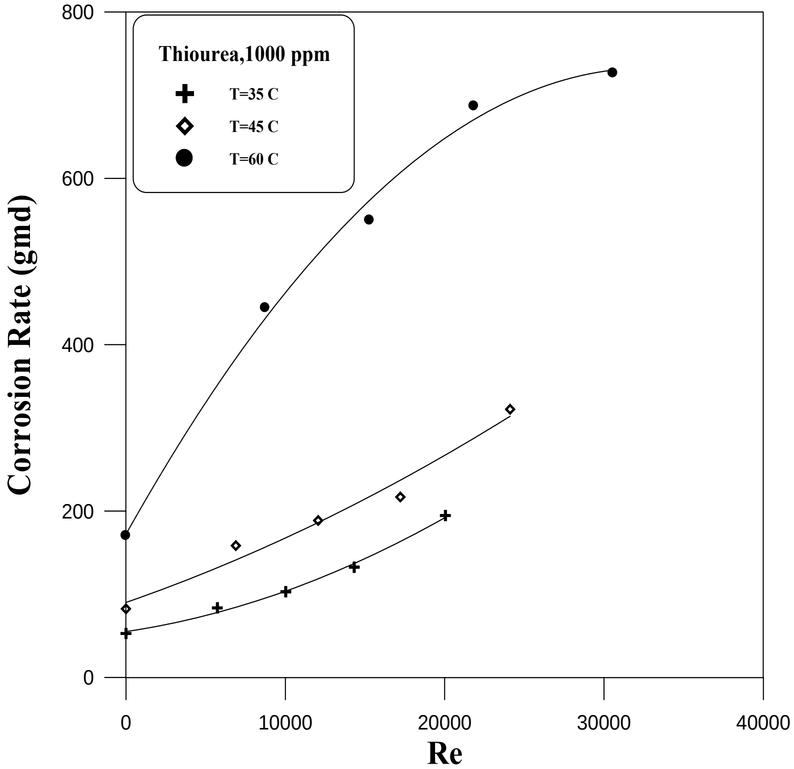

Figure 5-12 Corrosion Rate versus Reynolds Number in Presence of Thiourea Inhibitor at Concentration of 1000 ppm.

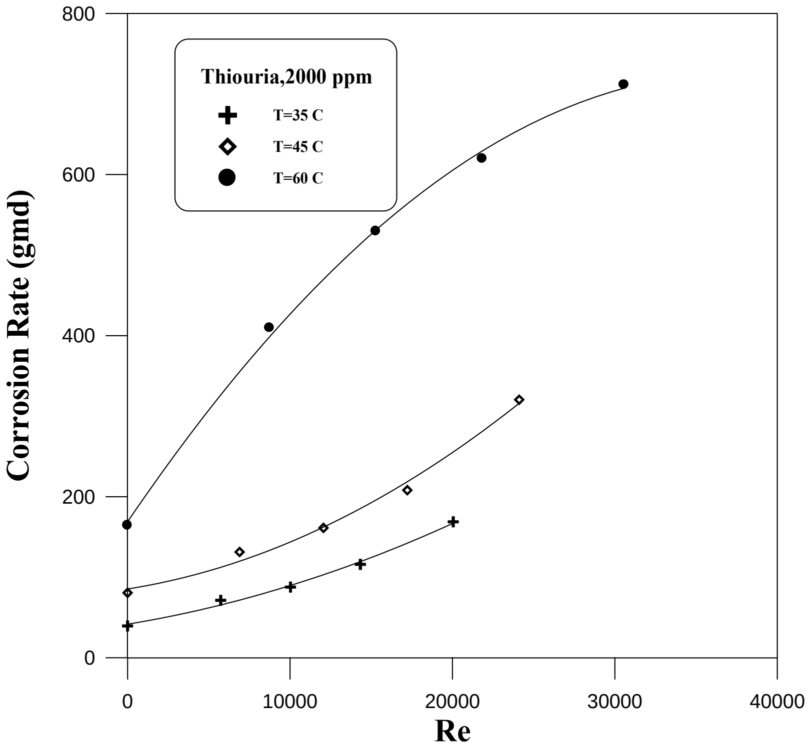

Figure 5-13 Corrosion Rate versus Reynolds Number in Presence of Thiourea Inhibitor at Concentration of 2000 ppm.

Figures 5.14 through 5.16 show the comparison of inhibitors efficiencies at temperature of 35ºC. It can be seen from these figures that the efficiency of thiourea is the highest followed by ethylene diamine, diethanol amine and formaldehyde inhibitor. As shown in fig. 5.14 it is clear that inhibitor efficiency of any inhibitor used, increased with increasing its concentration and decreased with increasing rotational speeds (or Re) at a given temperature. The inhibition efficiency of thiourea decreased from 64.42% under stationary conditions to 31.2% at Re = 20,000 and concentration of 400 ppm. Figure 5.15 shows likewise that the inhibition efficiency of thiourea decreased from 69.93% under static conditions to 48.41% at a concentration of 1000 ppm. Also the inhibition efficiency of thiourea at static condition (u=0 rpm) is equal to 77.59% but decreased at Re = 20,000 to 55.27. It is evident from figure 5.14 at (0 – 400) rpm the inhibition efficiency (η %) for each inhibitor was clearly decreasing but this decrease from (400-1400) rpm gradually became stable. This trend of behavior is the same in figure 5.15 at 1000 ppm concentration of each inhibiter except for formaldehyde inhibitor, where its inhibition efficiency (η) is uniformly decreasing with increasing from (0-1400) rpm. As shown in figure 5.16 it is evident that (η) only for thiourea and formaldehyde inhibitor becomes nearly stable in the Re range of 14322.55 – 20051.58.

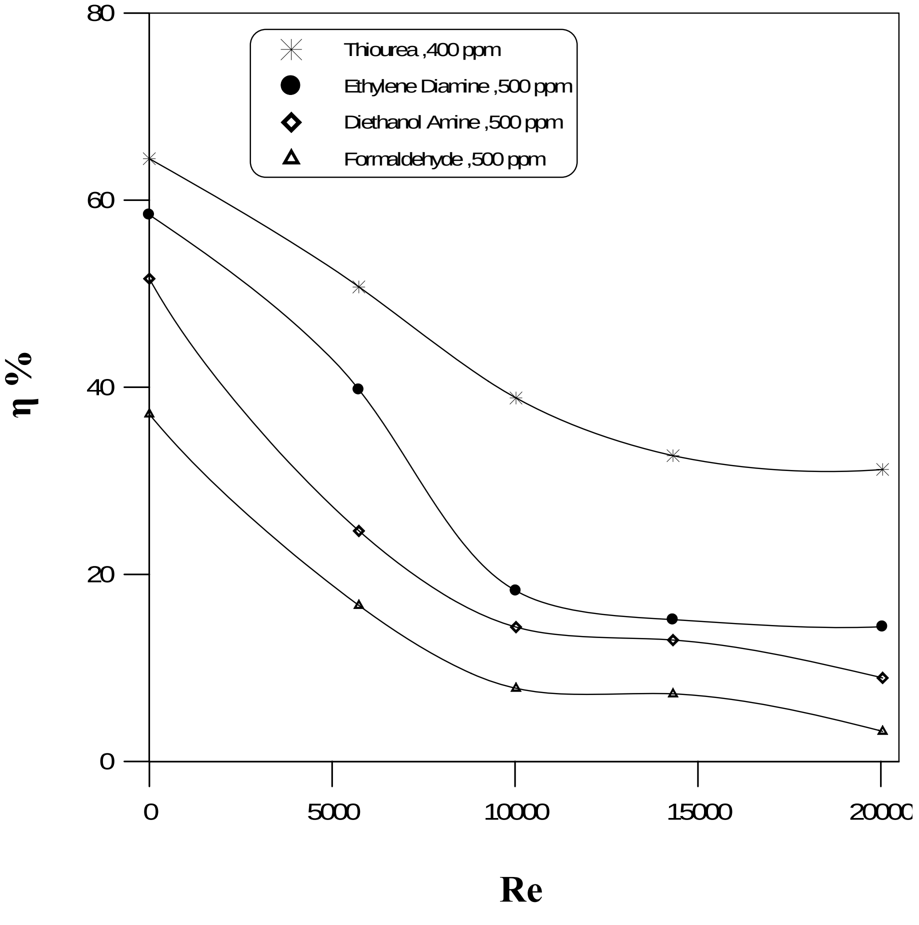

Figure 5-14 Comparison among Inhibitors Efficiencies at T= 35°C.

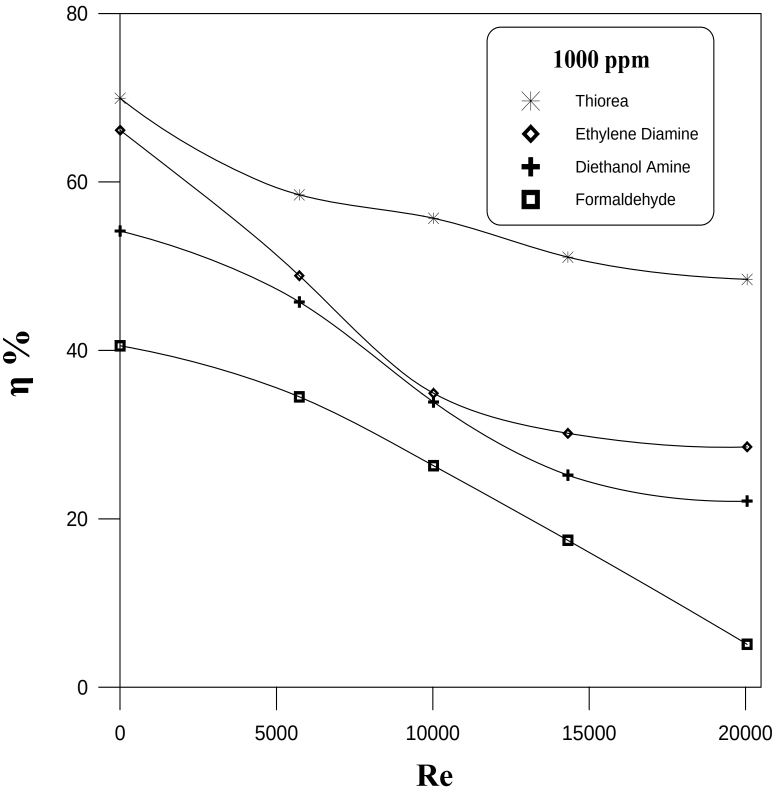

Figure 5-15 Comparison among Inhibitors Efficiencies at the Same Concentration of 1000 ppm at T= 35°C.

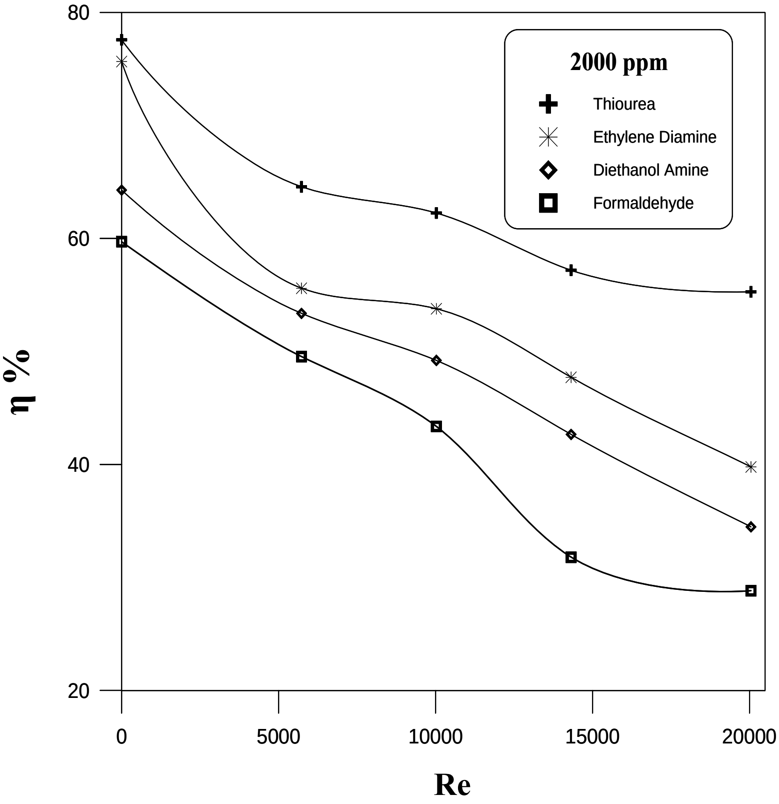

Figure 5-16 Comparison among Inhibitors Efficiencies at the Same Concentration of 2000 ppm at T= 35°C.

Figures 5.17 through 5.20 show the variation of inhibition efficiency (η) with Re in the presence of thiourea, formaldehyde, diethanol amine and ethylene diamine respectively. It is evident from these figures that the inhibition efficiencies of thiourea are better than other inhibitors at the same temperature, Re, and inhibitor concentration. At static conditions, T = 35ºC, 2000 ppm, the inhibition efficiency of each inhibitor is 77.59%, 59.7%, 64.3% and 75.7% respectively. As shown in figure 5.17, the inhibition efficiencies (η) of thiourea at a concentration of 2000 ppm are better than other concentrations. Also it is observed that its efficiency for each concentration decreases with increasing the rotational velocity (or Re). The same behavior is observed in figures 5.18 – 5.20 at a concentration of 500 ppm and Re > 10,000 (or rpm > 700) as the inhibition effect becomes nearly gradually constant. Figure 5.20 shows the efficiency behavior of ethylene diamine is similar to the behavior observed for thiourea inhibitor.

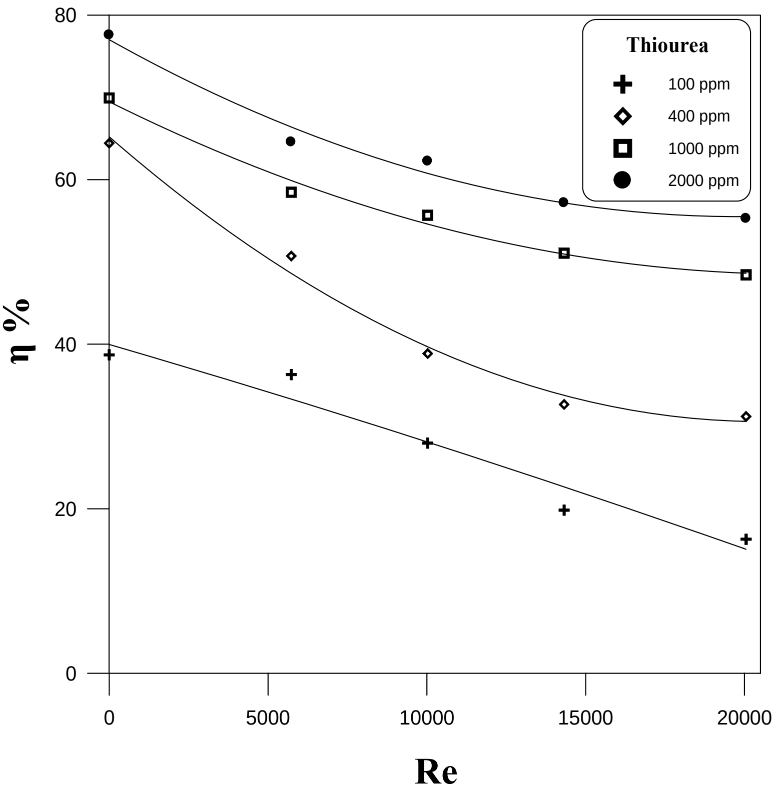

Figure 5-17 Variation of Inhibition Efficiency with Reynolds Number in Presence of Thiourea Inhibitor at T= 35°C.

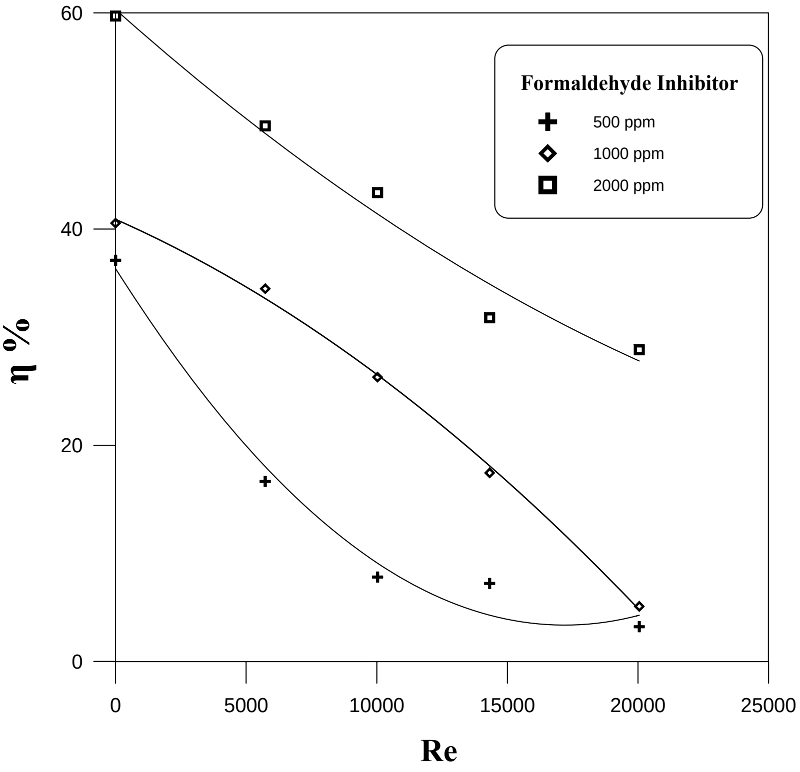

Figure 5-18 Variation of Inhibition Efficiency with Reynolds Number in Presence of Formaldehyde Inhibitor at T= 35°C.

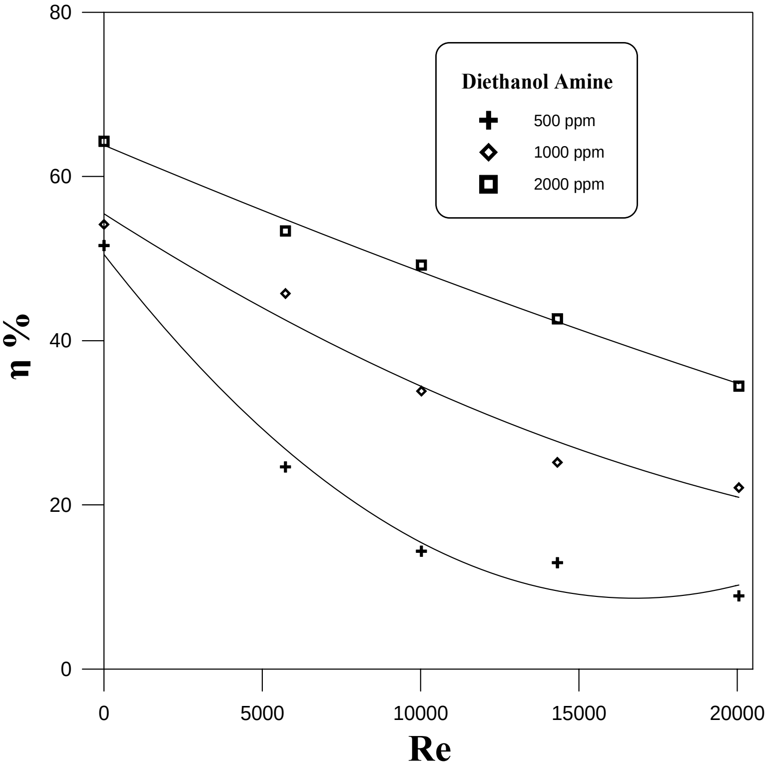

Figure 5-19 Variation of Inhibition Efficiency with Reynolds Number in Presence of Diethanol Amine at T= 35°C.

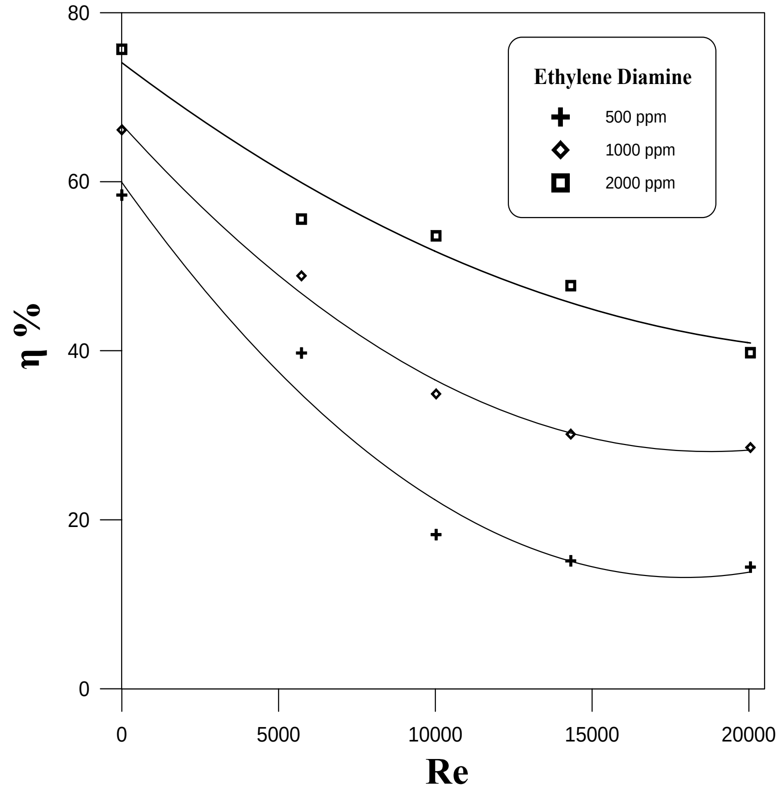

Figure 5-20 Variation of Inhibition Efficiency with Reynolds Number in Presence of Ethylene Diamine Inhibitor at T= 35°C.

The variation of inhibition efficiency versus Re in the presence of thiourea inhibitor at concentrations of 1000 ppm and 2000 ppm and three temperatures 35, 45 and 60ºC has been calculated. These are presented in figures 5.21 and 5.22. The inhibition efficiency (η) of thiourea at 35ºC is higher than at 45ºC and the latter is slightly higher than at 60ºC. It is evident that the inhibition efficiency at inhibitor concentration of 1000 ppm is lower than at 2000 ppm for the same temperature, as an example the (η) at 1000 ppm, 35ºC, and (0 rpm) is equal to 69.93%, and at 2000 ppm and similar conditions it is equal to 77.59%.

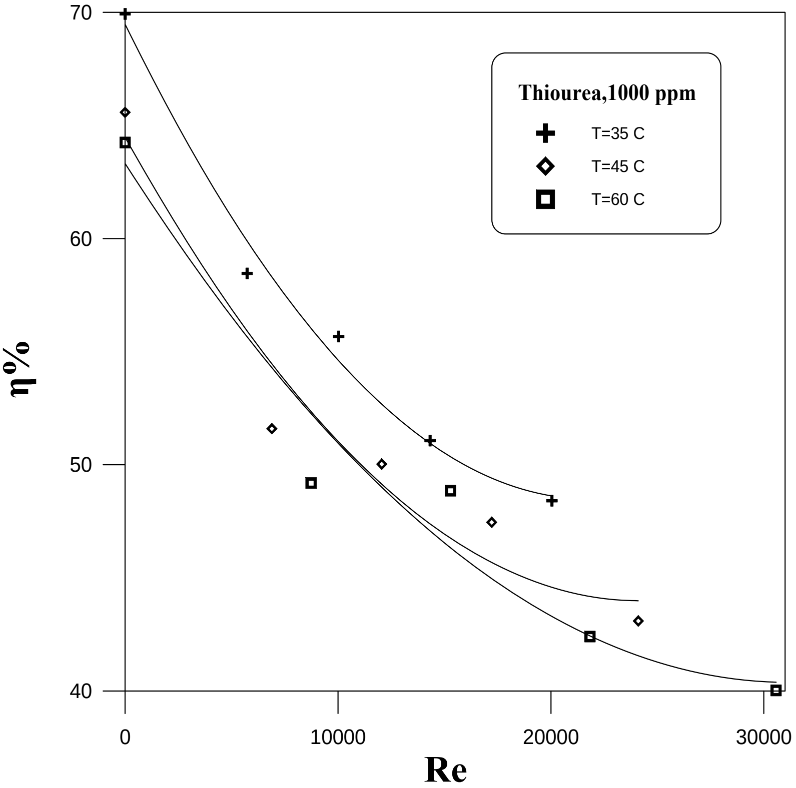

Figure 5-21 Inhibition Efficiency for Thiourea Inhibitor at Concentration of 1000 ppm versus Reynolds Number.

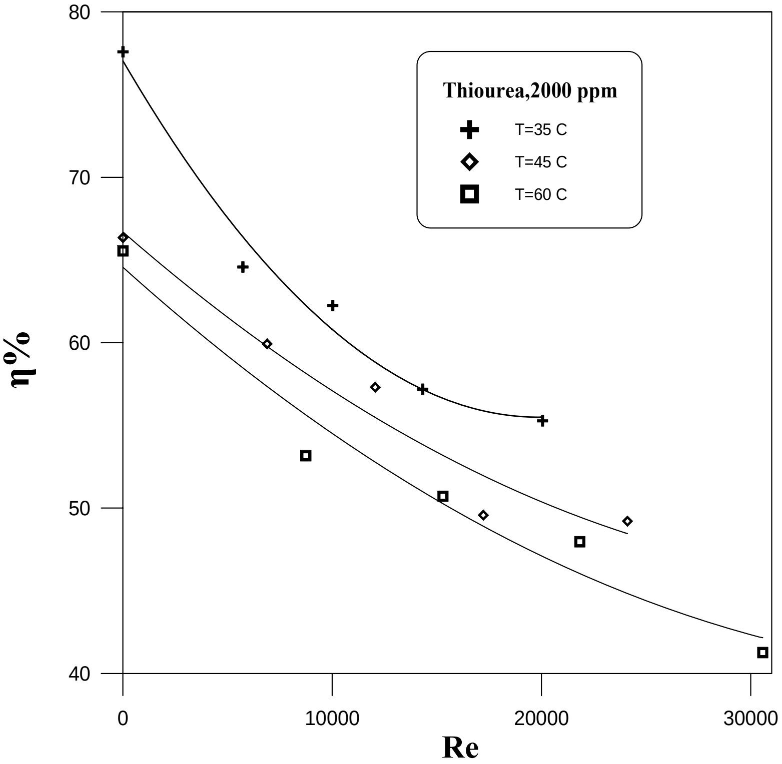

Figure 5-22 Inhibition Efficiency for Thiourea Inhibitor at Concentration of 2000 ppm versus Reynolds Number.

Figures 5.23 and 5.24 shows a gradual decrease in inhibition efficiency of thiourea with increasing rotational velocity for each concentration. Also it is observed that the inhibition efficiency for this inhibitor at a constant concentration decreases with increasing temperature, and it is clear that at concentrations of 1000 ppm and 2000 ppm and for the two temperatures 45ºC and 60ºC the range of inhibition efficiency at higher velocities (1400 rpm) is between 40 – 45% as it is shown in table (5-2).

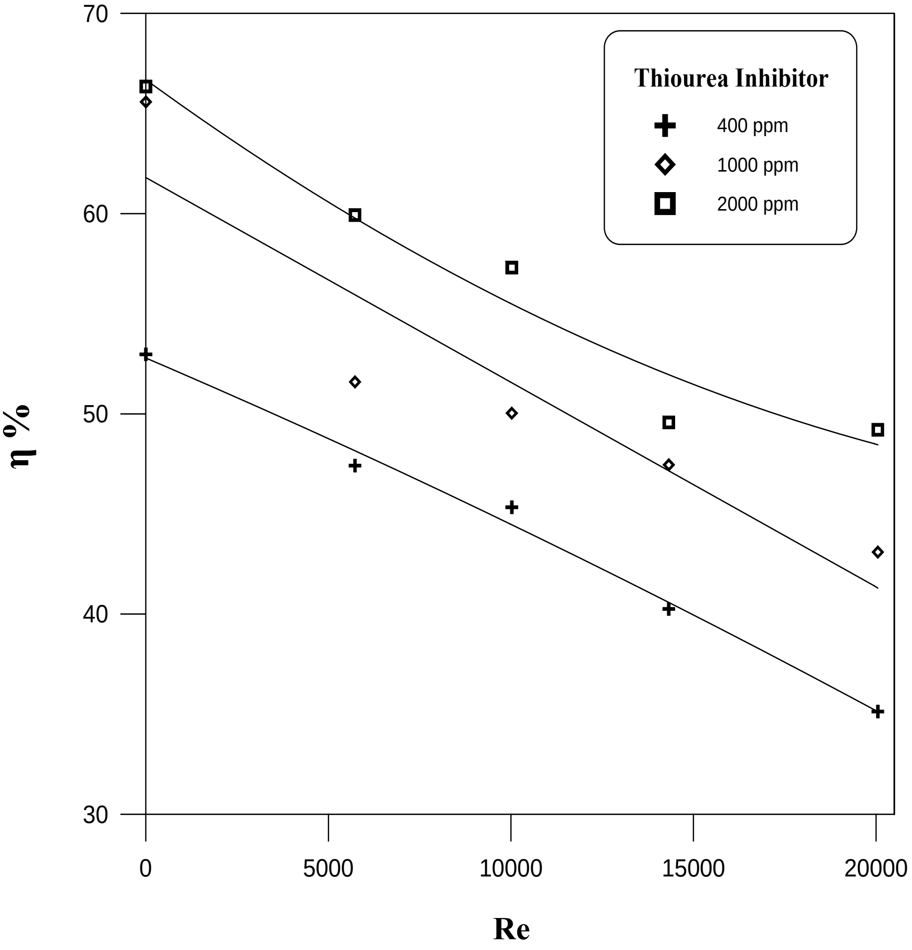

Figure 5-23 Variation of Inhibition Efficiency with Reynolds Number in Presence of Thiourea Inhibitor at T=45°C.

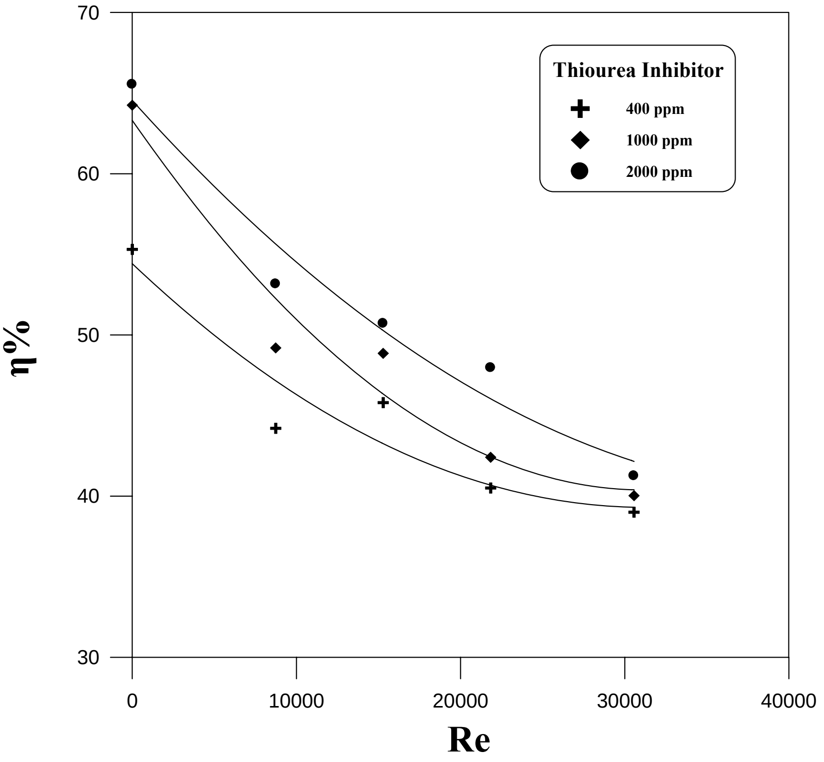

Figure 5-24 Variation of Inhibition Efficiency with Reynolds Number in Presence of Thiourea Inhibitor at T=60°C.

5.3 Corrosion Current of Iron (i_{Fe})

The molar flux is estimated from weight loss using the following equation [16]:

$$N_{A_{Fe}} = \frac{\left(\Delta W / M.Wt\right)}{A \times t \times 3600} \qquad (\text{Mole}/\text{m}^2.\text{s}) \qquad \ldots (5.4)$$

Molecular weight of iron metal ($M.Wt_{Fe}$) = 55.857 g/gmol.

The corrosion current of iron is calculated from the following equation [16]:

$$i_{Fe} = N_{A_{Fe}} \times Z \times F \qquad (\text{A}/\text{m}^2) \qquad \ldots (5.5)$$

$$\text{Fe} \longrightarrow \text{Fe}^{2+} + 2e \quad , \quad Z=2$$

5.3.1 Effect of Temperature and Rotational Velocity

Figure 5.25 shows the variation of corrosion current of iron (i_{Fe}) as calculated from weight loss values of iron metal (i_{Fe}) with Re at three temperatures. It is clearly seen that the behavior is similar to that observed in figure 5.1. It is observed that i_{Fe} increases with increasing temperature being much higher at 60ºC due to its exponential behavior with temperature.

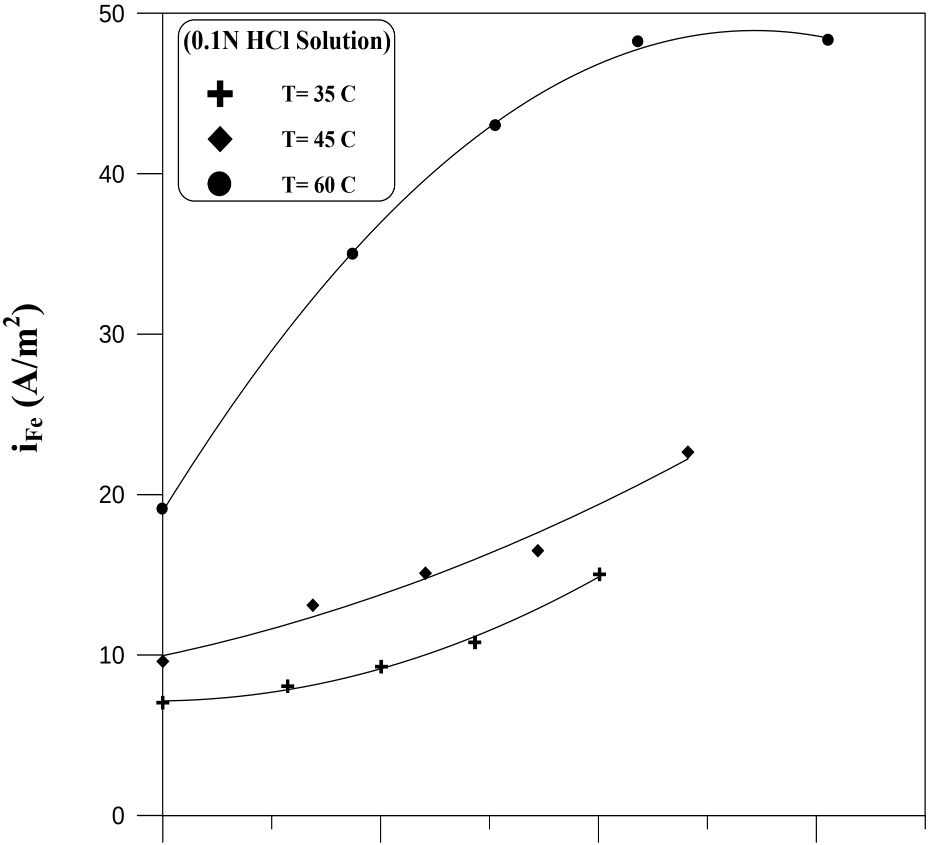

Figure 5-25 Corrosion Current of Iron Metal versus Reynolds Number Without Inhibitor.

5.3.2 Effect of Inhibitor Concentration

The relationship between Re and corrosion current of iron metal (i_{Fe}) in presence of formaldehyde, diethanol amine, ethylene diamine and thiourea inhibitors are shown in figures 5.26 and A.1-A.3 (appendix A) as a function of the inhibitor concentration at 35ºC. It is clear that the trend in these figures is almost similar to that of figures 5.2 through 5.5.

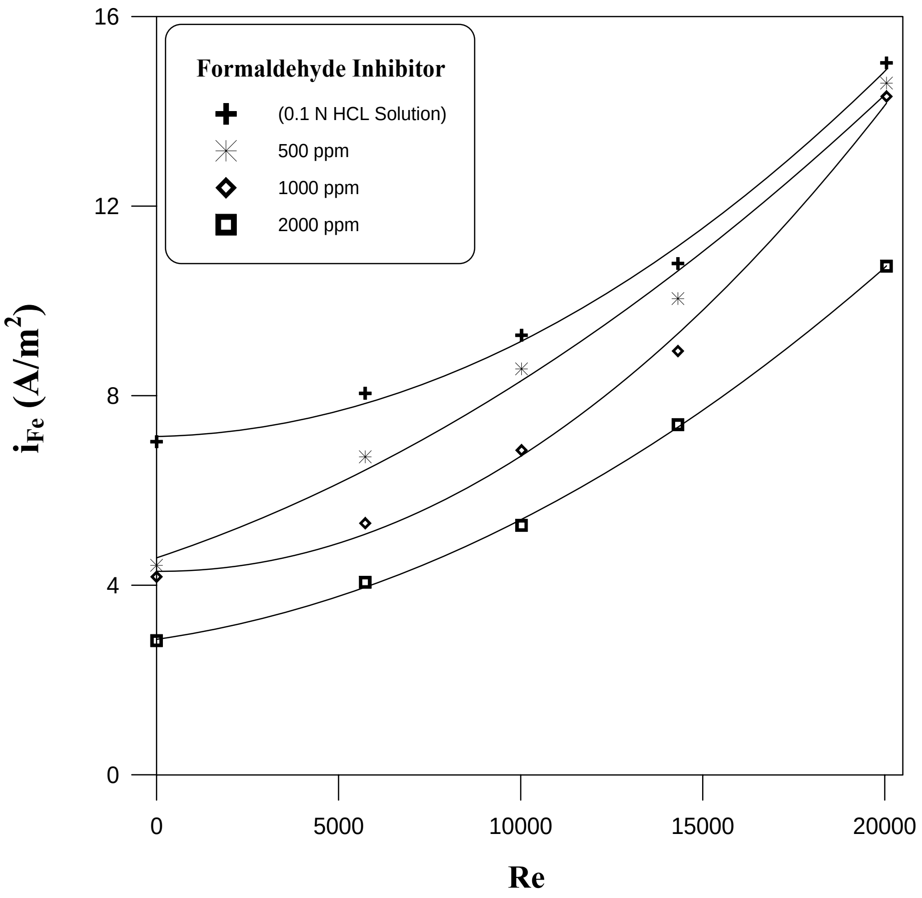

Figure 5-26 Variation of Corrosion Current of Iron Metal with Reynolds Number in Presence of Formaldehyde Inhibitor at T= 35°C.

Figures A.4 and A.5 (appendix A) show the variation of corrosion current of iron metal (i_{Fe}) with Re as a function of concentration of thiourea at 45ºC and 60ºC. It is clearly seen that the behavior of (i_{Fe}) in the presence of thiourea inhibitor with Re is similar to that presented in figures 5.9 and 5.10 under the same conditions of concentrations of thiourea and temperature.

Figures 5.27, A.6 and A.7 show the variation of corrosion current of iron metal with Re at three temperatures 35ºC, 45ºC and 60ºC and at constant thiourea concentrations of 400, 1000 and 2000 ppm respectively .

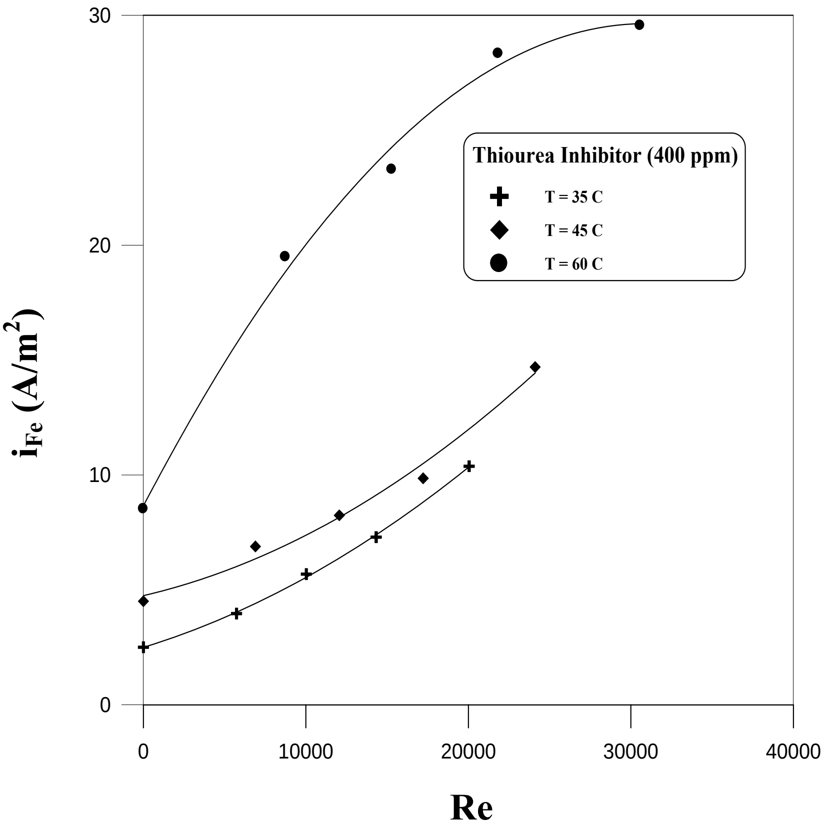

Figure 5-27 Corrosion Current of Iron Metal versus Reynolds Number for Thiourea Inhibitor at Concentration of 400 ppm.

The comparison among corrosion currents of iron metal among the four inhibitors at one temperature 35ºC is shown in figures 5.28, A.8 and A.9. Such behavior is similar to that observed in figures 5.6 through 5.8.

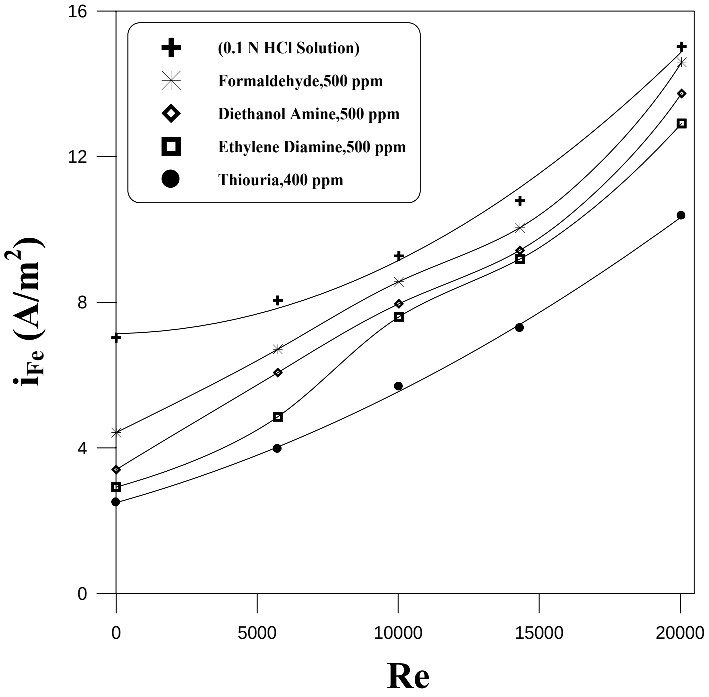

Figure 5-28 Variation of Corrosion Current of Iron Metal with Reynolds Number for Various Inhibitors at T=35°C.

5.4 Corrosion Current of Oxygen (i_{O2})

Corrosion current of oxygen is mass transfer controlled and is highly affected or influenced by the temperature of the corrosive solution and the rotational velocities, i.e., Reynolds number.

For oxygen transfer in a stirred solution (flow condition), the mass transfer coefficient is estimated from equation (5.6) [81].

$$Sh=\left(\frac{K\times d}{D}\right)=0.0791\times \mathrm{Re}^{0.7}\times SC^{0.356} \qquad \ldots (5.6)$$

$$\mathrm{Re} = \frac{\rho \times d^2 \times N}{\mu} \qquad ... (5.7)$$

$$Sc = \frac{\mu}{\rho \times D} \qquad \ldots (5.8)$$

$$K \times C_b = \left(\frac{i_L}{Z \times F} \right) \qquad \dots (5.9)$$

where:

$$i_L = i_{O_2} \quad , \quad Z = 4$$

While for oxygen transfer in an unstirred solution (static condition), the mass transfer coefficient is estimated from equation (5.10) [2]. The physical properties of the solution are presented in table B-2 in appendix B [13, 16].

$$i_{O_2} = i_l = \frac{D \times Z \times F}{\delta \times t_n} \times C_b \times 10^{-3} \; (\text{A/cm}^2) \qquad \dots (5.10)$$

where:

δ = Thickness of the stagnant layer of electrolyte next to the electrode Surface (about 0.05 cm in an unstirred solution).

t_n = transference number = 1

Figure 5.29 shows the variation of oxygen current at E_{corr} with Reynolds no. at three temperatures as a parameter, where it is clear from this figure that the value of i_{O2} under static conditions and flow conditions increases with increasing the rotational velocity and increasing the temperature of the corrosive solution as shown in table 5-3.

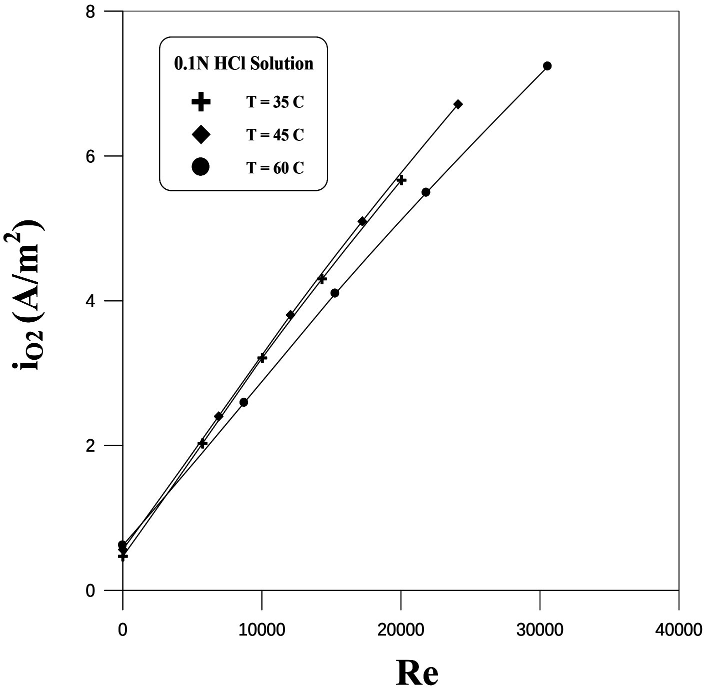

Figure 5-29 Variation of Corrosion Current of Oxygen with Reynolds Number at Various Temperatures.

Table 5-3 The Effect of Temperature and Rotational Velocity on the Corrosion Current of Oxygen (i_{O2}).

Temperature	Re	i_{O2} (A/m^2)
35ºC	static	0.47
	5729	2.0285
	10025.78	3.2097
	14322.55	4.3002
	20051.58	5.6665
45ºC	static	0.563
	6887.8	2.4039
	12053.77	3.8038
	17219.67	5.0960
	24107.54	6.7152
60ºC	static	0.62
	8734.89	2.5906
	15286.07	4.0992
	21837.24	5.4918
	30572.139	7.2367

5.5 Current of Hydrogen Evolution (i_{H2})

At the corrosion potential (E_{Corr}).

$$\sum i_a = \sum i_C \ ,$$

hence

$$i_{Fe} = i_{O_2} + i_{H_2}$$

$$\therefore i_{H_2} = i_{Fe} - i_{O_2}$$

Current of hydrogen evolution (i_{H2}) is activation controlled and is highly affected or influenced by: inhibitor concentration, temperature, and it is not affected by velocity [4]. The decrease in hydrogen evolution current with increasing corrosion potential because of oxygen transfer from the bulk solution to the metal surface, leads to make the corrosion potential more positive, while the increase in hydrogen evolution current at high velocity may arise from the removal of protective oxide layer that forms on the metal surface in oxygenated systems.

Figure 5.30 shows the variation of hydrogen evolution current at the corrosion potential (i_{H2}) with Re at three temperatures. This figure shows that the values of (i_{H2}) at 35ºC is slightly lower than at 45ºC and the latter is markedly lower than at 60ºC, so the behavior of (i_{H2}) is similar to that of (i_{Fe}) and the corrosion rate at the same temperature.

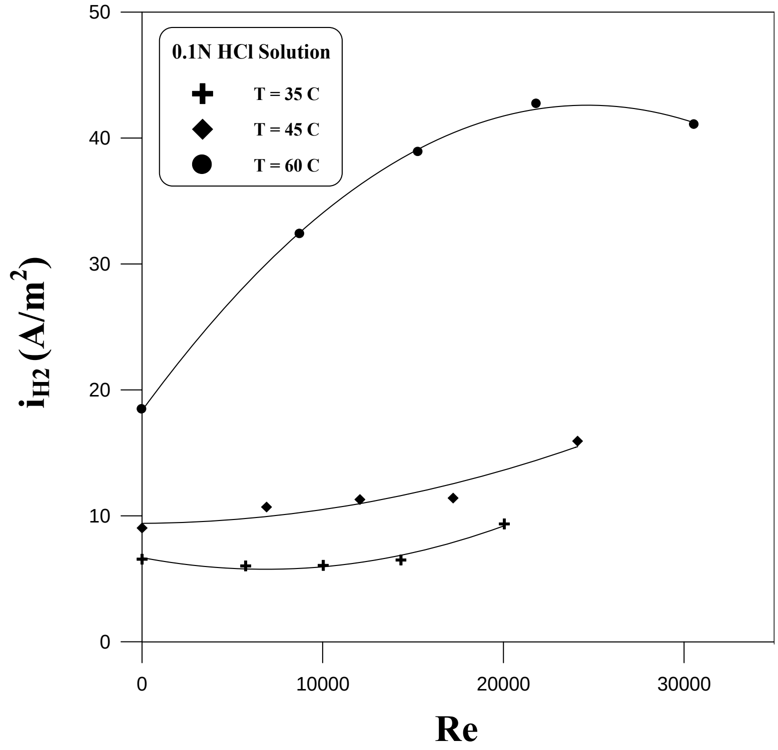

Figure 5-30 Current of Hydrogen Evolution at E_{corr} versus Reynolds Number without Inhibitor at Various Temperatures.

Figures 5.31–5.34 show the effect of inhibitor concentration on hydrogen evolution current at the corrosion potential (i_{H2}) in the presence of formaldehyde, diethanol amine, ethylene diamine and thiourea inhibitors respectively. It is revealed that the values of (i_{H2}) decrease with increasing the concentration of these inhibitors at the same temperature of 35°C. From table 5-4 it is clear that the order of values of (i_{H2}) at the same velocity for the four inhibitors is in the following decreasing order: formaldehyde > diethanol amine > ethylene diamine > thiourea.

Table 5-4 Hydrogen Evolution Current at E_{corr} in Presence of 1000 ppm of Various Inhibitors at 35°C.

Rotational Velocity (rpm)	i_{H2} (A/m^2)				
	$C_{inh.}$=0	Formaldehyde	Diethanol amine	Ethylene diamine	Thiourea
static	6.5575	3.7086	2.7514	1.9095	1.6446
400	6.0220	3.2792	2.3397	2.0886	1.3157
700	6.0630	3.6374	2.9350	2.8384	0.9082
1000	6.4879	4.6396	3.8025	3.2654	0.9988
1400	9.3573	8.6469	6.0832	5.1104	0.9531

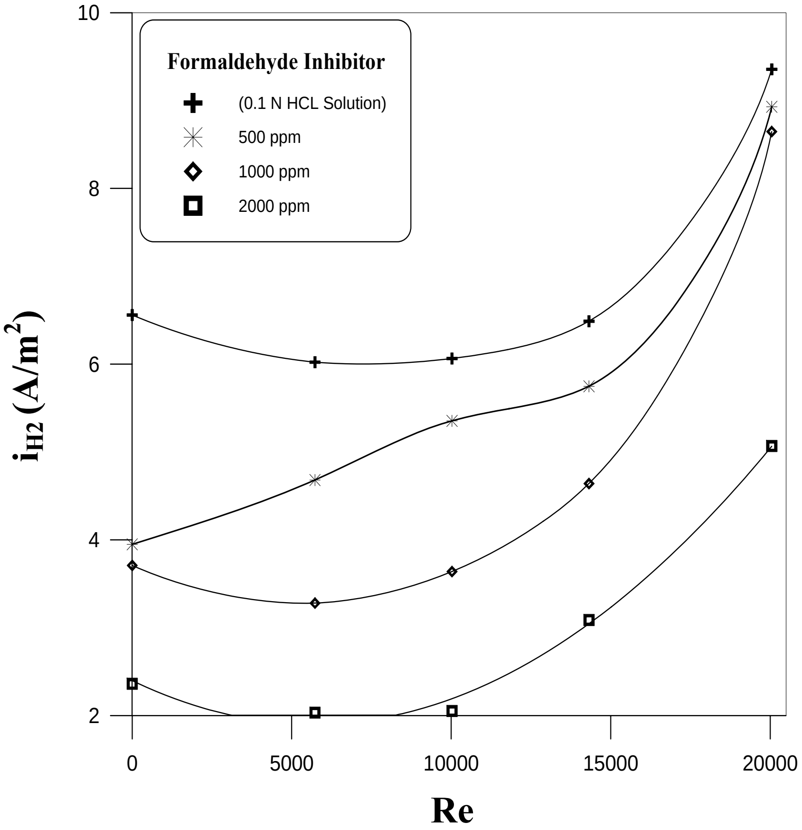

Figure 5-31 Variation of Current of Hydrogen Evolution at E_{corr} with Reynolds Number in Presence of Formaldehyde Inhibitor at T=35°C.

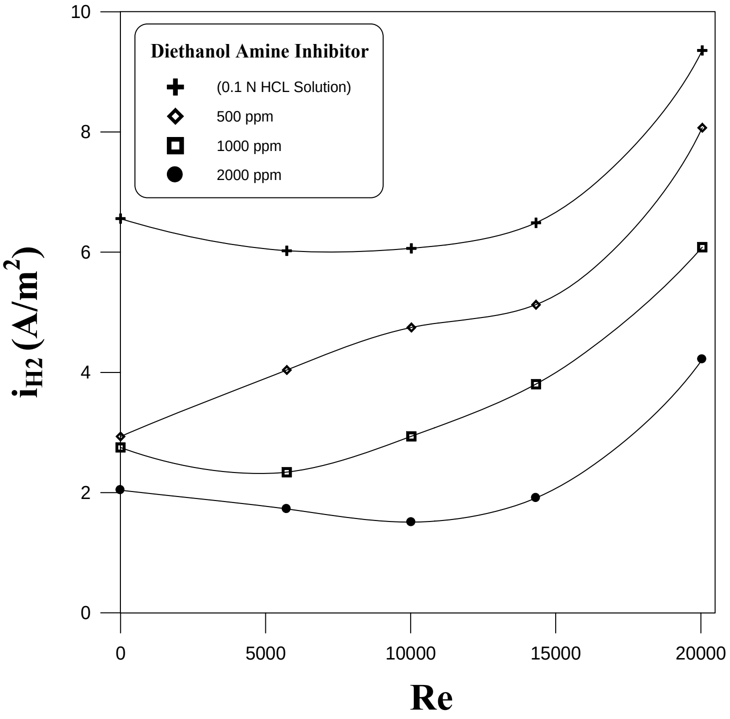

Figure 5-32 Variation of Current of Hydrogen Evolution at E_{corr} with Reynolds Number in Presence of Diethanol Amine Inhibitor at T=35°C.

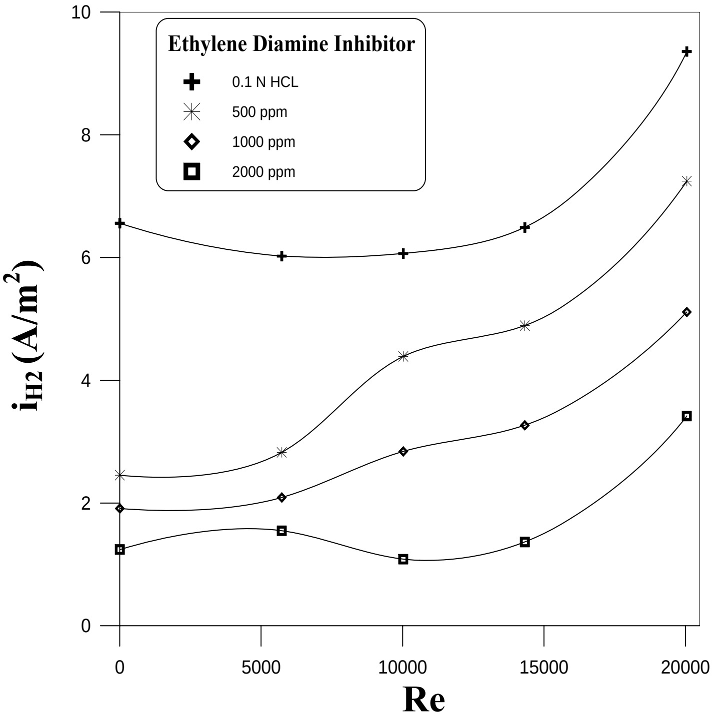

Figure 5-33 Variation of Current of Hydrogen Evolution at E_{corr} with Reynolds Number in Presence of Ethylene Diamine Inhibitor at T=35°C.

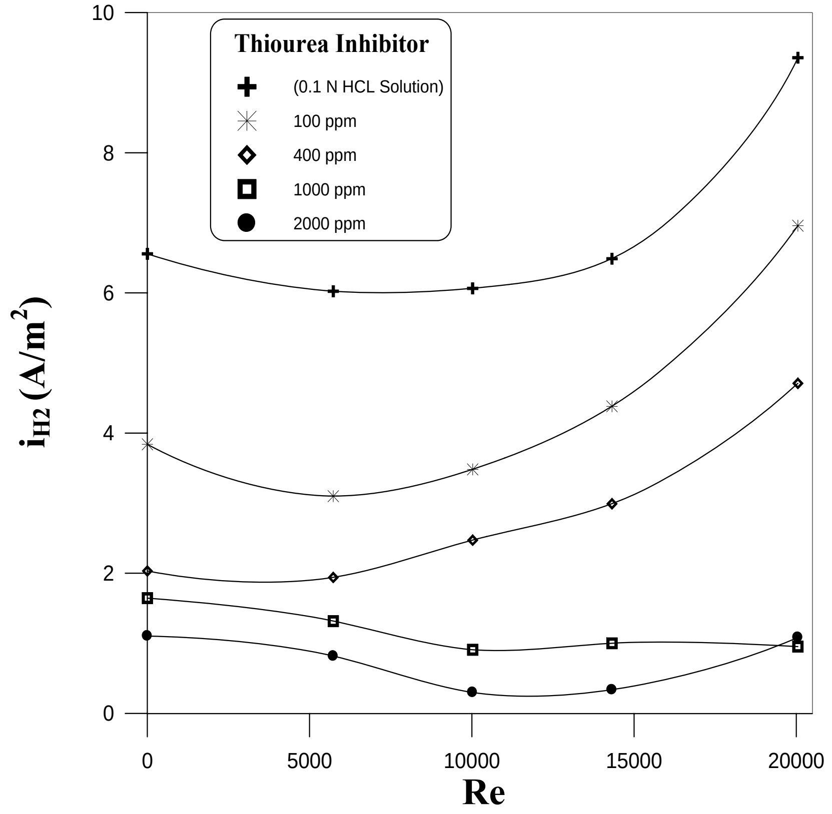

Figure 5-34 Variation of Current of Hydrogen Evolution at E_{corr} with Reynolds Number in Presence of Thiourea Inhibitor at T=35°C.

Figure 5.35 shows the effect of inhibitor concentration as a parameter on the hydrogen evolution current at the corrosion potential (i_{H2}) in the presence of thiourea inhibitor at 45°C. It is evident from table 5-5 that the values of (i_{H2}) with this inhibitor increase with increasing the temperature of the corrosive solution and decrease with increasing the concentration of this inhibitor.

Table 5-5 Hydrogen Evolution Current at E_{corr} under the Influence of Concentration of Thiourea Inhibitor and the Temperature of the Corrosive Solution.

Temperature	Rotational Velocities (rpm)	i_{H2} (A/m^2)			
		$C_{inh.}$=0	400 ppm	1000 ppm	2000 ppm
35ºC	static	6.5575	2.0303	1.6446	1.1048
	400	6.0220	1.9396	1.3157	0.8152
	700	6.0630	2.4706	0.9082	0.2979
	1000	6.4879	2.9904	0.9988	0.3364
	1400	9.3573	4.7093	0.9531	1.0819
45ºC	static	9.0322	3.9396	2.7326	2.6587
	400	10.6924	4.4833	3.9350	2.84
	700	11.2896	4.4392	3.7381	2.6409
	1000	11.4056	4.7565	3.5685	3.2254
	1400	15.9282	7.9761	6.1709	6.0947
60ºC	static	18.4486	7.9046	6.1903	5.9453
	400	32.3706	16.9033	15.1767	13.7875
	700	38.8785	19.1952	17.8861	17.0882
	1000	42.7128	22.8484	21.9782	19.2865
	1400	41.0657	22.3248	21.8278	21.2116

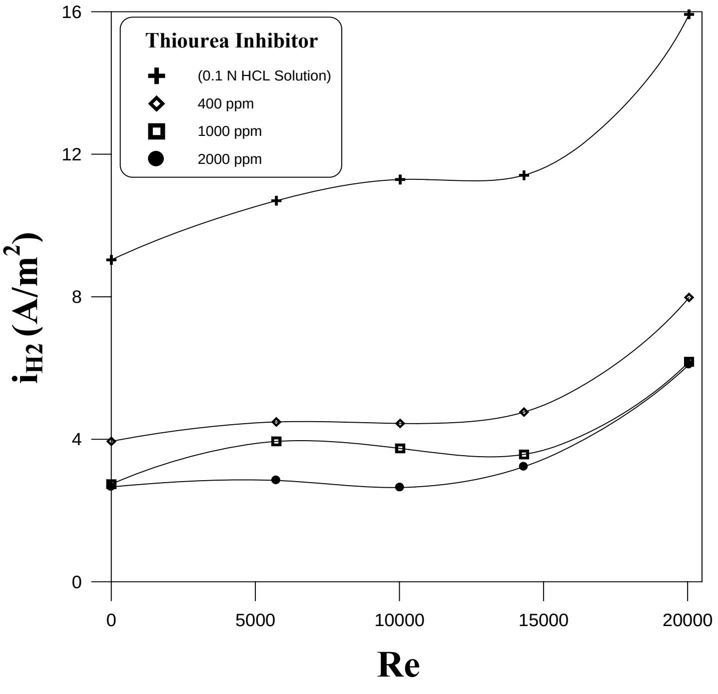

Figure 5-35 Variation of Current of Hydrogen Evolution at E_{corr} with Reynolds Number in Presence of Thiourea Inhibitor at T=45°C.

Figure A.10 shows the effect of inhibitor concentration as a parameter on the hydrogen evolution current at the corrosion potential (i_{H2}) in presence of thiourea inhibitor at 60°C, where it is also clear that the values of (i_{H2}) increase with decreasing the concentration of this inhibitor as shown in table 5-5.

Figures 5.36, A.11 and A.12 show the variation of hydrogen evolution current at the corrosion potential (i_{H2}) in the presence of thiourea inhibitor with Re at three temperatures 35ºC, 45ºC and 60ºC as a parameter and at constant thiourea concentrations of 400, 1000 and 2000 ppm respectively. It is clear from these figures that the values of (i_{H2}) with thiourea as inhibitor at 35ºC is slightly lower than that observed at 45ºC and the latter is markedly lower than at 60ºC and as shown in table 5-5.

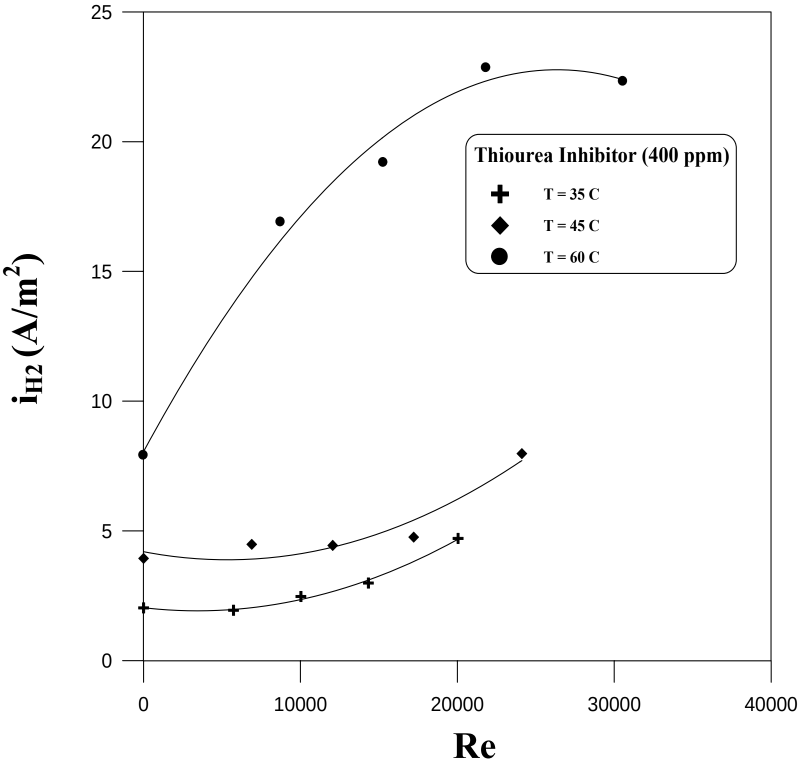

Figure 5-36 Variation of Current of Hydrogen Evolution at E_{corr} with Reynolds Number in Presence of Thiourea Inhibitor in Concentration of 400 ppm at Various Temperatures.

Figures 5.37, A.13 and A.14 show the effect of concentration of formaldehyde, diethanol amine, ethylene diamine and thiourea inhibitors respectively as a parameter on the hydrogen evolution current (i_{H2}) at one temperature 35°C. As shown in figure 5.37 which reveals that the values of (i_{H2}) at 35°C with thiourea inhibitor are lower than the other inhibitors then come ethylene diamine, diethanol amine and formaldehyde inhibitors. The same behavior is observed in figures A.13 and A.14 for these inhibitors at the same temperature and concentration of 1000 and 2000 ppm respectively. It is also observed from these figures that the values of (i_{H2}) as example for formaldehyde inhibitor at 35°C decreases with increasing the concentration of this inhibitor, and as shown in tables 5-6 and 5-7.

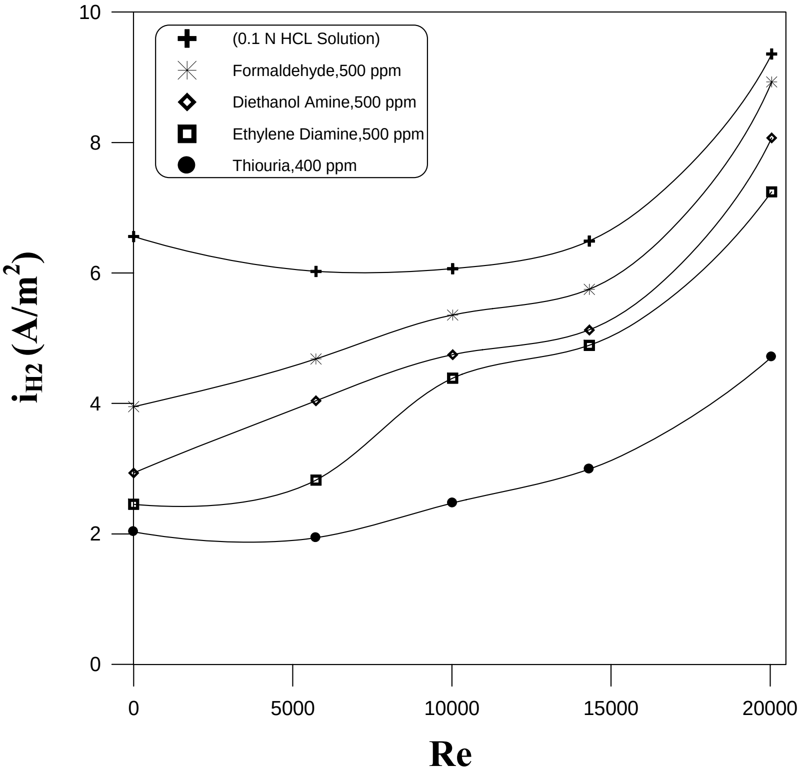

Figure 5-37 Current of Hydrogen Evolution at E_{corr} with Reynolds Number for Various Inhibitors at T= 35°C.

Table 5-6 Hydrogen Evolution Current at E_{corr} for Thiourea Inhibitor with Various Concentration at T=35°C.

Rotational Velocities (rpm)	i_{H2} (A/m^2)				
	$C_{inh.}$= 0	100 ppm	400 ppm	1000 ppm	2000 ppm
static	6.5575	3.8385	2.0303	1.6446	1.1048
400	6.0220	3.0997	1.9396	1.3157	0.8152
700	6.0630	3.4812	2.4706	0.9082	0.2979
1000	6.4879	4.3816	2.9904	0.9988	0.3364
1400	9.3573	6.9598	4.7093	0.9531	1.0819

Table 5-7 Hydrogen Evolution Current at E_{corr} in Presence of Various Inhibitors at 35°C.

Concentration (ppm)	Rotational velocity (rpm)	i_{H2} (A/m^2)		
		Formaldehyde	Diethanol amine	Ethylene diamine
500	Static	3.9488	2.932	2.452
	400	4.6808	4.0391	2.8243
	700	5.3539	4.7455	4.3860
	1000	5.7473	5.1246	4.8886
	1400	8.9297	8.0693	7.2429
1000	Static	3.7086	2.7514	1.9095
	400	3.2792	2.3397	2.0886
	700	3.6374	2.9350	2.8384
	1000	4.6396	3.8025	3.2654
	1400	8.6469	6.0832	5.1104
2000	Static	2.3613	2.04	1.2398
	400	2.033	1.7262	1.5475
	700	2.0516	1.5082	1.0837
	1000	3.0868	1.9098	1.3629
	1400	5.0667	4.2161	3.4168

5.6 Activation Energy for Experimental Results

Activation energies of the metal (Carbon Steel) in 0.1N HCl solution in the presence of different thiourea inhibitor concentrations (i.e., 400, 1000 and 2000 ppm) were calculated from Arrhenius plots, which represent the relationship between the logarithm of corrosion rate and the reciprocal of absolute temperature [16, 55]:

$$\text{Log CR} = \log A - \frac{E_a}{2.303\,RT} \qquad \text{... (5-11)}$$

Figures 5.38 through 5.47 represent this relation for thiourea concentration as a parameter and this means how the concentration of this inhibitor affects the activation energies under static and flow conditions. It is observed for 400, 1000 and 2000 ppm as concentration of thiourea inhibitor in 0.1N HCl solution, the activation energies of dissolution process at Re=5729 (or U=400 rpm) is 54.45, 56.93 and 59.84 KJ/mol respectively, as shown in table (5-8).

Table 5-8 Effect of Thiourea Concentration on Activation Energy at Various Velocities.

Rotational Velocity (rpm)	Activation Energy E_a (kJ/mol)		
	400 ppm	1000 ppm	2000 ppm
0	41.4	39.9	49.4
400	54.45	56.93	59.8
700	48.6	57.2	61.55
1000	47	56.53	57.3
1400	35.86	44.8	48.8

From table (5-8) it can be deduced that:

- Generally the higher the inhibitor concentration the higher the activation energy recorded for the dissolution process of the metal .This indicates that the reaction at the metal surface in the presence of thiourea inhibitor requires higher activation energy to proceed when the inhibitor concentration is increased.

- Except under static conditions, the activation energy which is required at 400 ppm thiourea concentration is higher than that required at 1000 ppm while the latter requires smaller activation energy compared to concentration of 2000 ppm.

Figures 5.38, 5.40, 5.42, 5.44 and 5.46 show the variation of corrosion rate with thiourea concentration at three temperatures 35, 45 and 60ºC as a parameter for 0-1400 rpm respectively, and it is clear that the values of corrosion rates decreased with increasing the concentration of thiourea inhibitor.

Figure 5.38 shows, under static conditions and at 35ºC, the corrosion rate decreased from 62.532 to 39.3857 gmd as thiourea concentration increased from 400 to 2000 ppm. Similar behavior was observed at 45ºC and 60ºC, as shown in table 5-9.

Table 5-9 Effect of Thiourea Concentration on Corrosion Rate of Iron at Three Temperatures under static conditions.

Thiourea Conc. (ppm)	Corrosion Rate (gmd)		
	35ºC	45ºC	60ºC
400	62.532	112.6063	213.1951
1000	52.8481	82.4215	170.4205
2000	39.3857	80.5734	164.27

Saliyan and Adhikari [70] stated that increasing the concentration of N-(3, 4-dihydroyxybenzylidene)-3-[[8-(tri-fluoromethyl) quinolin-4-yl] thio] propanehydrazide (DHPTPH) as a corrosion inhibitor for mild steel in HCl (1M, 2M) and H_2SO_4 (0·5M, 1M) solutions using weight-loss method, led to a decrease in the activation corrosion energy.

Elewady, et. al. [71] concluded that increasing the concentration of anion surfactants as corrosion inhibitors leads to increase in the value of activation energy of corrosion and consequently, decreasing the rate of dissolution of aluminum in HCl solution.

Mahmoud [82]. stated that the values of activation energy of corrosion increases with increasing the concentration of methyl-substituted piperidines as a corrosion inhibitor for Zn-Al-Cu alloy in HCl solution.

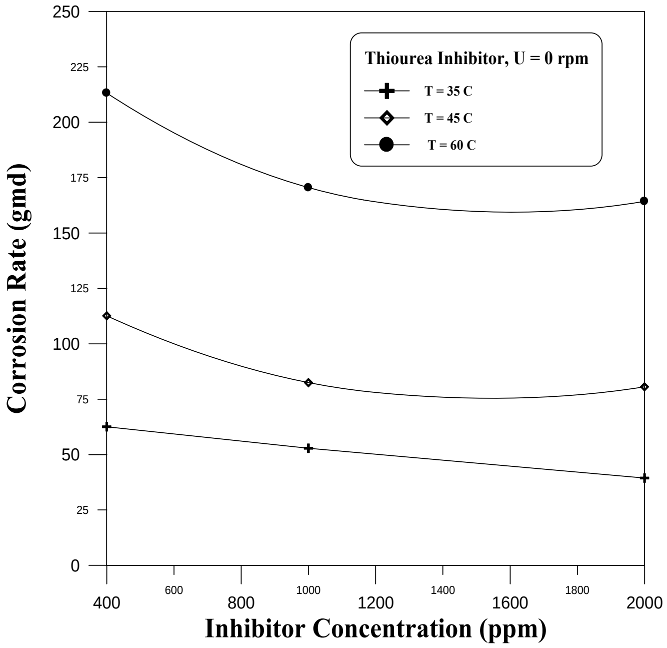

Figure 5-38 Variation of Corrosion Rate with the Concentration of Thiourea Inhibitor under Static Conditions at Various Temperatures.

Figure 5.39 represents Arrhenius equation .It is observed that at temperatures of 35, 45, and 60ºC under static condition, the activation energies of dissolution process ($Fe \Rightarrow Fe^{+2} + 2e$) are 41.4, 39.9, and 49.4 kJ/mol respectively as shown in table 5-8.

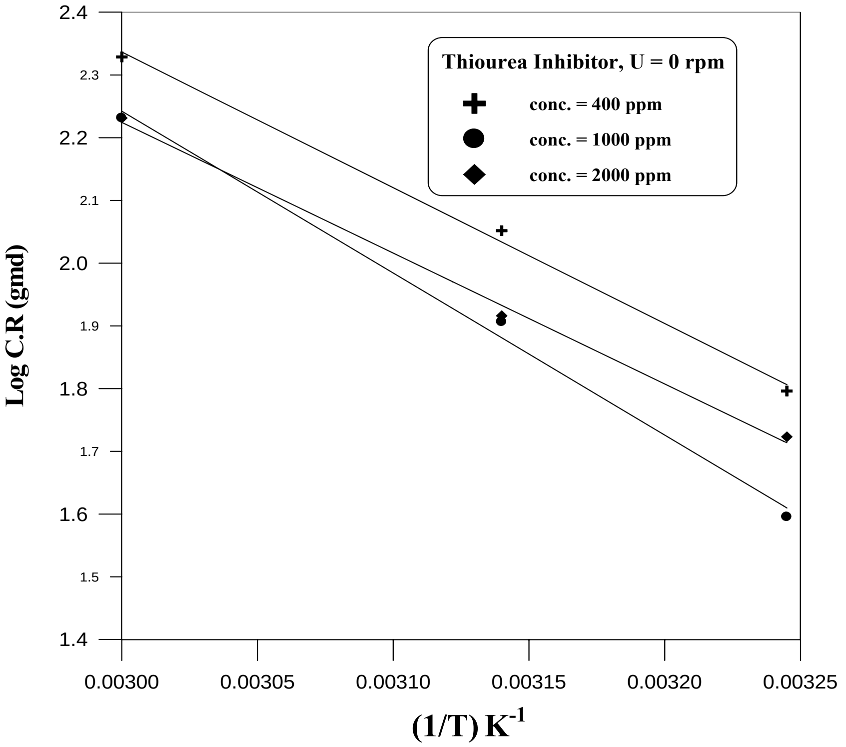

Figure 5-39 Arrhenius Plot for log Corrosion Rate (gmd) versus Reciprocal of Absolute Temperature under Static Conditions.

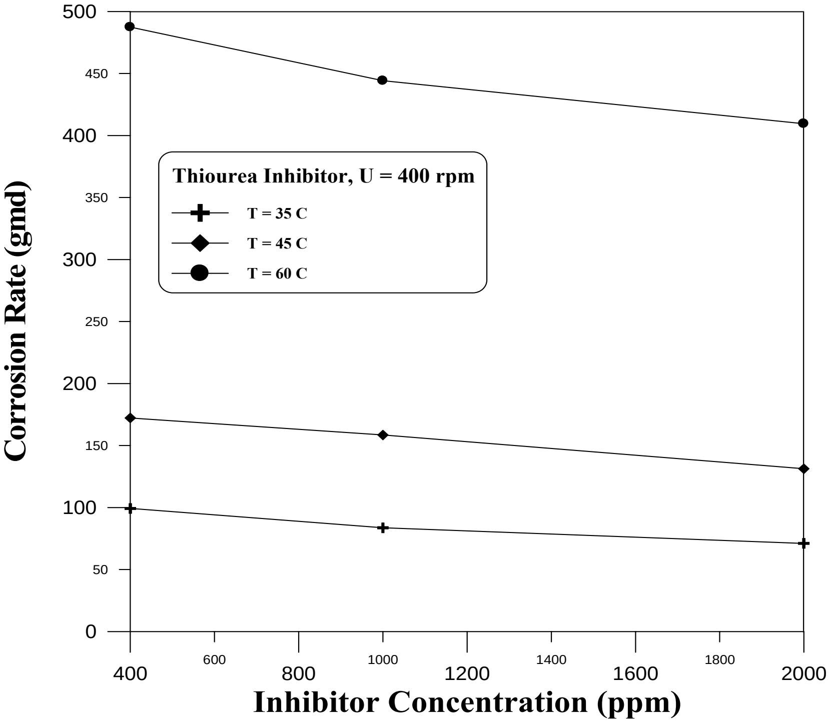

Figure 5-40 Variation of Corrosion Rate with the Concentration of Thiourea Inhibitor at Various Temperatures and 400 rpm.

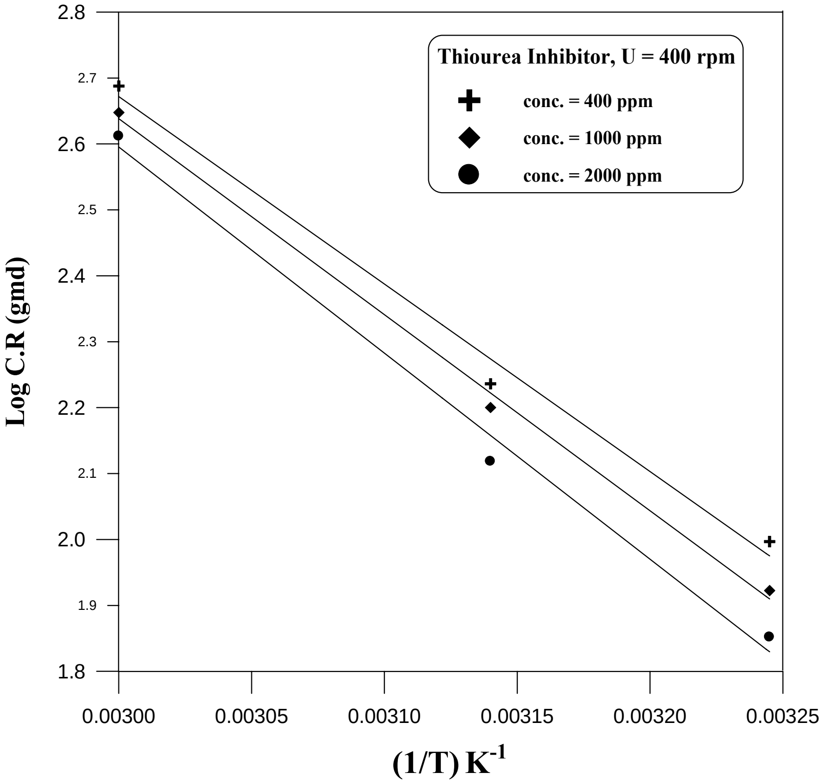

Figure 5-41 Arrhenius Plot for log Corrosion Rate (gmd) versus Reciprocal of Absolute Temperature and 400 rpm.

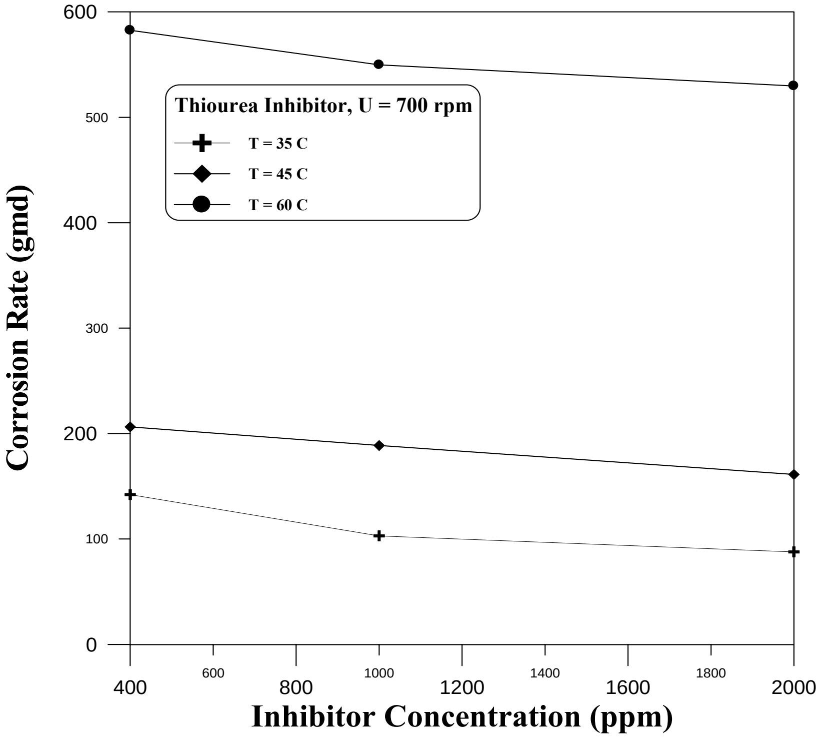

Figure 5-42 Variation of Corrosion Rate with the Concentration of Thiourea Inhibitor at Various Temperatures and 700 rpm.

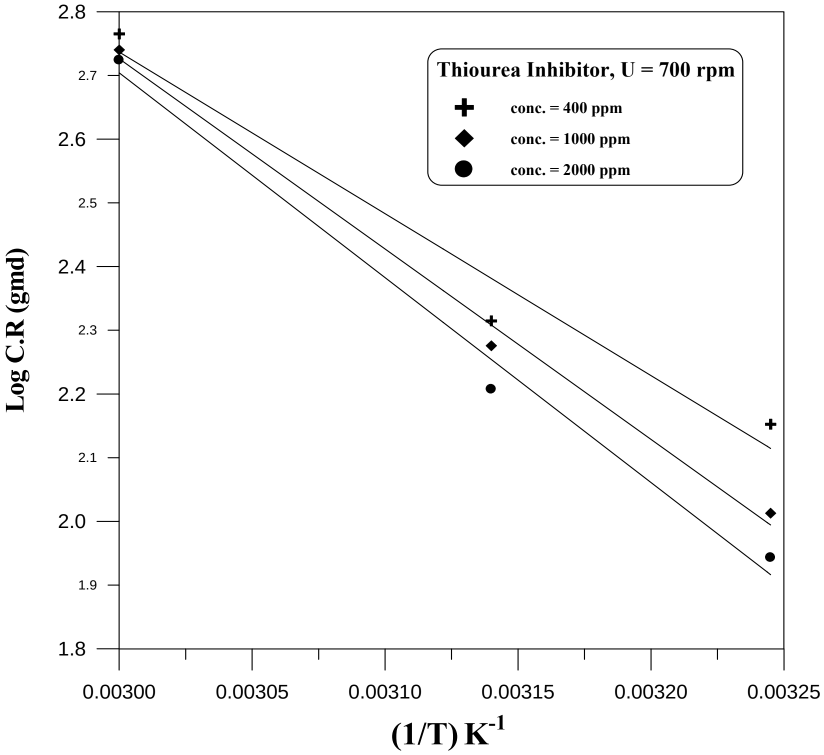

Figure 5-43 Arrhenius Plot for log Corrosion Rate (gmd) versus Reciprocal of Absolute Temperature and 700 rpm.

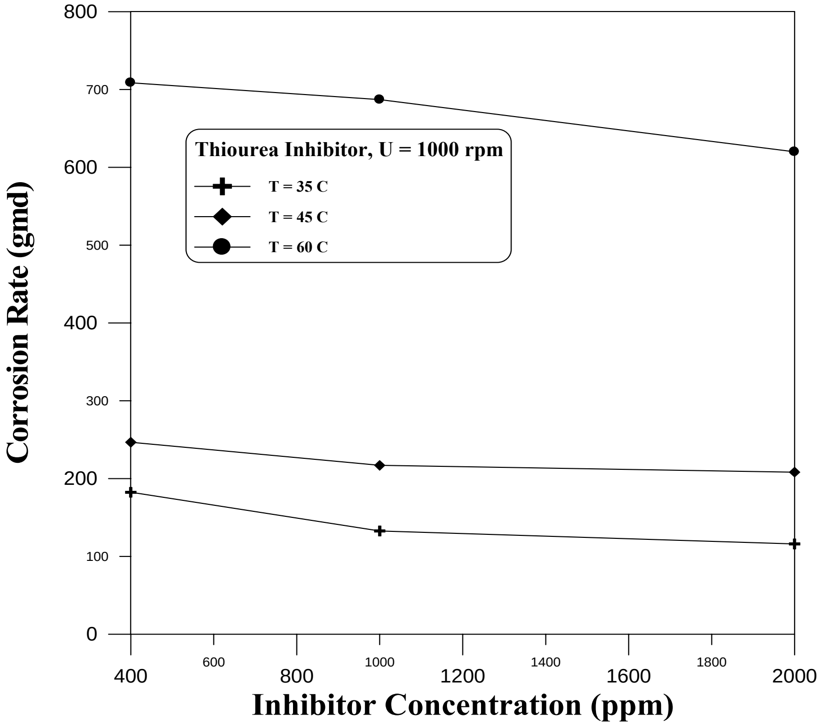

Figure 5-44 Variation of Corrosion Rate with the Concentration of Thiourea Inhibitor at Various Temperatures and 1000 rpm.

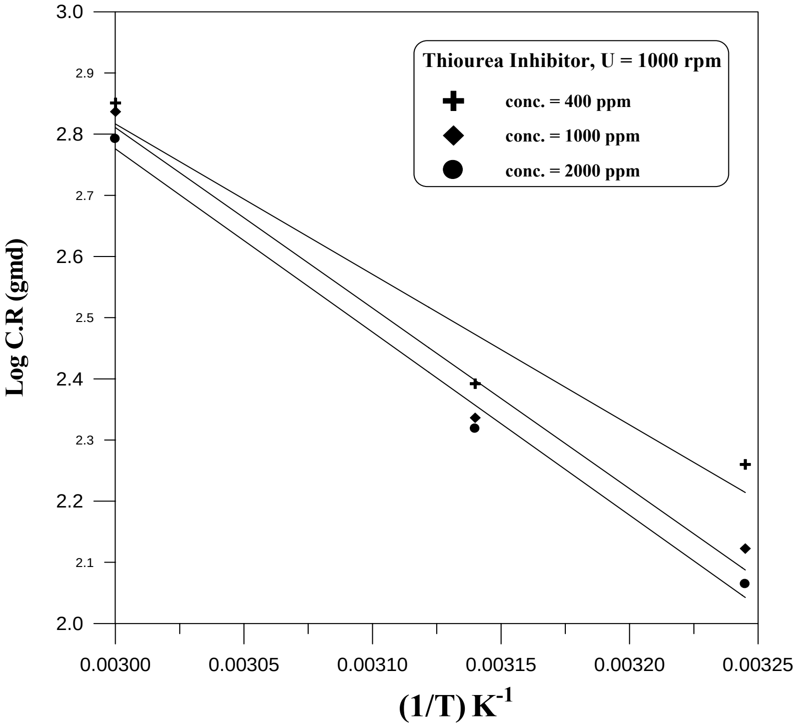

Figure 5-45 Arrhenius Plot for log Corrosion Rate (gmd) versus Reciprocal of Absolute Temperature and 1000 rpm.

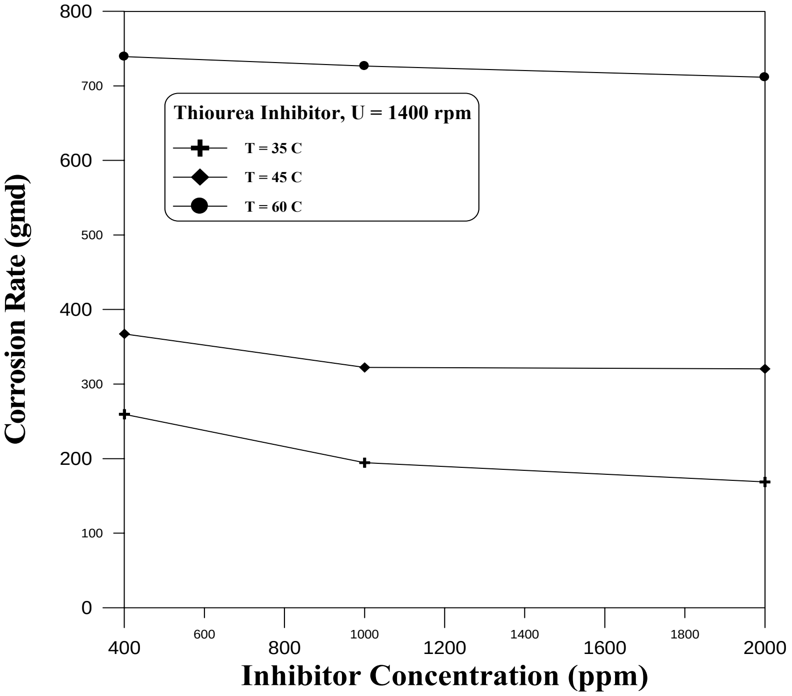

Figure 5-46 Variation of Corrosion Rate with the Concentration of Thiourea Inhibitor at Various Temperatures and 1400 rpm.

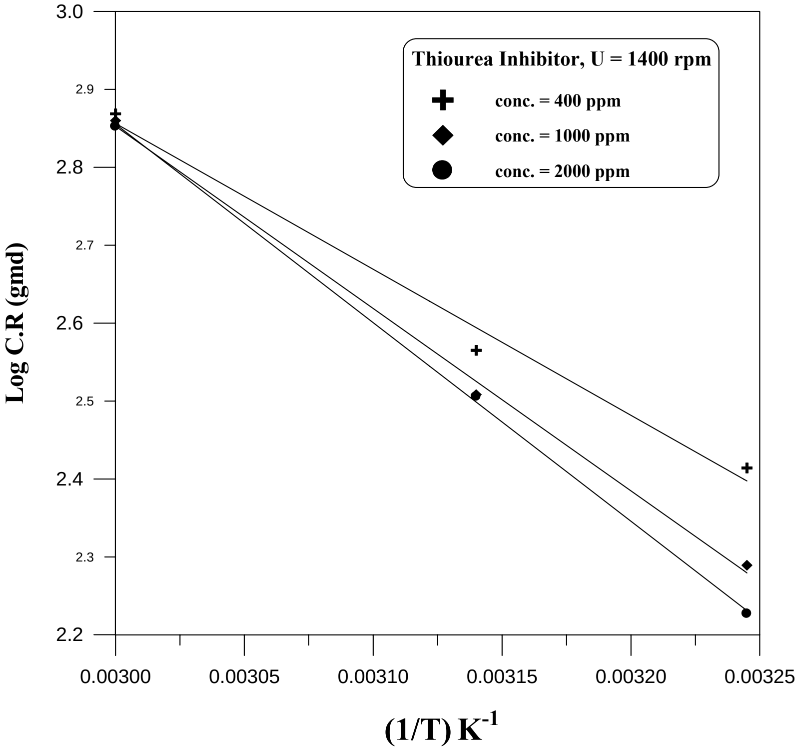

Figure 5-47 Arrhenius Plot for log Corrosion Rate (gmd) versus Reciprocal of Absolute Temperature and 1400 rpm.

Table 5-10 Effect of Rotational Velocity on Activation Energy for Thiourea Inhibitor at

Thiourea Concentration (ppm)	Activation Energy E_a (kJ/mol)		
	U = 400 rpm	U = 700 rpm	U = 1000 rpm
400	20.3	15.2	12.94
1000	48.46	51.26	49
2000	51.64	53.88	50.7

Various Concentrations.

Figures 5.48-5.53 also represent Arrhenius relationship for thiourea inhibitor while the parameter is the Reynolds number and this indicates the influence of the rotational velocity on activation energies at 400, 1000 and 2000 ppm respectively. It is observed for 400, 700 and 1000 rpm as rotational velocity to rotate the cylindrical electrode in 0.1N HCl solution as example which contains 400 ppm of thiourea inhibitor, the activation energies of the dissolution process are 20.3, 15.2 and 12.94 kJ/mol respectively as shown in table 5-10.

From table (5-10) it can be deduced that:

- For a concentration of 400 ppm and by increasing Reynolds number, the higher the rotational velocity the smaller the activation energies recorded for the dissolution process of the metal.
- For concentrations of 1000 and 2000 ppm the activation energies which were recorded for the dissolution process at 700 rpm is higher than that recorded at 400 rpm. And the activation energy recorded at 1000 rpm is lower than to that recorded at 700 rpm.

Table 5-11 Reynolds Number as a Function of Temperature.

Temperature	U(rpm)	Re
35ºC	0	static
	400	5729
	700	10025.78
	1000	14322.55
	1400	20051.58
45ºC	0	static
	400	6887.8
	700	12053.77
	1000	17219.67
	1400	24107.54
60ºC	0	static
	400	8734.89
	700	15286.07
	1000	21837.24
	1400	30572.139

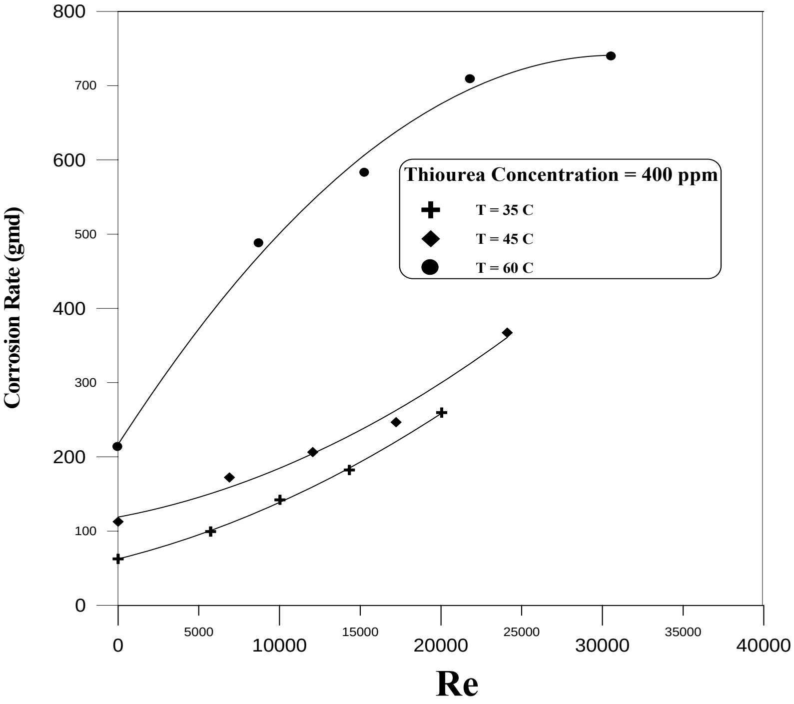

Figure 5-48 Variation of Corrosion Rate with Reynolds Number in Presence of Thiourea Inhibitor in Concentration of 400 ppm at Various Temperatures.

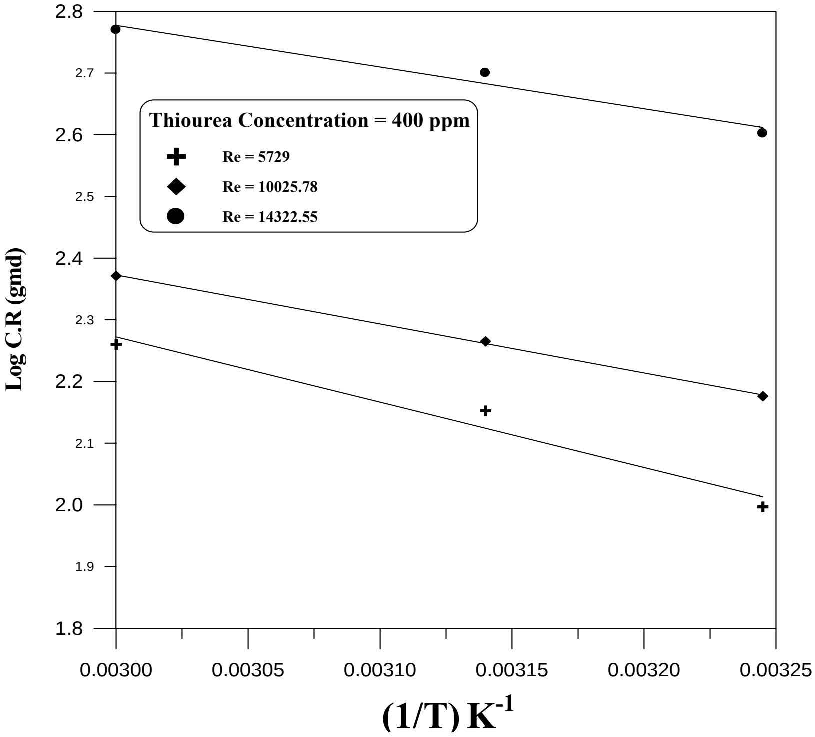

Figure 5-49 Arrhenius Plot for log Corrosion Rate (gmd) versus Reciprocal of Absolute Temperature for Thiourea Concentration of 400 ppm at Various Rotational Velocity.

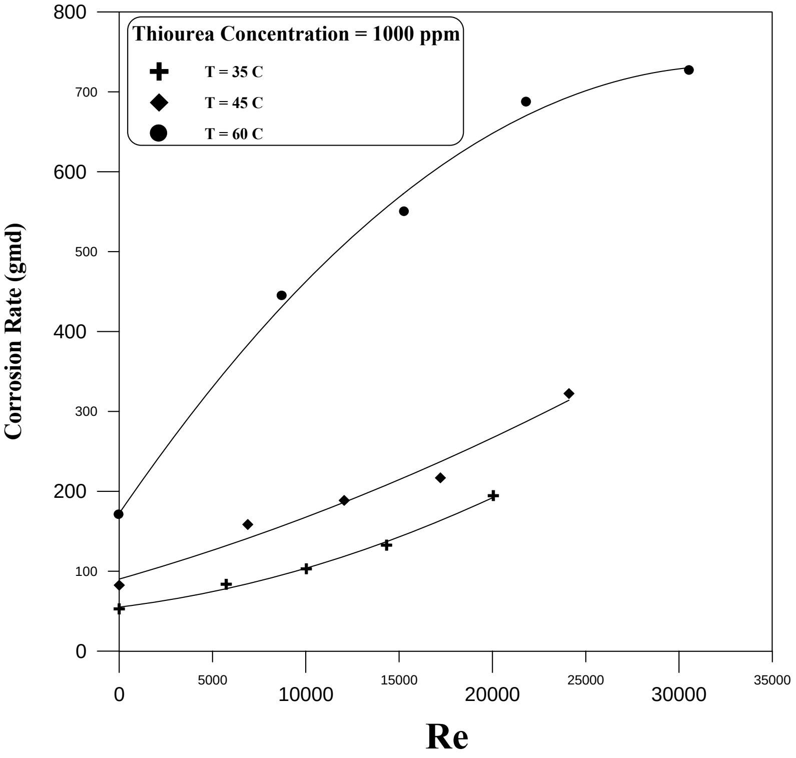

Figure 5-50 Variation of Corrosion Rate with Reynolds Number in Presence of thiourea Inhibitor in Concentration of 1000 ppm at various temperatures.

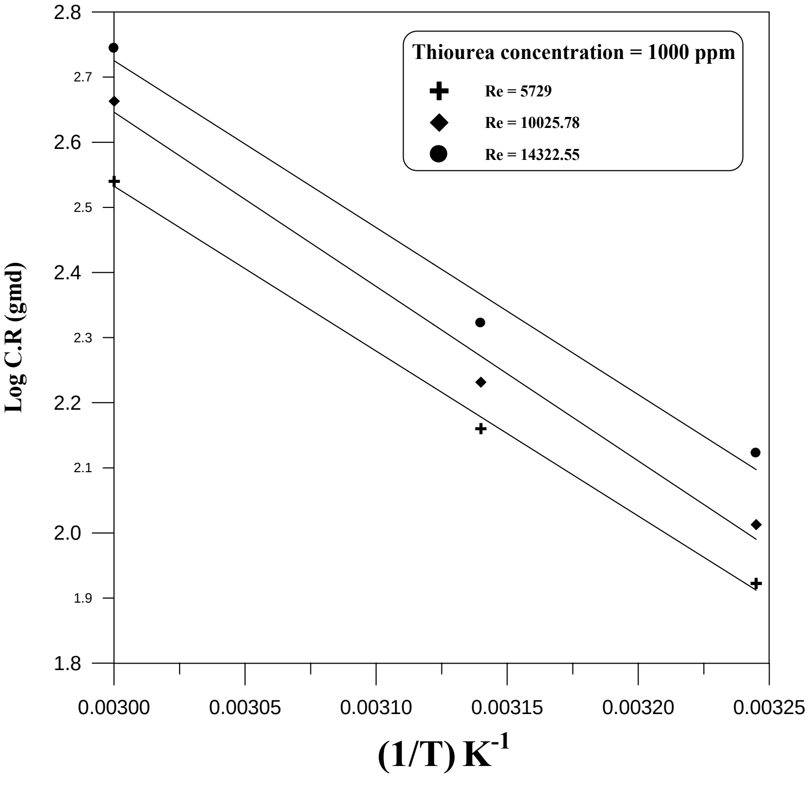

Figure 5-51 Arrhenius Plot for log Corrosion Rate (gmd) versus Reciprocal of Absolute Temperature for Thiourea Concentration of 1000 ppm at Various Rotational Velocity.

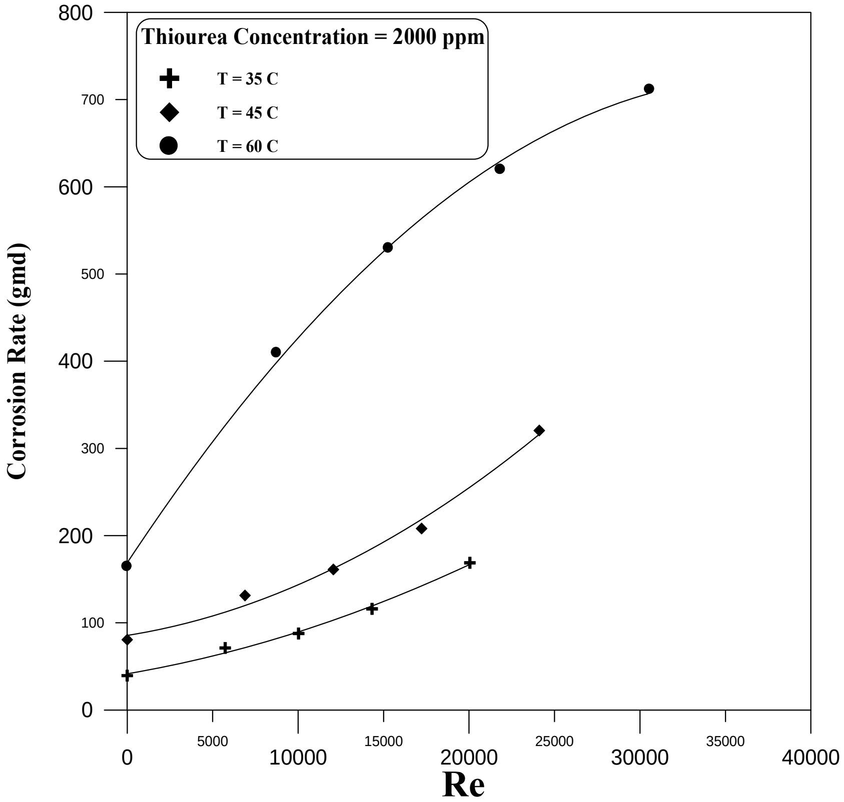

Figure 5-52 Variation of Corrosion Rate with Reynolds Number in Presence of Thiourea Inhibitor in Concentration of 2000 ppm at Various Temperatures.

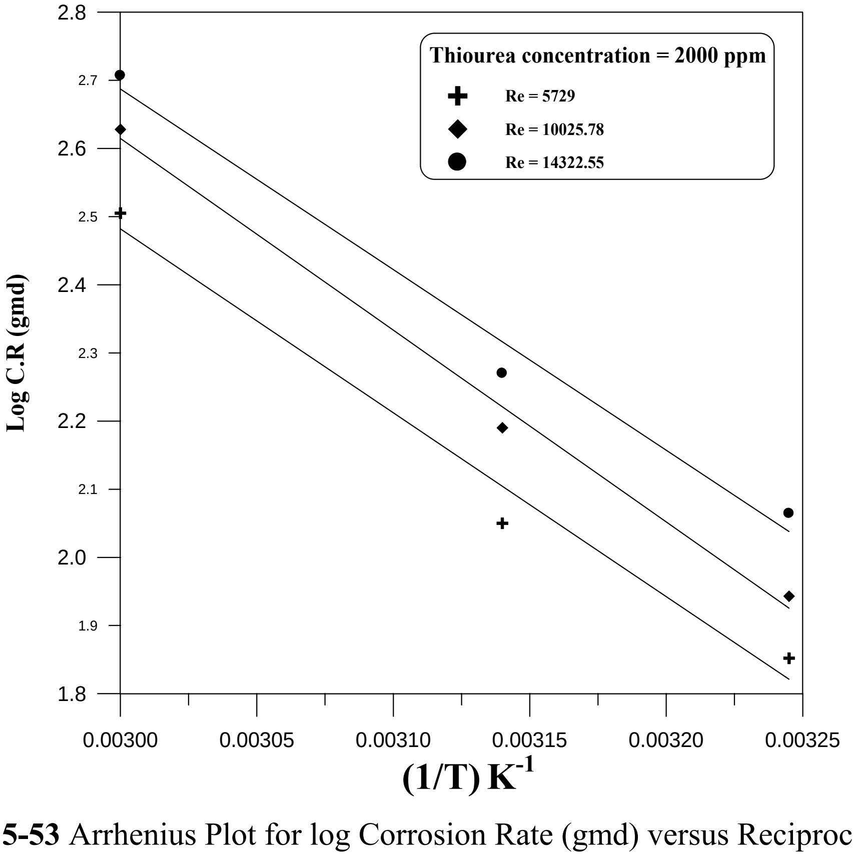

Figure 5-53 Arrhenius Plot for log Corrosion Rate (gmd) versus Reciprocal of Absolute Temperature for Thiourea Concentration of 2000 ppm Various Rotational Velocity.

CHAPTER SIX

Conclusions and Recommendations for Future Work

6.1 Conclusions

The followings are concluded from the experimental results:

1- In aerated 0.1N HCl solution, increasing rotational velocity increases the corrosion rates for the investigated range of temperature in the presence and absence of inhibitors.

2- In the absence and presence of corrosion inhibitors, increasing the temperature increases the corrosion rates for the entire range of Re and inhibitors concentration.

3- The corrosion rate, for the four inhibitors which were used, decreased with increasing the concentration of inhibitor. It was found also that the most efficient inhibitor was thiourea, followed by ethylene diamine, diethanol amine and formaldehyde. The minimum inhibition efficiency attained by thiourea was (38.7%) and maximum was (77.6%).

4- The variation of corrosion rate with temperature for thiourea inhibitor obeys Arrhenius equation. From Arrhenius plot it was found that the activation energy increases with increasing the concentration and decreases with increasing Reynolds number.

5- For mass transfer controlled oxygen reduction, increasing Re leads to increase in the corrosion rate of free corrosion and for activation controlled (hydrogen evolution reaction) not clearly affected by rotational velocity (or Re).

6- The inhibition efficiency of all inhibitors which were used decreases with increasing temperature of the corrosive solution and the rotational velocity.
7- Increasing the oxygen transport from the bulk solution to the metal surface with increasing Re (or rotational speed), increase the corrosion rate of the carbon steel in the presence and absence of inhibitors.

6.2 Recommendations for Future Work:

The followings are recommended for future work:

1. Use another types of organic amine inhibitors at the same conditions which were used.
2. The effect of acid concentration on the inhibitors efficiency.
3. The effect of inhibitors under other temperatures and rotational velocity ranges.
4. The effect of inhibitors in deaerated acid solution.
5. Use the polarization method to measure the instantaneous currents, the effect of inhibitors and the influence of the exposure time on the corrosion rate using different time intervals.
6. Studying the efficiency of inhibitors in other acids such as H_2SO_4 or HNO_3.
7. Analyze the data obtained by weight loss to find the effect of variables studied by modeling through a mathematical expression.
8. Use ANOVA analysis to find the significance of the variables on the response.

References

1. Evans, V., “The Corrosion and Oxidation of Metals”, Arnold, London, (1961).
2. Uhlig, H. H., “Corrosion and Corrosion Control”, 3rd Edition, Wiley-Interscience Publication, New York, (1985).
3. Tretheway, K. R. and J. Chamberlain, “Corrosion Science and Engineering”, Longman, Second Edition, London, (1996).
4. Fontana, M. G. and N. D. Greene, “Corrosion Engineering”, London, Third Edition (1987).
5. Steigerwald, R. F., “Corrosion-NACE”, (1968).
6. Kruger, J., “Electrochemistry of Corrosion“, the Johns Hopkins University, Baltimore, MD 21218, USA, April (2001).
7. Cost of Corrosion, NACE International, July (2002) http://www.battlle.org.
8. Y. T. AL-Janabi, “Chronoamperometric Evaluation of Several Organic Corrosion Inhibitors by the Hydrogen Permeation Flux”, Dhahran, Saudi Arabia, (1993).
9. Garry E. Means and Robert E. Feeney, “Chemical Modification of Proteins”, Holden-Day Inc. London, chapter six, pp. 126.
10. Shen, C. B., S. G. Wang, H. Y. Yang, K. Long and F. H. Wang, “Corrosion and Corrosion Inhibition by Thiourea of Bulk Nanocrystallized Industrial Pure Iron in Dilute HCl Solution”, Corrosion Science 48, (2006) pp. 1655-1665.
11. Hamm, E. R. and Captain, CEC, U.S. Navy, Corrosion Control, 200 Stovall Street, Alexandria, Virginia 22332-2300, September, (1992).

12. A. Sarafis, “Environmentally Friendly Inhibitors to Control Corrosion of Copper, Steel and Aluminium”, M.SC in Advanced Materials, Cranfield University, (2007).
13. Perry, R. H. and Green, D. W., “Perry Chemical Engineers Handbook” ,7th ed, McGraw Hill ,United states , (1997).
14. Henry, S. D. and W. M. Scott, “Corrosion in the Petrochemical Industry”, ASM International, First Edition USA,(1999).
15. Conway, B. E., E. M. Beatty and P. A. D. DeMaine, Electo. Chem. Acta., Vol. 7, (1962) pp. 39.
16. Shreir, L. L., “Corrosion Handbook”, Newnes -Butter, London, 2nd Edition, Part 1, (2000).
17. Uhlig, H. H., “The Corrosion Handbook”, John Wiley and Sons, New York, (1976).
18. Poulson, B., “Corrosion Science”, Vol. 23, No. 1, (1983) pp. 391.
19. Stern, M. Corrosion-NACE, Vol. 13, (1957) pp. 97.
20. Kolman, D. G. D. K. Ford, D. P. Butt, and T. O. Nelson, “Materials Corrosion and Environmental Effects Laboratory”, Los Alamos, NM 87545, (2002).
21. S. S. Bahar, MSc. Thesis, Chem. Eng. Dept., Saddam University, Baghdad, (2002).
22. Barnartt, S., “Electrochemical Techniques for Corrosion”, Baboian, (1977).
23. Fontana, M. G., and N. D. Greene, “Corrosion Engineering”, McGraw-Hill Inc., second Edition, (1978).
24. Heitz, E. and G. Kreysa, “Principles of Electrochemical Eng.”, an Extended Version of a Dechema, Experimental Course, VCH, (1986).

25. Bergman, J., “Corrosion Inhibitors”, the Macmillan Company, New York (1963).
26. Butler, G. and Ison, H. C. K., “Corrosion and its Prevention in water Leonard”, Hill-London, (1966).
27. Revie, R., Winston Uhlig’s, “Corrosion Handbook”, Second addition, John Wiley & Sons, Ottawa, Ontario (Canada), (2000).
28. Classification of corrosion inhibitors, http://www.corrosindoctors.org/Modules/mod-prevention.htm.
29. Rozenfeld, I. L., "Corrosion Inhibitors", McGraw-Hill Inc, United States of America, (1981).
30. Moore, W. J., “Physical Chemistry”, Longman, fifth Edition, (1972) pp. 500.
31. Nathan, C., “Corrosion Inhibitor”, NACE, (1973).
32. Chin, R. J., and K. Nobe, J., “Electro. Chem. Soc.”, Vol. 4, (1971) pp. 118.
33. Glusstone, S. and D. lewis, “Elements of physical Chemistry”, MacMillan and Co. Ltd, second Edition, (1960) pp. 559.
34. AL-Kadhimi, E., “M. Sc. Thesis University of Baghdad”, June, (1979).
35.. Agrawal, R. T. and K. G. Namboohiri, “Corros. Sci.”, Vol. 30, No. 1, (1989) pp. 37.
36. Ali, S. A., M. T. Saeed and S. V. Rahman, “Corros. Sci.”, Vol. 45, No. 3, (2003) pp. 253.
37. Singth, I., “Corrosion”, Vol. 49, No. 9, (1993) pp. 726.
38. Kuztnetsov, Y. I., “Corrosion”, Vol. 49, No. 6, (1993) pp.726.
39. Formaldehyde. http://www.chem.unep.ch/irptc/sids/OECDSIDS/FORMALDEHYDE.pdf.

40. Chronic toxicity summary (Formaldehyde).
http://www.oehha.org/air/chronic_rels/pdf/50000.pdf
41. Joe E. Heimlich, "The Invisible Environment Fact Sheet Series (Formaldehyde)", the OHIO State University.
http://ohioline.osu.edu/cd-fact/pdf/0198.pdf
42. Formaldehyde council.
http://www.bifma.com/news/newsrelease.pdfs/IARCimpact.pdf.
43. Trabanelli, G. and V. Carassiti, "Mechanism and phenomenology of Organic Inhibitors", Advances in Corrosion Science and Technology, Vol. 1, M.G. Fontanna and R.W. Staehle, eds., Plenum Press, New York, (1970), pp. 147-228.
44. Lorenz, W. J. and F. Mansfeld, "Corrosion Inhibition", R. H. Hausler.ed., NACE, Texas (1988), pp. 7-13.
45. Hackerman, N., "Corrosion", Vol. 18, 332t (1962) September.
46. Craig, B. D., "Fundamental Aspects of Corrosion Films in Corrosion Science", Plenum Press, New York, (1991) pp. 89-108.
47. Rosenfeld, I. L., "Corrosion", Vol. 37, (1981) pp.371.
48. Kaesche, H. and N. Hackerman, "Electrochem. Soc.", Vol. 7, (1958) pp. 105-191.
49. P. Dupin, D. A. Viloria-Vera, A. de Savignac, A. Lattes, B. Sutter and Ph. Haicour, Proc. 5th Europ. Symp. Corros. Inhibitors, Vol. 1, p. 301, Universita delgi Studi di Ferrara, Ferrara, Italy (1980).
50. Raicheva, S. N., B. V. Aleksiev and E. I. Sokolova, "Corros. Sci.", Vol. 34, No. 2, (1993) pp. 343.
51. Cox. P. F., R. L. Every and O. L. Riggs, Jr., "Corrosion", Vol. 20, 299t (1964) September.

52. Nathan, C. C. ed., "Corrosion Inhibitors", Nace, Texas, (1973) pp. 7- 27.

53. Szklarska-Smialowska, Z., "Corrosion Inhibition", R. H. Hausler, ed. NACE, Texas, (1988) pp. 1-6.

54. James, A. O., N. C. Oforka, and O. k. Abiola, "Inhibition of Acid Corrosion of Mild Steel by Pyridoxal and Pyridoxol Hydrochlorides", Int. J. Electrochem. Sci., (2007) pp. 278-284.

55. West, J.M., "Electrodeposition and Corrosion processed, V. N. R.Co., (1971).

56. Soror, T. Y., H. A. EL Dahan and N. G. EL Sayed Ammer, "Corrosion Inhibition of Carbon Steel in Hot Hydrochloric Acid Solutions", J. Mater. Sci. Technol, Vol. 15, No. 6, (1999) pp. 559-562.

57. Bentiss, F., M. Lagrenee, M. Traisnel, and J. C. Hornez, "The Corrosion Inhibition of Mild Steel in Acidic Media by a New Triazole Derivative", Corrosion Science 41, (1999) pp. 789-803.

58. Harek, Y. and Larabi, **"**Corrosion Inhibition of Mild Steel in 1 mol dm^{-3} HCl by Oxalic *N*-Phenylhydrazide *N*-Phenylthiosemicarbazide", Corrosion Inhibition of Mild Steel, Kem. Ind., (2004) pp. 55-61.

59. Sorkhabi, H. A. and D. Seifzadeh, "The Inhibition of Steel Corrosion in Hydrochloric Acid Solution by Juice of Prunus Cerasus", International Journal of Electrochemical Science, (2006) pp. 92-98.

60. Jeyaprabha, C., S.Sathiyanarayanan, S.Muralidharan and G.Venkatachari, "Corrosion Inhibition of Iron in 0.5 mol L-1 H2SO4 by Halide Ions", J. Braz. Chem. Soc., Vol. 17, No. 1, (2006) pp. 61-67.

61. Abd Elhamid, M. H., B. G. Ateya and H.W. Pickering, "J. Electro. Chem. Soc.", Vol. 147, (2000) pp. 2258.

62. Vracar, L. J. and D. M. J. Drazic, "Electroanal. Chem.", Vol. 339, (1992) pp. 269.
63. Shetty, S. D., P. Shetty and H. V. S. Nayak, "The Inhibition Action of *N*-furfuryl-*N'*-phenyl Thiourea on the Corrosion of Mild Steel in Acid Media", J. Serb. Chem. Soc 71, (2006) pp. 1073–1082.
64. Olorunniwo, O. E., L. E. Umoru and O. R. Bamigboye, "Sodium Chromate and Diethylene Amine as Corrosion Inhibitors for Mild Steel in Cassava Fluid", Journal of Applied Sciences, Vol. 6, No. 4, (2006) pp. 878-882.
65. EL-Mhammedi, M. A. and Abdelilah Chtaini, "Investigation of the Inhibitive Effect of Pyrazolo [3, 4-b] Pyridine on Corrosion of Stainless Steel in 1M HCl Solutions", Leonardo Electronic Journal of Practices and Technologies, Issue 11, (2007) pp. 37-46.
66. Arora, P., S. Kumar, M. K. Sharma and S. P. Mathur, "Corrosion Inhibition of Aluminium by Capparis Decidua in Acidic Media", E-Journal of Chemistry, Vol. 4, No. 4, (2007) pp. 450-456.
67. Atul Kumar, "Corrosion Inhibition of Mild Steel in Hydrochloric Acid by Sodium Lauryl Sulfate (SLS)", E-Journal of Chemistry, Vol. 5, No. 2, (2007) pp. 275-280.
68. Srisuwan, N., N. Ochoa, N. Pebe`re, and B. Tribollet, "Variation of Carbon Steel Corrosion Rate with Flow Conditions in the Presence of an Inhibitive Formulation", Corrosion Science 50, (2008) pp. 1245-1250.
69. Begum, A., S. Harikrishna, I. Khan and K. Veena, "Enhancement of the Inhibitor Efficiency of Atropine Methochloride in Corrosion Control of Mild Steel in Sulphuric Acid", E-Journal of Chemistry, Vol. 5, No. 4, (2008) pp.774-781.

70. Saliyan, V. R. and A. V. Adhikari, **“**Inhibition of Corrosion of Mild Steel in Acid media by N′-benzylidene-3-(quinolin-4-ylthio) Propanohydrazide”, Bull. Mater. Sci., Vol. 31, No. 4, (2008) pp. 699–711.
71. Elewady, G. Y., “Pyrimidine Derivatives as Corrosion Inhibitors for Carbon-Steel in 2M Hydrochloric Acid Solution”, Int. J. Electro. chem. Sci., (2008) pp. 1149-1161.
72. Abdallah, M., A. S. Fouda, S. A. Shama1 and E. A. Afifi1, “Azodyes as Corrosion Inhibitors for Dissolution of C-Steel in Hydrochloric Acid Solution”, African Journal of Pure and Applied Chemistry, Vol. 2, No. 9, (2008) pp. 083-091.
73. Elbeik, S., A. C. C. Tseung and A. L. Mackay, “Corrosion Science”, Vol. 26, (1986) pp. 669.
74. Chapion, F. A., Corrosion Testing Procedure, 2nd Edition. Chapman and Hall, London, 1964.
75. Skold, R.V. and T. E. Larson, Corrosion-NACE, Vol. 13, (1957) pp. 69.
76. Samh, S. A., Ph.D. Thesis, Dept. of Chem. Eng., University of Technology, Baghdad, (1994).
77. Al-Hadithi, F. M., Ph.D. Thesis, Chem. Eng. Dept., Saddam Univ., Baghdad, 2002.
78. Mahato, B. K., F. R. Stewrd and L. W. Shimlit, “Corrs. Sci.”, Vol. 8, (1968) pp. 737.
79. Yee, Y. J., “Green Inhibitors for Corrosion Control”, M. Sc. Thesis, University of Manchester Institute of Science and Technology, (2004) pp. 23.

80. Musa, A.Y., A. H. kadhum, M. S. Takriff, A. R. Daud and S. K. Kamarudin, "Evaluation of Ethylenediaminetetra-Acetic Acid Di-Sodium Salt as Corrosion Inhibitor for Mild Steel in 1m Hydrochloric Acid", Australian Journal of Basic and Applied Sciences , (2008) pp. 956-960.
81. Eisenberg, M. C. W., A. R. Tobias and J. Wilke, Electrochem. Acta. Soc., Vol. 101, (1954) pp.306.
82. Mahmoud, S. S., "Hydrochloric Acid Corrosion Inhibition of Zn-Al-Cu Alloy by Methyl-Substituted Piperidines", Portugaliae Electrochimica Acta, vol. 26, (2008) pp. 245-256.

APPENDIX -A-

Iron Dissolution Rates and Hydrogen Evolution Current in Presence and Absence of Inhibitors in Acid Solution

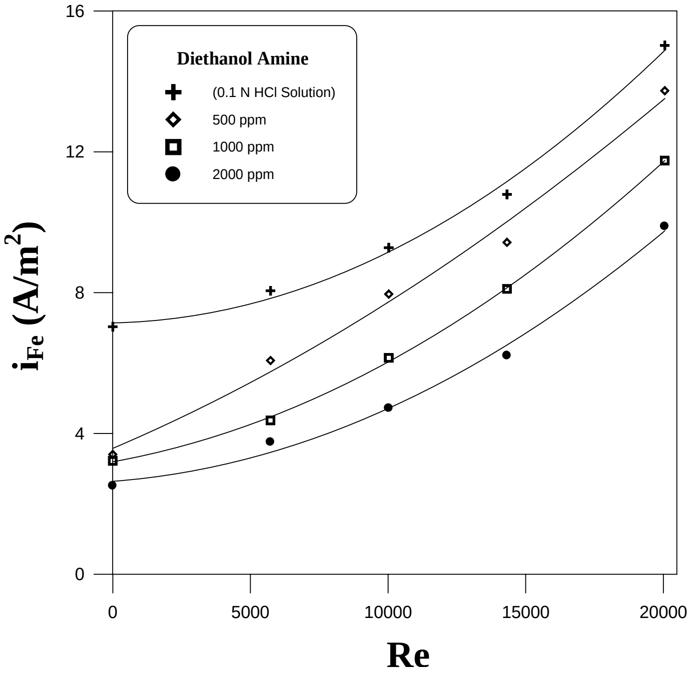

Figure A-1 Variation of Corrosion Current of Iron Metal with Reynolds Number in Presence of Diethanol Amine Inhibitor at T= 35°C.

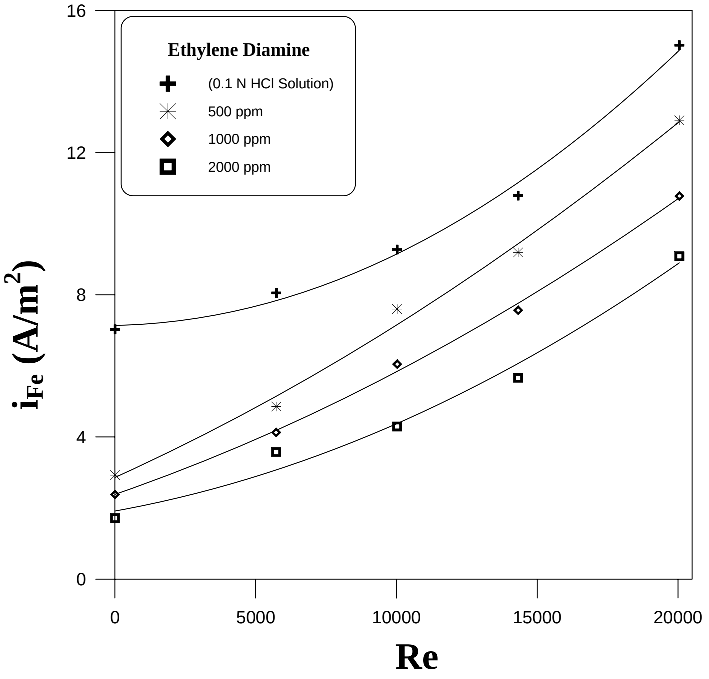

Figure A-2 Variation of Corrosion Current of Iron Metal with Reynolds Number in Presence of Ethylene Diamine Inhibitor at T= 35°C.

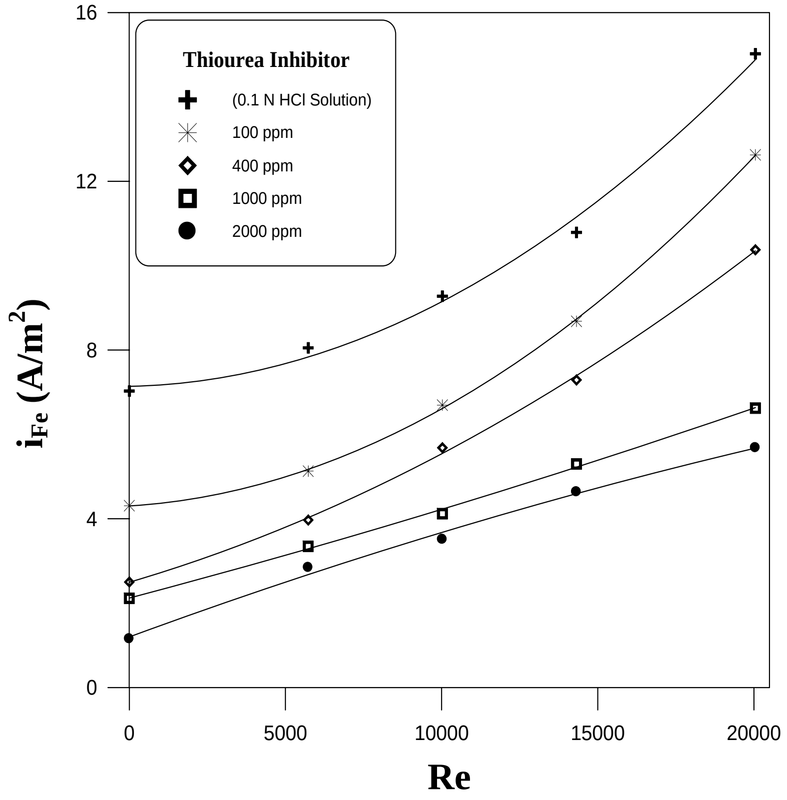

Figure A-3 Variation of Corrosion Current of Iron Metal with Reynolds Number in Presence of Thiourea Inhibitor at T= 35°C.

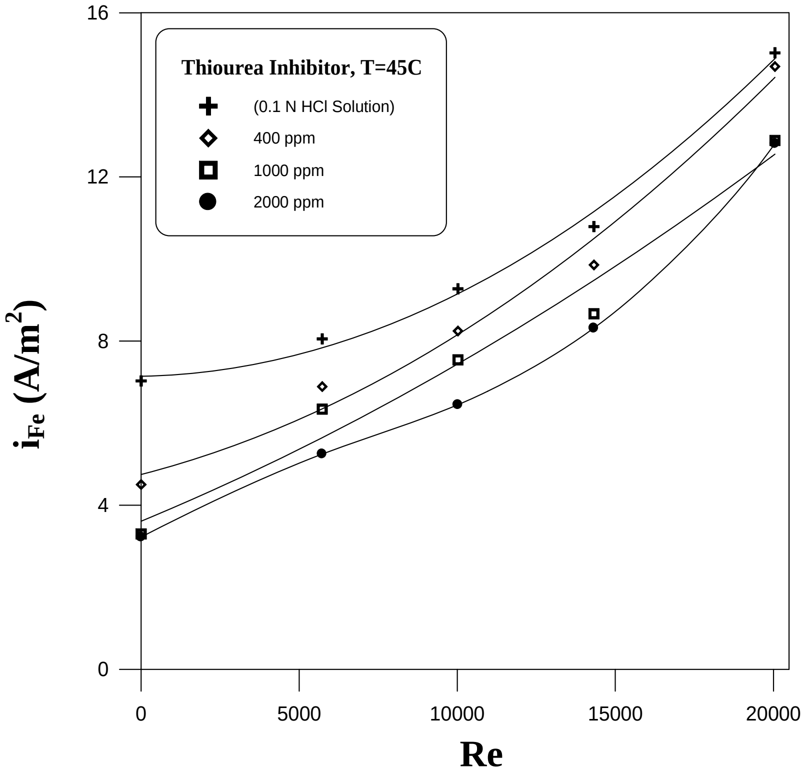

Figure A-4 Variation of Corrosion Current of Iron Metal with Reynolds Number in Presence of Thiourea Inhibitor at T= 45°C.

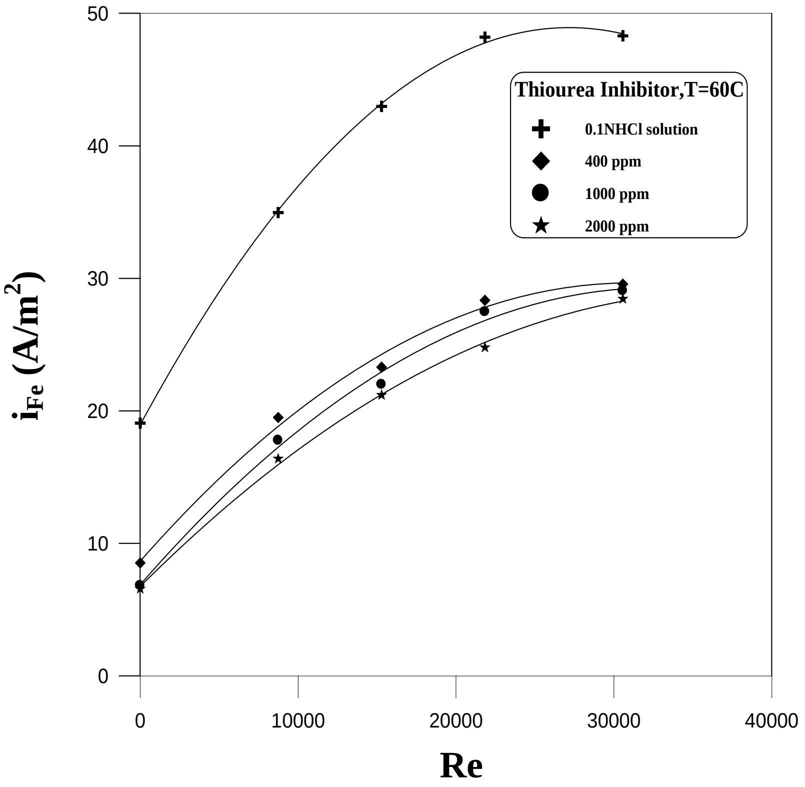

Figure A-5 Variation of Corrosion Current of Iron Metal with Reynolds Number in Presence of Thiourea Inhibitor at T= 60°C.

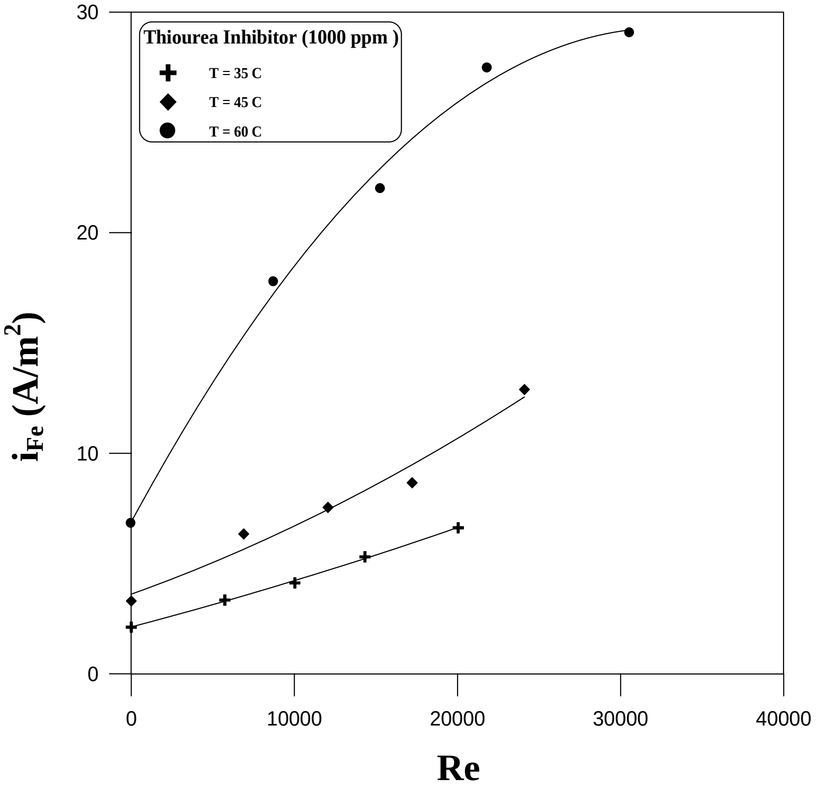

Figure A-6 Corrosion Current of Iron Metal versus Reynolds Number in Presence of Thiourea Inhibitor at Concentration of 1000 ppm at Various Temperatures.

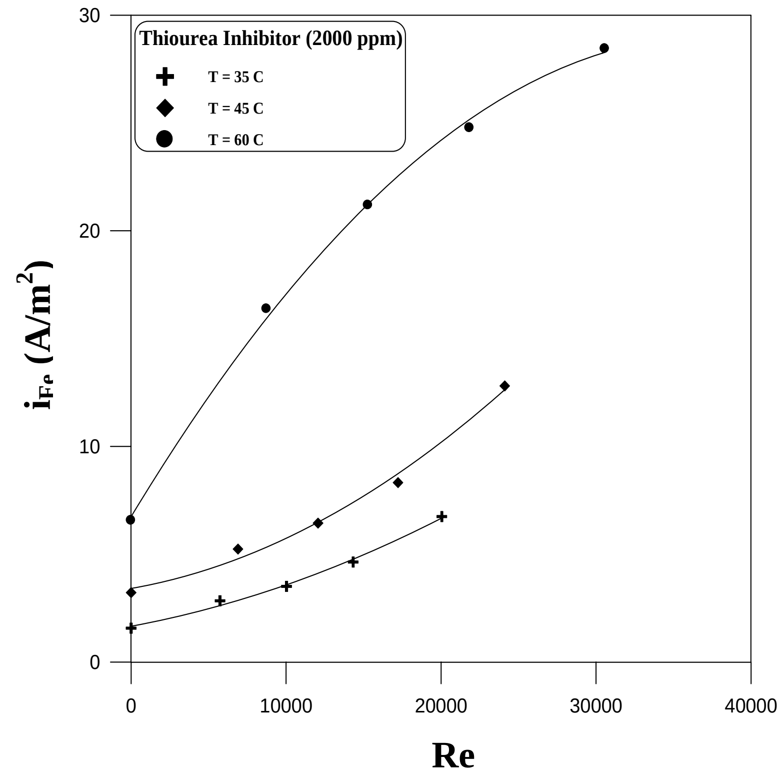

Figure A-7 Corrosion Current of Iron Metal versus Reynolds Number in Presence of Thiourea Inhibitor at Concentration of 2000 ppm at Various Temperatures.

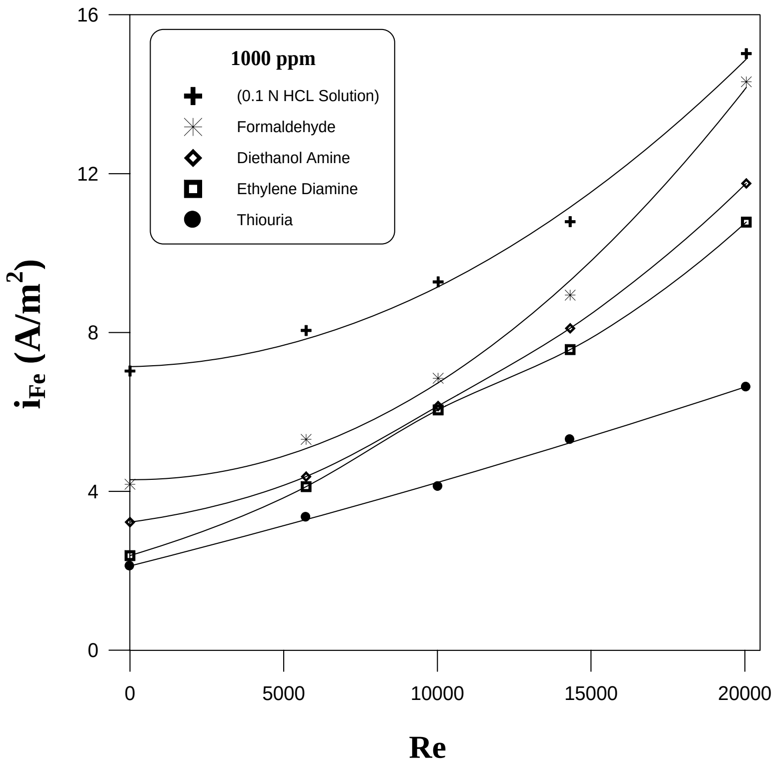

Figure A-8 Variation of Corrosion Current of Iron Metal with Reynolds Number for Various Inhibitors in Concentration of 1000 ppm at T= 35°C.

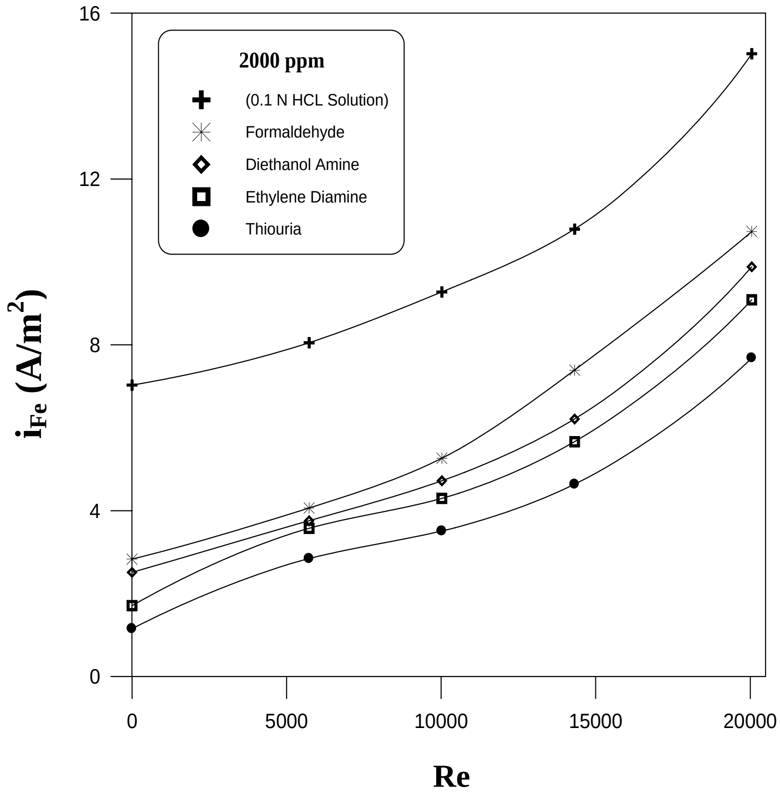

Figure A-9 Variation of Corrosion Current of Iron Metal with Reynolds Number for various Inhibitors in Concentration of 2000 ppm at T=

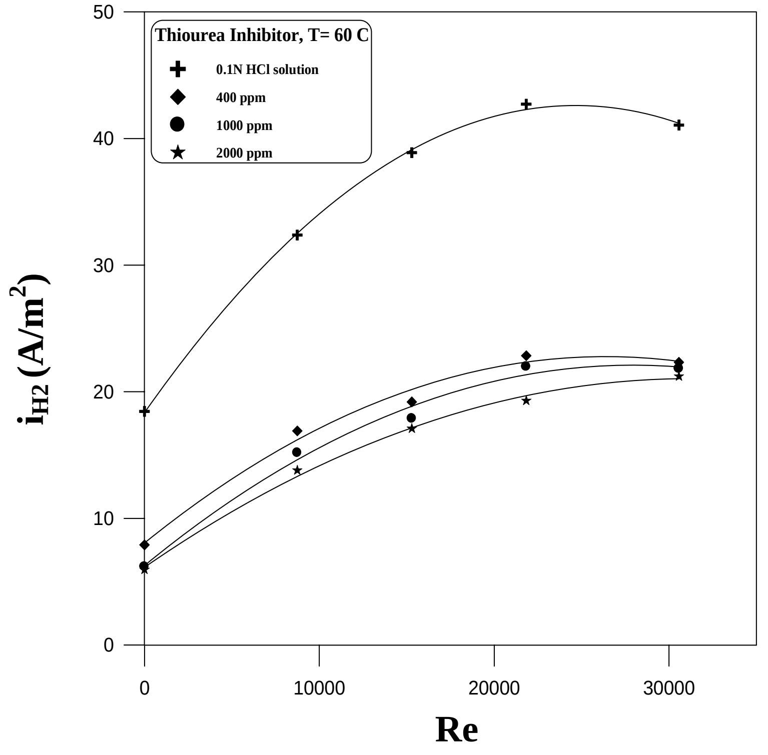

Figure A-10 Variation of Current of Hydrogen Evolution at E_{corr} with Reynolds Number in Presence of Thiourea Inhibitor at T=60°C.

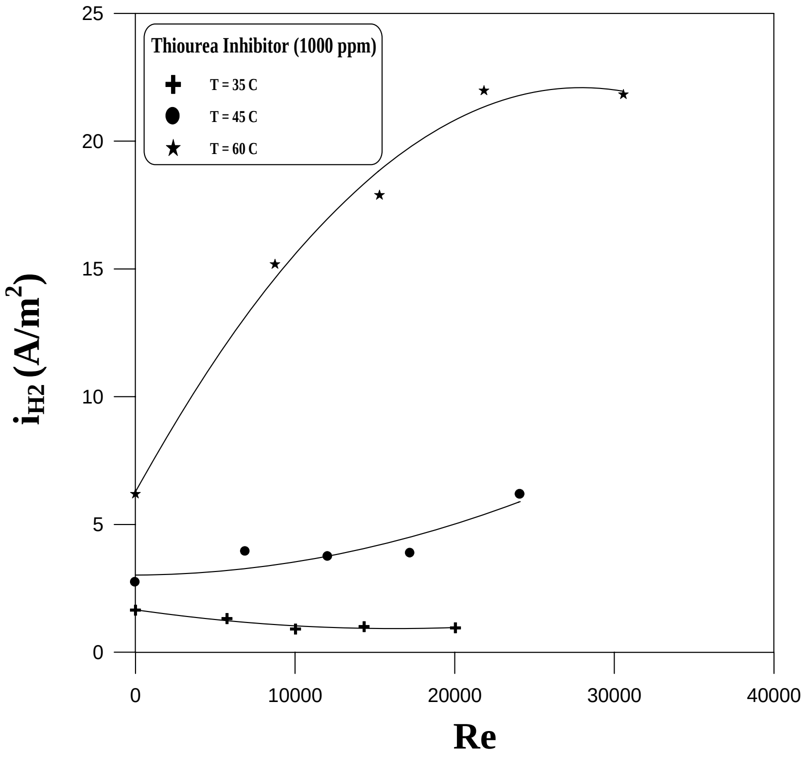

Figure A-11 Variation of Current of Hydrogen Evolution at E_{corr} with Reynolds Number in Presence of Thiourea Inhibitor in Concentration of 1000 ppm at Various Temperatures**.**

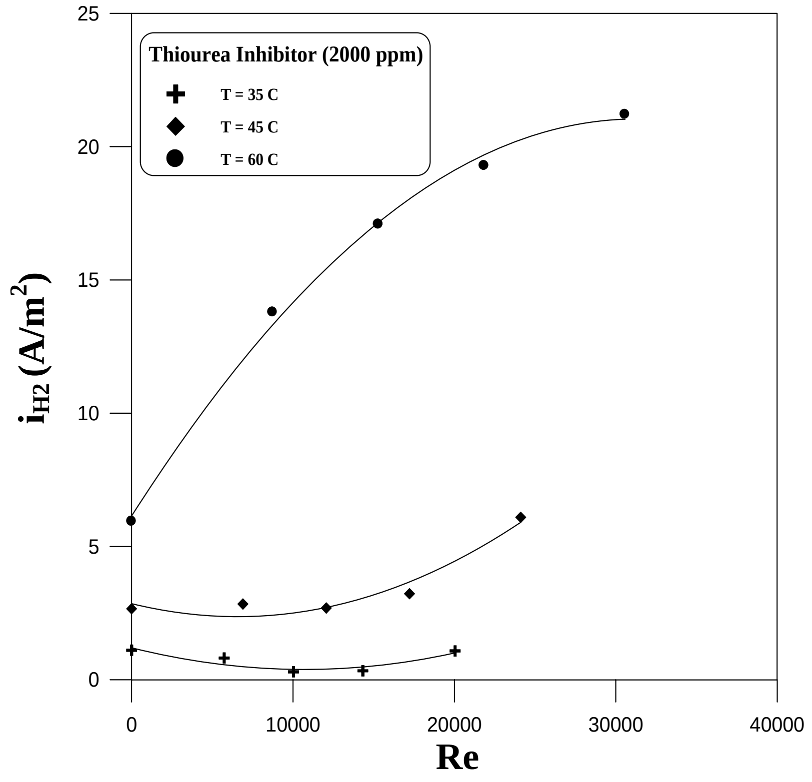

Figure A-12 Variation of Current of Hydrogen Evolution at E_{corr} with Reynolds Number in Presence of Thiourea Inhibitor in Concentration of 2000 ppm at Various Temperatures**.**

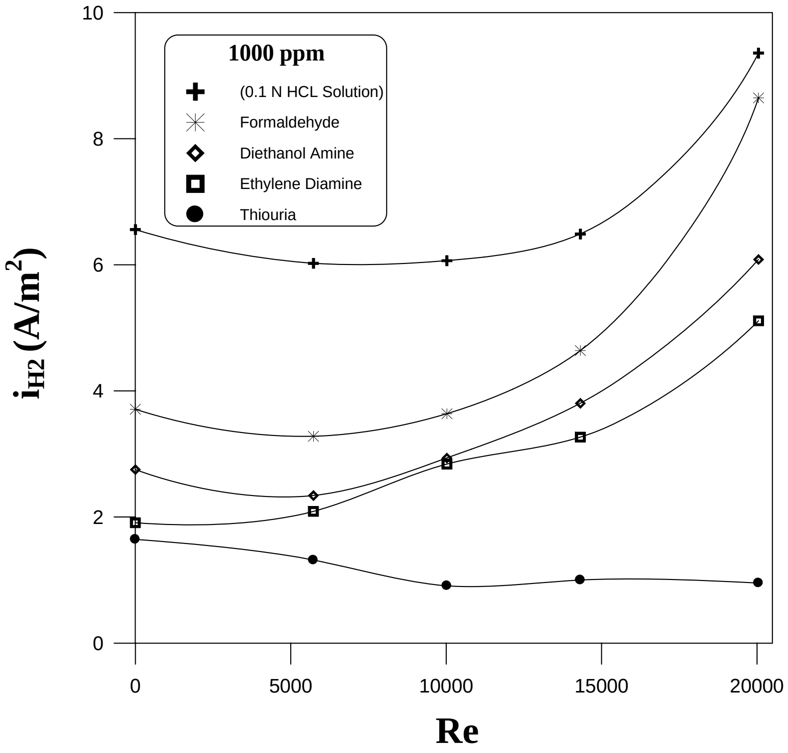

Figure A-13 Variation of Current of Hydrogen Evolution at E_{corr} with Reynolds Number for Various Inhibitors in Concentration of 1000 ppm at T= 35°C.

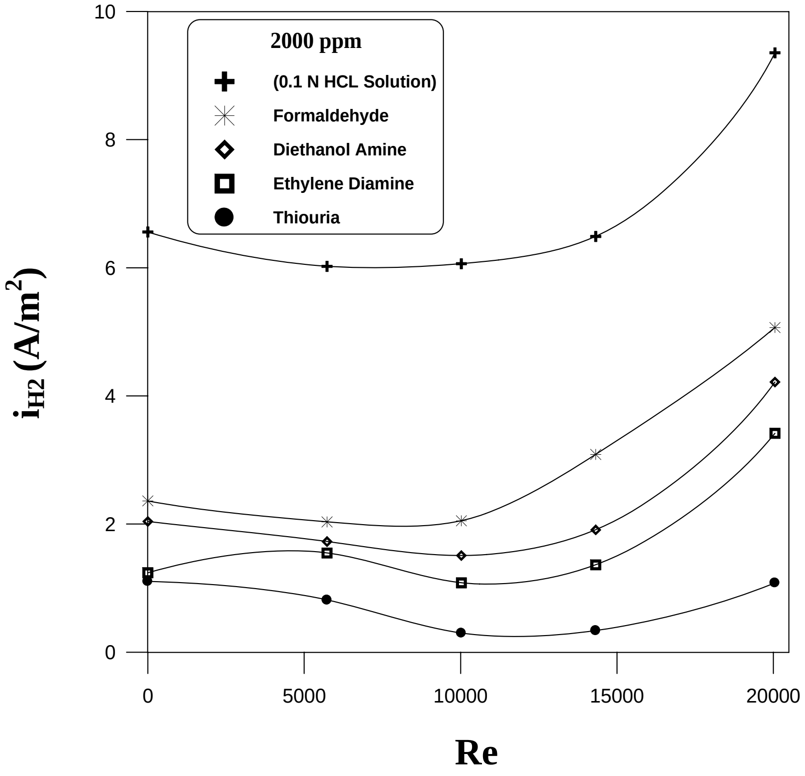

Figure A-14 Variation of Current of Hydrogen Evolution at E_{corr} with Reynolds Number for Various Inhibitors in Concentration of 2000 ppm at T= 35°C.

APPENDIX -B-

Solution and Inhibitors Properties

Table B-1 Properties of Corrosion Inhibitors [13].

Inhibitor	Structure	Density g\cm^3	Molecular Weight
Ethylenediamine	$H_2N\text{-}CH_2\text{-}CH_2\text{-}NH_2$	0.8984	60.1
Diethanolamine	$HN(CH_2CH_2OH)_2$	1.02134	105.14
Formaldehyde	HCHO	1.09	30
Thiourea	$CH_{2=}CH\text{-}CH2\text{-}NHCSNH2$	1.129	116.18

Table B-2 Physical Properties of the Solution [13, 16].

Temperature	ρ (kg/m^3)	$\mu * 10^4$ (kg/m.s)	$D * 10^9$ (m^2/s)	C_b (mole/m^3)
35ºC	994.1	7.235	2.94	0.207
45ºC	990.2	6.0052	3.88	0.188
60ºC	983.2	4.71	5.7	0.141

الخلاصة

تم أجراء دراسة لمعدلات التآكل للحديد الكاربوني في حامض الهيدروكلوريك المخفف ضمن نظام حاوي على الأوكسجين بوجود وعدم وجود المواد المانعة للتأكل والتي هي :
ثايويوريا TU، أثلين داي أمين EDA، داي أيثانول أمين DEA، فورمالديهايد، تحت درجات حرارة من (60-35)ºم وتركيز الحامض 0.1 مولاري وسرع من 1400-400 دورة/دقيقة وبوجود المواد المانعة بتركيز 2000-400 ملغم/لتر، حيث تم أستخدام طريقة الفقدان بالوزن لتحديد معدلات التآكل.

البيانات الناتجة بوجود وعدم وجود المواد المانعة للتآكل بينت بأن معدلات التآكل تزدادبزيادة كل من درجات الحرارة والسرع وتقل بزيادة تراكيز المواد المانعة للتأكل ضمن المدى المعتمد من درجات الحرارة والسرع. كما وجد أيضاً بأن تسلسل تلك المواد حسب كفائتها في تثبيط تآكل الحديد الكاربوني هو: ثايويوريا>أثيلين داي أمين>داي أيثانول أمين>فورمالديهايد حيث ان أعلى كفاءة سجلت كانت للثايويوريا والتي كانت (77.59%) واقل كفاءة سجلت لمادة الفورمالديهايد والتي كانت (37 %).

كما واضهرت النتائج العملية زيادة انتقال الأوكسجين من المحلول الى سطح المعدن مع زيادة السرعة، اي زيادة معدل اختزال الأوكسجين بالأضافة الى عدم وجود تأثير واضح للسرعة على معدل اختزال الهايدروجين باستثناء السرعة العالية (1400 rpm). إن معاملَ انتقال الكتلة يعتمد بالاساسُ على السرعة،لأنه يزداد عند زيادة عدد رينولدز أو (rpm) عند ثبوت الحرارة.

وقد وجد أن التغير في معدلات التآكل مع درجة الحرارة يتبع معادلة أرينيس بوجود المادة المانعة للتآكل (ثايويوريا-TU) اعتمادا على تأثير تركيز الثايويوريا والسرع على الطاقة المنشطة للتفاعل.

شكر وتقدير

الحمد لله رب العالمين والصلاة والسلام على أشرف الخلق محمد وعلى آله وصحبه أجمعين ..

أقف عاجزاً عن التعبيرعن مدى الشكر والأمتنان الذي أود أن أبديه إلى أستاذيِ الفاضلين المشرف الأستاذ الدكتور قاسم جبار سليمان والمشرف الدكتور باسم عبيد حسن لما بذلاه من جهد وعناء لأخراج هذا النتاج العلمي بهذه الحلة الغراء.

واتقدم بالشكر الجزيل الى الاستاذ الدكتور قاسم جبار سليمان رئيساً للقسم وجميع الكادر في قسم الهندسه الكيمياويه لما بذلوه في مساعدتي لانجاز هذا العمل.

كما أتقدم بالشكر والإجلال الى والدي الكريمين اللذان حفوني بالدموع والدعاء كما أشكر أخوتي وأخواتي اللذين لطالما كابدوا عناء البعد والفراق.
ولا أستطيع أن أنسى زوجتي العزيزة التي وقفت معي في السراء والضراء طيلة فترة البحث.

وشكري الجزيل الى جميع زملائي الذين لم يقصروا في مساعدتي.

حيدر محمد الناجي

دراسة عملية لأداء بعض مثبطات التآكل المعدني في محاليل حامضية مشبعة بالهواء

رسالة
مقدمة إلى كلية الهندسة في جامعة النهرين
وهي جزء من متطلبات نيل درجة ماجستير علوم
في الهندسة الكيمياوية

من قبل

حيدر محمد تركي

(بكالوريوس علوم في الهندسة الكيمياوية ٢٠٠٦)

جمادي الأولى ١٤٣٠
آيار ٢٠٠٩